POTENTIATION OF U-937 CELL DIFFERENTIATION BY NITRIC OXIDE DONORS AND ASSESSMENT OF HEPARANASE AS A DIFFERENTIATION MARKER

Amy Yamazaki

Thesis submitted to the Department of Biochemistry in partial fulfillment of the requirements for the degree of Master of Science

University of Ottawa
Ottawa, Ontario, Canada

National Library
of Canada

Acquisitions and
Bibliographic Services Branch

395 Wellington Street
Ottawa, Ontario
K1A 0N4

Bibliothèque nationale
du Canada

Direction des acquisitions et
des services bibliographiques

395, rue Wellington
Ottawa (Ontario)
K1A 0N4

Your file Votre référence

Our file Notre référence

ISBN 0-612-15777-6

Canada

UNIVERSITÉ D'OTTAWA
UNIVERSITY OF OTTAWA

ABSTRACT

Our laboratory has been interested in the effects on leukocytes of reactive oxygen intermediates (ROI), such as superoxide (O_2^-), produced during the "respiratory burst". Upon stimulation, such cells employ the NADPH oxidase to reduce O_2 to form O_2^- using NADPH from the hexose monophosphate shunt (HMPS). In order to further study the effects of ROI, we planned to perform genetic manipulations on U-937 cells, a monoblastic cell line capable of differentiation into more mature leukocytes. In ***Part A***, conditions to promote maximal U-937 differentiation into respiratory burst-competent cells were developed, thus allowing for such manipulations. Retinoic acid (RA) was found to be a potent inducer of a functional NADPH oxidase and HMPS, and of various mRNAs for their components. RA also reduced cell proliferation and altered cell morphology. The effects of RA were augmented by nitric oxide (NO·) donors, believed to act by increasing intracellular cGMP levels. Among the NO· donors tested, only glyceryl trinitrate induced differentiation in the absence of RA.

Since heparanase, an endoglycosidase which degrades heparan sulfate (HS), is active in mature leukocytes, the possibility that heparanase might serve as another U-937 differentiation marker was investigated. Because of a laboratory interest in cloning a heparanase cDNA based on enzymatic activity, ***Part B*** was devoted to the development of heparanase assays for these purposes and for characterization of heparanases. A refined PAGE-based heparanase assay was used to test various cell types; KNRK cells were found to be the most active. Not previously characterized, KNRK heparanase was found to be a

relatively stable enzyme with pH 6 optimum, inhibitable by heparin and able to digest a variety of HS substrates. Heparanase activity was virtually absent in immature U-937 cells and was only marginally increased during differentiation. Development of a more sensitive fluorescence-based heparanase assay was initiated.

ACKNOWLEDGEMENTS & DEDICATION

The completion of my Masters degree has been a long and arduous journey; however, through the contributions of many, I have been able to see its completion. I would like to acknowledge some of the individuals with whom I have had the pleasure of working with and whose input is greatly appreciated.

I wish to thank the following for their kindness and generosity: Dr. Israel Vlodavsky, for samples of heparan sulfate substrates, heparin and heparanases; Dr. Peter Anderson for providing me with dansyl chloride, dansylated amino acids and polyamide TLC sheets; Dr. Brian G. Carter of Hoechst-Roussel Canada for samples of molsidomine and CAS 936; Dr. M. Buchwald from Hospital for Sick Children for HSC 93 cells; and Dr. Joshua Stahl from Molecular Probes for fluorescein-X-biotin.

In offering words of wisdom, showing support, and patiently enduring my lengthy meetings, I wish to thank the members of my committee, Dr. Barbara Vanderhyden, Dr. Denis Williamson, and Dr. Martin Young. Thanks also to Dr. Martin Tenniswood for his advice and excellent teaching over the years. Many thanks to Joanne and Julie, the dedicated office staff in the Biochemistry department, for always taking care of my various student needs.

In terms of the Bimboim lab, I have been truly blessed with a fantastic group of people with whom to work. I would like to extend my deepest gratitude to all members of the lab, those with us now as well as those who haved moved on, for offering words of advice and encouragement, for being sources of great inspiration and enthusiasm, for

helping me to keep my sanity, for knowing how to make the best of things and for knowing how to have fun...basically, for being like family to me throughout the years! Thanks to: Diana for getting me started on tissue culture way back when and for always keeping up the cheer in the lab; Paula for keeping me company on those odd hour shifts (and simply those odd hours), and showing me the importance of shoes: Steff for offering advice on cell and molecular biology stuff, being a great inspiration and showing your support for my teaching aspirations; Deep for being a symbol of hard work and sharing with us your great cooking; Randy for being a walking reference manual, travelling buddy and bench hog; Mike, John, Chantal, Phil, Steff, Dan and Howard with whom I enjoyed working with as a team on the heparanase project; Irith, Amanda, Sat and Deepali for being younger than I; and last, but not at all least, Rick, Cai-Ying, Eileen, Tina, Chantal, Phil, Angie and the office staff for their their knowledge, expertise and technical support, as well as their patience with me and my many questions and requests. Wishing the new members of the lab a warm welcome and wishing all of you continued success!!

Now, special thanks to the one who made this all possible, with his great wisdom, advice, and words of encouragement: my supervisor, Dr. Chaim Bimboim.

Finally, I would like to thank: God, the Lord and Creator of all things, and whose wonders and intricacies never cease to amaze me; and my family and friends, especially my "other half" Tim, whose enduring support and love got me through this experience.

To my faithful family and friends, I dedicate this thesis.

FOREWORD

This thesis is divided into two parts. **Part A** represents work done on developing a differentiation protocol that would give the highest yield of differentiated U-937 cells capable of producing superoxide. **Part B** represents work done towards developing heparanase activity assays to assess whether heparanase would be useful as another U-937 differentiation marker, to aid in the cloning of the heparanase cDNA and to characterize various heparanases. The projects were carried out in parallel and came together with the testing of heparanase activity in differentiated U-937 cells. The organization of the thesis is outlined below.

There is one combined abstract and list of abbreviations for both parts found at the beginning of the thesis. Materials, suppliers and solution compositions for both parts are detailed in the text, in the figure legends and/or in Appendix I.

Except for Materials being listed elsewhere, **Part A** is arranged in the form of a typical paper with Introduction, Methods, Results, Discussion and Summary sections. In contrast, **Part B** begins with an Introduction section and the remainder of the text is divided into three *chapters*, each of which is divided into numerous *sections*. ***Chapter I*** describes the refinement of a PAGE-based heparanase activity assay. ***Chapter II*** describes the application of the PAGE assay to the heparanase cloning project, to the characterization of different heparanases and to the U-937 differentiation project described in Part A. ***Chapter III*** outlines the development of a fluorescence-based heparanase activity assay. Due to the nature of the work done for Chapters I and III (i.e., development of methods), there is no

actual "Methods" section since the methods are part of the text itself. Details of the methods are given either in the text, in the figure legends, or in Appendix II. Since the results of Chapter II are obtained using methods developed in Chapter I, again there is no Methods section. For all three chapters, the Results and Discussion sections have been placed together in one *subsection* within each section of each chapter. Several Summary sections are provided. The thesis draws to a close with an Overall Conclusion section.

TABLE OF CONTENTS

LIST OF FIGURES AND ILLUSTRATIONS

LIST OF ABBREVIATIONS USED

α,MM	human placental heparanase purified by Dr. I. Vlodavsky
ANOVA	analysis of variance
B16F10	murine melanoma cell line
BSS	balanced salt solution
BXXSE	6-((6-((biotinoyl)amino)hexanoyl)amino) hexanoic acid, succinimidyl ester
cAMP	cyclic adenosine 3':5'-monophosphate
CAS	persidomine or CAS 936 or 3-(cis-2,6-dimethylpiperidino)-N-(4-methoxybenzoyl)sydnonimine)
cDNA	complementary deoxyribonucleic acid
CDTA	*trans*-1,2-diaminocyclohexane-*N,N,N',N'*-tetraacetic acid
CGD	autosomal chronic granulomatous disease
cGMP	cyclic guanosine 3':5'-monophosphate
CHAPS	3-((3-cholamidopropyl)dimethylammonio)-1-propane sulfonate
CT	CDTA-Tris solution
CTAP-III	connective tissue activating peptide-III
CYS	L-cysteine
cyt b_{558}	cytochrome b_{558} (also known as cytochrome b-245); catalytic component of the NADPH oxidase
dCTP	2'-deoxycytidine 5'-triphosphate
DEAE	diethylaminoethyl
DMEM	Dulbecco's modified eagle's medium
DMMB	dimethylmethylene blue
DMF	dimethyl formamide
DMSO	dimethyl sulfoxide
DNA	deoxyribonucleic acid
DTT	dithiothreitol
ECM	extracellular matrix
EDTA	ethylenediaminetetraacetic acid
FAD	flavin-adenine dinucleotide
FCS	fetal calf serum
FITC	fluorescein isothiocyanate isomer 1
FITC-HS	HS randomly labelled with FITC
FITC-HS-N-XXB	HS biotinylated with BXXSE after reductive amination and randomly labelled with FITC
fMLP	*N*-formyl-methionylleucylphenylalanine
G6PD	glucose-6-phosphate dehydrogenase
GAG	glycosaminoglycan
GAP	GTPase activating protein
GAPDH	glyceraldehyde-3-phosphate dehydrogenase
GDI	GDP dissociation inhibitor
GDP	guanosine diphosphate

GDS	GDP dissociation stimulator
GRP 94	glucose regulated protein (94 kDa), also called endoplasmin
$gp91^{phox}$	91 kDa glycosylated β chain of cyt b_{558} (NADPH oxidase component)
GTN	glyceryl trinitrate (also known as nitroglycerin)
GTP	guanosine triphosphate
GTPase	GTP phosphohydrolase
Hep III	heparinase III from *Flavobacterium heparinum*; heparin lyase, EC 4.2.2.7
HEPES	*N*-(2-hydroxyethyl)piperazine-*N'*-(2-ethanesulfonic acid)
HL-60	human promyelocytic leukemia cell line
HMPS	hexose monophosphate shunt (also called pentose phosphate pathway)
HMW	high molecular weight
hr	hour(s)
HS	heparan sulfate (also known as heparan sulphate or heparitin sulfate)
HSC 93	human lymphoma cell line
$HS\text{-}NH_2$	reductively aminated HS
HS-N-XXB	reductively aminated and N-biotinylated HS
hsp	heat shock protein
HSPG	heparan sulfate proteoglycan
IPTG	isopropyl-β-D-thiogalactopyranoside
KNRK	Kirsten murine-sarcoma-virus-transformed normal rat kidney cell line
λgt11	λ bacteriophage-based expression library
MAPK	mitogen-activated protein kinase
min	minute(s)
MNase	micrococcal nuclease
MOL	molsidomine or N-carboxy-3-morpholino-sydnonimine-ethylester
MOPS	3-(*N*-morpholino)propanesulfonic acid
M_r	molecular weight
mRNA	messenger ribonucleic acid
MWCO	molecular weight cutoff
NA	NeutrAvidin
$NaBH_3CN$	sodium cyanoborohydride
$NADP^+$	oxidized nicotinamide-adenine dinucleotide phosphate
NADPH	reduced nicotinamide-adenine dinucleotide phosphate
NBT	nitroblue tetrazolium
NEM	N-ethyl maleimide
NF-κB	nuclear factor-kappa B
NIH 3T3	NIH Swiss murine embryo (fibroblast) cell line
NRK	normal rat kidney cell line
O.D.	optical density units
$p21^{rac\ (or\ Rap1A)}$	small GTP-binding proteins necessary for NADPH oxidase activation
$p22^{phox}$	22 kDa non-glycosylated α chain of cyt b_{558} (NADPH oxidase component)
$p40^{phox}$	possible cytosolic factor for the NADPH oxidase
$p47^{phox}$	47 kDa cytosolic protein component of the NADPH oxidase

pp47^{phox}	phosphorylated p47^{phox}
p67^{phox}	67 kDa cytosolic protein component of the NADPH oxidase
PAGE	polyacrylamide gel electrophoresis
PBP	platelet basic protein
PBS	phosphate buffered saline
pbs	heparan sulfate prepared by Sigma
PBST	phosphate buffered saline containing Triton X-100
pfs	heparan sulfate prepared for Sigma
phox	phagocyte oxidase
PKC	protein kinase C
PMNs	polymorphonuclear neutrophils (here used interchangeably with granulocytes)
PMSF	phenylmethylsulfonyl fluoride
PreS1R8	preimmune rabbit serum preparation
R8IS5	antibody preparation against putative heparanase peptide
RA	all-*trans* retinoic acid (also known as tretinoin)
Rec	rat embryo fibroblast cell line
RecRas	ras-transformed rat embryo fibroblast cell line
ROI	reactive oxygen intermediates
RNA	ribonucleic acid
RT	room temperature
SA	streptavidin
SA-ag	streptavidin linked to agarose beads
SAL	saccharic acid 1,4-lactone
^{35}S-ECM	^{35}S-labelled extracellular matrix
SEM	standard error of the mean
SDS	sodium dodecyl sulfate
SLSR	Soft-Link Soft-Release resin
SSC	sodium chloride, sodium citrate buffer
SOD	Cu,Zn-superoxide dismutase (EC 1.15.1.1)
TAC	Tris-acetate-CDTA electrophoresis buffer for DNA and HS
TEMED	*N,N,N',N'*-tetramethylethylenediamine
THP-1	human monocytic leukemia cell line
TK6	human lymphoblastic cell line
TLC	thin layer chromatography
TNM	tetranitromethane
TPA	12-*O*-tetradecanoylphorbol-13-acetate (also known as PMA, phorbol 12-myristate 13-acetate)
Tris	tris(hydroxymethyl)aminomethane
U-937	human monoblastic leukemia cell line
UV	ultraviolet
X-CGD	X-linked chronic granulomatous disease

PART A

POTENTIATION OF RETINOIC ACID-INDUCED U-937 CELL DIFFERENTIATION INTO RESPIRATORY BURST-COMPETENT CELLS BY NITRIC OXIDE DONORS

PART A: Potentiation of Retinoic Acid-Induced U-937 Cell Differentiation Into Respiratory Burst-Competent Cells by Nitric Oxide Donors

INTRODUCTION

Objective

Our laboratory has been interested in the mechanisms by which reactive oxygen intermediates (ROI), such as superoxide anion ($O_2^{\cdot-}$), hydrogen peroxide (H_2O_2), hypochlorous acid (HOCl), nitric oxide (NO·) and peroxynitrite ($ONOO^-$), produced by mature peripheral blood leukocytes during a variety of processes cause breaks in cellular DNA [1-6]. Although granulocytes (mostly polymorphonuclear neutrophils, PMNs) have been satisfactory for many types of experiments, such terminally-differentiated, non-dividing cells do not allow for genetic manipulations that are needed to better understand the mechanisms involved in inducing DNA breaks. My objective in this part of the thesis was to develop a differentiation protocol that, starting with immature precursor cells, would generate the highest yield of differentiated cells capable of producing $O_2^{\cdot-}$ through the "respiratory burst". This would allow for genetic manipulation of growing cells prior to induction of differentiation, which is not possible in mature monocytes or PMNs.

Background

The term "respiratory burst" refers to the rapid consumption of diatomic oxygen (O_2) by stimulated phagocytes (namely neutrophils, monocytes, macrophages, and eosinophils) [7-9]. This phenomena was originally believed to be the result of increased

mitochondrial respiration; however, this process was observed to be insensitive to inhibitors of mitochondrial respiration such as cyanide and azide [7,9,10]. The dramatic rise in O_2 consumption was later attributed to the formation of superoxide anion ($O_2^{\cdot-}$) via the NADPH oxidase (also referred to as the "respiratory burst oxidase"), a key contributor to oxyradical generation during the respiratory burst [10,11]. In response to appropriate stimuli, this membrane-bound oxidase catalyzes the one electron reduction of O_2 to $O_2^{\cdot-}$ using NADPH (reduced nicotinamide-adenine dinucleotide phosphate) as the electron donor [7]. The overall reaction is:

$$NADPH + 2O_2 \xrightarrow{2e^-} NADP^+ + H^+ + 2O_2^{\cdot-}$$

$O_2^{\cdot-}$ production and release primarily occur extracellularly at the plasma membrane on the luminal membranes surfaces of phagocytic vacuoles or on the membranes of specific neutrophilic cytoplasmic granules which eventually fuse with the phagocytic vacuoles [10]. $O_2^{\cdot-}$ production is not restricted to the "professional" phagocytes having a NADPH oxidase; it occurs in many other cell types including lymphocytes [10], fibroblasts, endothelial cells, kidney mesangial cells, spermatozoa and tumour cells [7,12].

The NADPH oxidase itself is a multicomponent enzyme (Figure 1). It contains a membrane-bound electron transport chain whose catalytic component is a flavocytochrome called cytochrome b_{558} (cyt b_{558}) due to its absorption maximum at 558 nm (also called cytochrome b-245 due to its extremely low midpoint redox potential of -245 mV) [7,10]. This flavocytochrome is the only known mammalian protein that is capable of reducing O_2 to $O_2^{\cdot-}$ directly. Cyt b_{558} is composed of a flavoprotein which binds FAD (flavin-adenine dinucleotide) and NADPH, and a b-type cytochrome bearing one or more electron-carrying

Figure 1. ***Model of the respiratory burst and related activities.***

1. *Respiratory burst activation.* Activation of the respiratory burst is accomplished by a variety of stimuli including protein kinase C (PKC) agonists such as phorbol esters (eg., 12-*O*-tetradecanoylphorbol-13-acetate (TPA)) and diacylglycerol (DAG), chemoattractant receptor agonists such as *N*-formyl-methionylleucylphenylalanine (fMLP), and bioactive lipids such as phosphatidic acid (PA), lysophosphatidic acid (Lyso-PA) and arachidonate. The latter could be generated from PA, phosphatidylinositol 4,5-bisphosphate (PIP_2) and phosphatidyl choline (PC) (or other phospholipid) by the action of phospholipases A_2, C and D (PLA_2, PLC, PLD), respectively, and DAG kinase (for DAG ⇌ PA interconversions). Where as PKC-mediated pathways are Ca^{2+}-independent, an increase in intracellular Ca^{2+} concentration ($[Ca^{2+}]_i$) by inositol (1,4,5)-trisphosphate (IP_3) and other intermediates accompanies activation of pathways involving PLC. The role of Ca^{2+} is uncertain although it may be involved in protein translocation and degranulation. fMLP-induced activation also activates the mitogen-activated protein kinase (MAPK) pathway which may have a role in oxidase deactivation.

2. *NADPH oxidase assembly and action.* Although the role of phosphorylation is unclear, the cytosolic p47 undergoes a stimulus-dependent phosphorylation possibly by PKC (indicated by a dashed line). pp47 and p67 translocate to the membrane and associate with cytochrome b_{558}, the membrane-bound catalytic component of the NADPH oxidase composed of gp91 and p22 subunits. Upon activation, the isoprenylated (indicated by a zigzag line) cytosolic $p21^{rac}$ dissociates from its GDP-dissociation inhibitor (GDI), possibly interacts with a GDP-dissociation stimulator (GDS) to facilitate binding of GTP, and translocates to the membrane to aid in oxidase assembly. Rap1A, a membrane-associated GTP-binding protein (also isoprenylated), is believed to regulate oxidase activation. Electrons are passed from NADPH donated from the hexose monophosphate shunt (HMPS) to cytochrome b_{558} and finally to O_2 to generate superoxide ($O_2^{\cdot-}$) which is released to the exterior. $O_2^{\cdot-}$ production can be measured by $O_2^{\cdot-}$ reduction of NBT to form insoluble formazan. Deactivation of the NADPH oxidase may occur by Rac GTPase-activating proteins (GAPs) which may in turn be regulated by MAPK pathways that are co-activated with the oxidase.

3. *Consequences of NADPH oxidase activity.* The HMPS is activated to replenish the supply of NADPH for the NADPH oxidase. Through a series of reactions starting with glucose, NADPH is regenerated from $NADP^+$ and the first carbon of glucose is liberated as CO_2. $O_2^{\cdot-}$ formed by the NADPH oxidase spontaneously or enzymatically (by superoxide dismutase (SOD)) dismutates to H_2O_2 which can diffuse into the cell where it is either detoxified to H_2O by catalase or by glutathione peroxidase (Gpx). (The latter, using reduced glutathione (GSH) as a reducing agent, generates oxidized glutathione (GSSG) which is reduced back to GSH by glutathione reductase (Gred) using NADPH from the HMPS). As part of the microbicidal and tumoricidal defense mechanism, H_2O_2 can be converted to the more reactive hypohalous acids such as hypochlorous acid (HOCl) in the presence of halides (Cl_2) by myeloperoxidase (Mpx) or the highly reactive hydroxyl radical ($\cdot OH$) in the presence of transition (trans.) metal ions.

Figure 1.

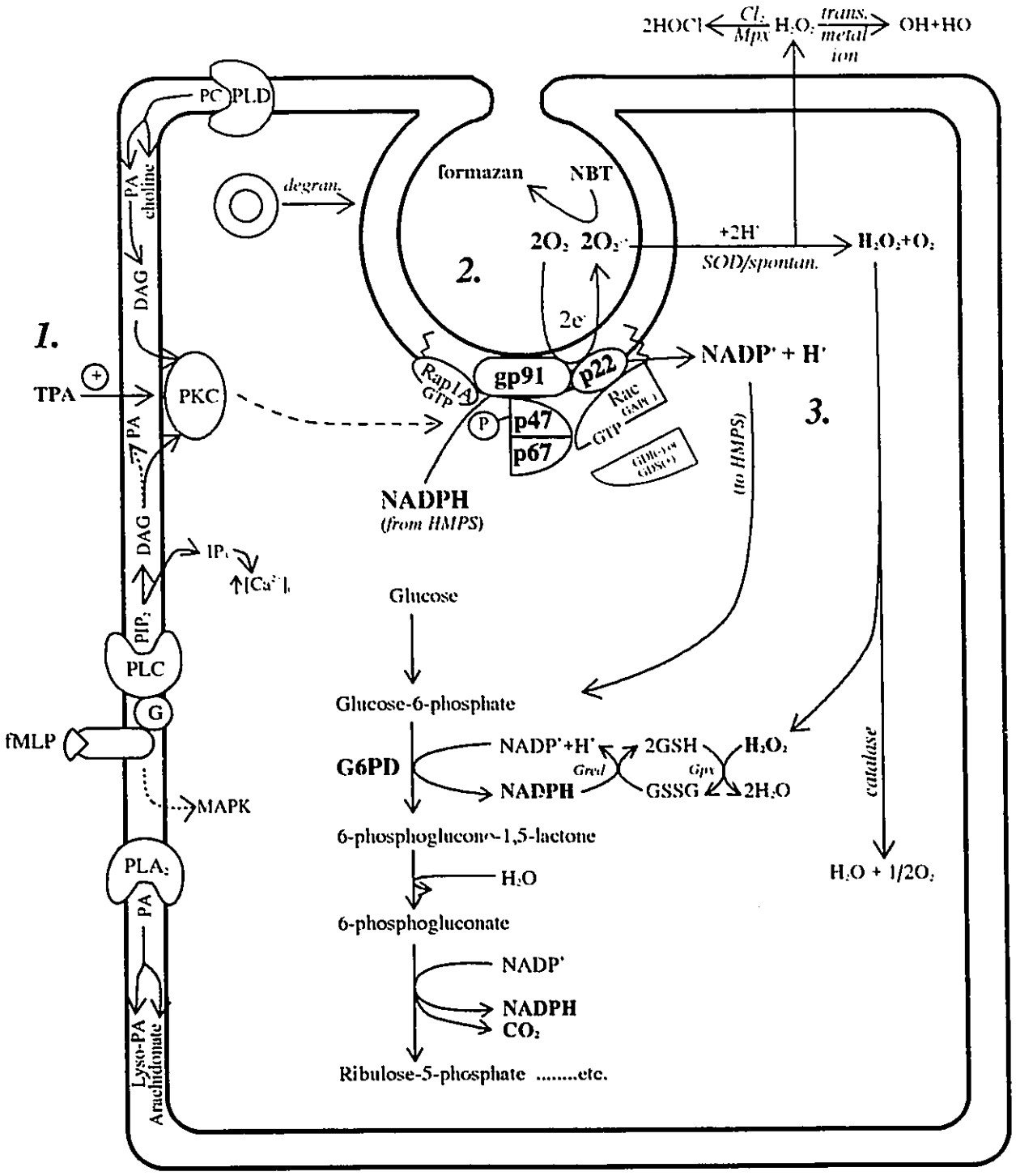
2HOCl
Cl⁻ Mpx
H₂O₂
trans. metal ion
OH+HO
PC
PLD
PA
choline
DAG
degran.
formazan
NBT
2O₂ 2O₂·⁻
+2H⁺
SOD/spontan.
H₂O₂+O₂
2.
1.
2e⁻
TPA
PKC
Rap1A GTP
gp91
p22
NADP⁺ + H⁺
3.
P
p47
p67
Rac GAP1 GTP
Gluc-6-P GDSCO
NADPH
(from HMPS)
(to HMPS)
PA
DAG
IP₃
↑[Ca²⁺]i
Glucose
PIP₂
PLC
Glucose-6-phosphate
G
fMLP
G6PD
NADP⁺+H⁺
NADPH
Grd
2GSH
GSSG
Gpx
H₂O₂
2H₂O
catalase
MAPK
6-phosphoglucono-1,5-lactone
PLA₂
H₂O
H₂O + 1/2O₂
6-phosphogluconate
PA
NADP⁺
NADPH
CO₂
Lyso-PA
Arachidonate
Ribulose-5-phosphate .....etc.

hemes [9]. With the combined FAD-dependent dehydrogenase and electron transferase activities of cyt b_{558} [13], the proposed electron flow from NADPH to O_2 is [12]:

$$\text{NADPH} \xrightarrow{2e^-} \text{FAD} \xrightarrow{2e^-} 2 \text{ cyt } b_{558} \xrightarrow{2e^-} 2\ O_2 \xrightarrow{2e^-} 2\ O_2^-$$

Unlike most other cytochromes, cyt b_{558} is composed of two types of subunits, a heavily glycosylated heavy chain (β chain or $gp91^{phox}$; "phox" denoting *ph*agocyte *ox*idase) and one or two non-glycosylated light chains (α chain or $p22^{phox}$) [9,10]. $gp91^{phox}$ is believed to contain the FAD-binding site while there remains debate as to whether $p22^{phox}$, $gp91^{phox}$ or both are the heme-binding proteins [9,10]. Cyt b_{558} was originally identified as being defective in X-linked chronic granulomatous disease (X-CGD) [14], an often-fatal syndrome which renders patients deficient in respiratory burst activity abnormally susceptible to severe infections [9]. The defect for X-CGD lies in the β-subunit.

Several other proteins have been identified to be necessary for NADPH oxidase activity (Figure 1). Two soluble cytosolic factors, the phosphoprotein $pp47^{phox}$ and $p67^{phox}$, play an essential role in oxidase activation [9]. Either $pp47^{phox}$ and $p67^{phox}$ can be deficient or absent in autosomal recessive forms of CGD [15]. $p47^{phox}$ undergoes a stimulus-dependent phosphorylation (possibly by protein kinase C (PKC) [16]) and translocates from the cytosol to the membrane to activate the oxidase; however, the exact relevance of phosphorylation in translocation or oxidase activation is unclear [9]. At the membrane, $pp47^{phox}$ and $p67^{phox}$ associate with cyt b_{558}. $pp47^{phox}$ and $p67^{phox}$ translocation is absent in X-CGD suggesting that their association with cyt b_{558} or some closely associated molecule may be necessary to reside at the membrane [9,10]. Both $pp47^{phox}$ and $p67^{phox}$ contain two *src* homology 3 domains which may be involved in submembranous

cytoskeletal attachment [9], interaction with GTP-binding proteins [10] or association with the cyt b_{558} itself. In addition to cyt b_{558}, $pp47^{phox}$ and $p67^{phox}$, small cytosolic or membrane-bound *Rac*- or *Ras*-related GTP-binding proteins, such as $p21^{rac}$ and $p21^{RapIA}$, and their respective GDP dissociation inhibitors (GDIs), GTPase activating proteins (GAPs) and GDP dissociation stimulators (GDSs) are believed to be important for regulation of oxidase assembly and/or translocation of the cytosolic factors to the membrane as well as for cytoskeletal rearrangements that occur during phagocytosis and degranulation [9,11,16]. More recently, $p40^{phox}$ has been shown to co-immunoprecipitate with $p67^{phox}$ from neutrophil cytosols and its levels are reduced with $p67^{phox}$ in autosomal forms of CGD [17]. Although $p40^{phox}$ has been implicated in NADPH oxidase regulation, it may not be essential for activity.

NADPH oxidase activation can be accomplished by a variety of different means (Figure 1) [8,10,12,16,18]. Agonists that activate PKC, such as 12-*O*-tetradecanoylphorbol-13-acetate (TPA) or diacylglycerol, appear to trigger the oxidase after a lag of about 25 seconds, in a calcium-independent manner, resulting in a more sustained respiratory burst [10]. This contrasts agonists such as *N*-formyl-methionylleucylphenylalanine (fMLP) which act more rapidly (within 5-10 seconds), accompanied by increased intracellular Ca^{2+} concentration and whose response is less sustained [8,10,18]. The significance of the increase in intracellular Ca^{2+} concentration is not clear, although Ca^{2+} may mediate vesicle or protein translocation during oxidase activation and vesicle fusion during degranulation events [8,19,20]. Other chemotactic agonists that are activators of the NADPH oxidase and that may act similarly to fMLP are

complement fragment C5a, platelet-activating factor, interleukin 8 and leukotriene B_4 [8,16]. Bioactive lipids (such as arachidonic acid, phosphatidic acid and phosphatidylinositols) may activate the NADPH oxidase directly through physical disruption of Rac-GDI complexes [10,11] or indirectly by other mechanisms [12,18,21]. Little is known about the deactivation of the oxidase. It has been speculated that dephosphorylation events involving phosphatases and/or GAP-stimulated intrinsic GTPase activity of GTP-binding proteins involved in oxidase activation (such as *Rac*) may be responsible for NADPH oxidase deactivation [10,11,16]. fMLP-initiated respiratory burst is accompanied by tyrosine phoshorylation and activation of a mitogen-activated protein kinase (MAPK) pathway, the role of which may be in the regulation of the GTP/GDP state of the GTP-binding proteins involved in NADPH oxidase activation [11].

O_2^- formed by the NADPH oxidase can subsequently be converted to H_2O_2 either spontaneously or by the enzyme superoxide dismutase (SOD) (Figure 1). Neither O_2^- nor H_2O_2 are highly reactive; however, in the presence of various trace metal ions, H_2O_2 can yield the hydroxyl radical, $^{\cdot}OH$, a very potent biological oxidant [10]. In the presence of halides such as chloride, oxidizing hypohalides such as hypochlorous acid may be formed from H_2O_2 by the enzyme myeloperoxidase [10]. O_2^- and nitric oxide ($NO^{\cdot}$) react to form peroxynitrite ($ONOO^-$), also a strong oxidant. The production of these reactive oxygen intermediates (ROI) is one of the phagocyte defense mechanisms to combat microbial infection, destroy tumor cells, or remove dying cells and cellular debris [9-11]. One key enzyme involved in self-defense against the potentially toxic effects of H_2O_2 is catalase, which converts H_2O_2 to O_2 and H_2O [9]. Additionally, glutathione peroxidase utilizes

reduced glutathione to detoxify harmful peroxides (such as membrane lipid peroxides and H_2O_2). Glutathione reductase uses NADPH to reduce oxidized glutathione back to its reduced form [22]. Another key role of $O_2^{\cdot-}$ production is to increase the basicity of the phagocytic vacuole. As electrons are pumped into the lumen of the vacuole, they are unaccompanied by protons. This results in a pH increase in the vacuole thereby activating neutral proteinases (normally inactive in the mildly acidic environment of the granules) upon granule fusion to the vacuolar membrane [10] (Figure 1).

Since ROI are also produced by non-phagocytic cells, a more subtle role particularly at lower concentrations of these agents has been proposed namely in the regulation of the expression of genes and in signal transduction pathways, including those involved in the inflammatory and immune responses [7,10,12,23]. $O_2^{\cdot-}$, H_2O_2, vanadyl peroxides and other ROI have been reported to enhance tyrosine phosphorylation by increasing tyrosine kinase and/or decreasing tyrosine phosphatase activities [24-27]. ROI are also implicated to be second messengers for TPA, tumor necrosis factor and interleukin-1 mediated pathways that activate the stress-responsive transcription factor, nuclear factor-kappa B (NF-κB) [23,26,28,29]. Ionizing radiation, H_2O_2 and TPA (known to activate genes including c-*fos*, c-*myc*, c-*jun*, and NF-κB) have also been found to activate the MAPK signalling pathway through generation of ROI [30]. One ROI target may lie upstream of receptor protein tyrosine kinase signalling pathways [31], which, via MAP kinase, may activate NF-κB (since ROI have been shown to activate *src*-related tyrosine kinases as well as NF-κB [27], and the downstream Raf-1 and MAP kinases have been shown to activate NF-κB [32,33]). Thiols, SOD, and other antioxidants are able to

inhibit the ROI-dependent effects on protein phosphorylation and transcription activation [23-28]. Our laboratory was interested in the role of ROI in tumour progression, more specificially, their role in inducing DNA strand breaks by means of a specific enzymatic mechanism (as opposed to a direct chemical attack) [4,5].

The increased demand for NADPH as a co-substrate for the NADPH oxidase and glutathione reductase necessitates the activation of the hexose monophosphate shunt (HMPS, also called pentose phosphate pathway) [7]. A drop in cellular NADPH removes the product inhibition experienced by glucose-6-phosphate dehydrogenase (G6PD), the regulatory enzyme at the first step of the pathway (Figure 1) [22,34]. Glucose-6-phosphate, from extracellular glucose transported into the cell or from glycogenolysis (of glycogen stored in the granules of granulocytes), is fed into the shunt to regenerate NADPH from $NADP^+$. The first carbon of glucose is released as CO_2 at the fourth step and it is the release of this CO_2 that has been used as a measure of HMPS activity [35]. Although normally a constitutive housekeeping enzyme, G6PD is also believed to be subject to tissue-specific regulation by hormones, growth factors and oxidant stress [36].

Thus, it is clear that the acquisition a fully functional respiratory burst oxidase during cell differentiation would not only rely upon acquisition of the NADPH oxidase components but also HMPS activity that would provide the necessary NADPH.

Experimental Approach

The human monoblastic leukemic cell line, U-937, has been used as a model

system for studying myelomonocytic differentiation *in vitro* [37]. These cells are arrested in an early stage of differentiation. This cell line was chosen for my studies since immature U-937 cells do not possess any significant O_2^- -generating ability; however, upon differentiation towards monocyte/macrophage- or granulocyte-like cells, they may acquire this ability. Use of this cell line offered the additional advantages of rapid growth and relative ease of maintainance of the cells in culture. Development of an optimal differentiation protocol would allow genetic manipulations to be performed on U-937 cells prior to induction of differentiation.

A variety of agents have been shown to induce U-937 differentiation. Depending on the inducing agent employed, these cells can be induced to differentiate along either the granulocytic or the monocytic/macrophage lineage. One of the earlier agents to be identified was all-*trans* retinoic acid (RA). Treatment of U-937 cells with RA results in their differentiation into monocyte-like cells [38-41]. RA is presumed to act *via* a specific nuclear receptor [42-44] to modulate transcription of genes related to cell cycling and differentiation [45,46] including those encoding leucocyte-specific proteins (reviewed in [47]).

RA alone is insufficient to induce complete differentiation to mature monocytes and other factors are presumed to be necessary. Attempts have been made by others to identify agents that further enhance the differentiation-inducing ability of RA. Among those agents previously identified are gamma-interferon [48,49], 1α,25-dihydroxycholecalciferol [41,50], cyclic adenosine monophosphate (cAMP)-elevating agents such as dibutyryl cAMP, prostaglandin E_2 or cholera toxin [39,40,51], bufalin [38], transforming growth factor-β1

[52], tumor necrosis factor-α, granulocyte colony stimulating factor, interleukin-1α, and interleukin-4 [49].

Prior to the present study, I screened RA and several other compounds for their potential in inducing U-937 cell differentiation into $O_2^{\cdot-}$-generating cells as assessed by their ability to reduce nitroblue tetrazolium (NBT) to formazan using $O_2^{\cdot-}$. High numbers of $O_2^{\cdot-}$-producing cells were obtained by using RA alone. Other compounds (such as 8-(4-chlorophenylthio) cAMP, dibutyryl cAMP, dibutyryl cGMP (cyclic guanosine monophosphate), gamma-interferon, indomethacin, granulocyte-macrophage colony stimulating factor) were only effective when combined with RA. Cyclic nucleotides, such as cAMP and cGMP, have been studied in the context of myeloid differentiation [40,53]. Because dibutyryl cGMP appeared to have an effect, the possibility that a cGMP pathway might enhance the effect of RA was investigated further with the use of cGMP-elevating agents.

Cyclic GMP levels can be elevated by the agents which release nitric oxide (NO·), an important endogenous activator of soluble guanylate cyclase [54,55]. NO· is endogenously produced from *L*-arginine by nitric oxide synthase [56]. A variety of drugs that release NO· either spontaneously or after metabolic activation have also been identified [57,58]. Some have recently been shown to modulate monocytic differentiation and gene expression in HL-60 human promyelocytic leukemia cells [59]. Glyceryl trinitrate (GTN, nitroglycerin) has been demonstrated to release NO· after metabolic activation in various tissues [57,60-62]. Sydnonimines such as molsidomine (MOL) and CAS 936 (CAS, persidomine) release NO· following ring-opening; bioactivation of MOL

and CAS is required for ring-opening to occur [57.63]. Tetranitromethane (TNM) is a novel agent that has not yet been tested for NO·-releasing potential or cGMP-elevating activities (although its structure bears resemblance to sodium nitrite, also believed to be a NO· donor [63]).

In the present study, potentiation of RA induction of differentiation by GTN, MOL, CAS, and TNM was examined using a variety of differentiation markers. NADPH oxidase activity in response to TPA stimulation was assessed by microscopically scoring the percentage of cells staining with formazan, the product of NBT reduction by $O_2^{\cdot-}$, as well as spectrophotometrically quantifying the total amount of formazan produced. HMPS activity was assessed by quantification of $[^{14}C]CO_2$ released from D-[1-^{14}C]glucose. mRNA levels for two NADPH oxidase components, $p47^{phox}$ and $gp91^{phox}$, the rate-limiting HMPS enzyme, G6PD, as well as SOD were assessed by Northern analysis. Other parameters examined for alteration were cell proliferation and cellular morphology.

MATERIALS and METHODS

Materials

A listing of the materials, chemical suppliers and solution compositions is found in Appendix I.

Cells and Cell Culture

U-937 cells were cultured 10 cm plastic tissue culture dishes for ≤ 4 weeks in complete medium (RPMI 1640 medium + 10% fetal calf serum (FCS)) at 37°C in a humidified atmosphere of 5% CO_2/95% air. Cell suspensions were maintained between 2-8 × 10^5 cells/mL by dilution with fresh medium.

For differentiation experiments, U-937 cells (2 × 10^5 cells/mL) were grown for up to 96 hr in the continuous presence of either RA (1 × 10^{-9} M to 1 × 10^{-4} M), GTN (0.1 mM), TNM (50 µM) with or without L-cysteine (CYS) (0.3 mM), MOL (1 × 10^{-3} M), or CAS 936 and various combinations thereof. While the other agents could be added from concentrated stocks, CAS 936 had very limited solubility and cells had to be centrifuged at 600*g* for 7 min in a IEC Centra-7R refrigerated centrifuge (International Equipment Co.) and resuspended in fresh culture medium containing 15 µM of the drug. The final concentration of ethanol (where used) did not exceed 0.2% except for 1 × 10^{-4} M RA treatment where the concentration was 1.0%. As a positive control for the functional assays, human granulocytes (mostly PMNs) were isolated from fresh whole blood of healthy donors as described previously [6].

For the priming experiments, the cells were treated with 1 x 10^{-5} M RA for 24 hr, then the cells were resuspended in fresh medium after centrifugation at 600×g for 7 min in a IEC Centra-7R refrigerated centrifuge, and incubated for another 72 hr in the presence or absence of the other inducers at concentrations as indicated above.

Cell number was determined at 24 hr intervals using a Model ZM Coulter Counter (Coulter Electronics Ltd.). Cell viability was assessed by trypan blue and by ethidium bromide dye exclusion methods. For the trypan blue dye exclusion assay, at least 200 to 400 cells from each culture were scored microscopically. For the ethidium bromide procedure, cell suspensions (0.2 to 1.5 × 10^6 cells/mL) in PBS (phosphate buffered saline: 2.7 mM KCl, 1.5 mM KH_2PO_4, 137 mM NaCl, 4.3 mM Na_2HPO_4) containing 4 µg/mL ethidium bromide were gently agitated after 3-5 min incubation and fluorescence was measured in a Perkin-Elmer Model LS-5 spectrofluorometer at λ_{ex} = 520 nm and λ_{em} = 590 nm. Triton X-100 was then added at 0.05% (w/v) final to permeabilize all cells and a second fluorescence reading taken after 3-5 min. The percentage of non-viable cells was calculated as $F_o/F_t \times 100$ where F_o represents the initial fluorescence reading and F_t represents the reading after addition of Triton X-100.

NBT Reduction and Spectrophotometric Determination of Solubilized Formazan Deposits

Formazan-Staining Assay. At indicated intervals, U-937 cells (1 mL per well in 12-well polystyrene plates) in complete medium were stimulated with TPA (final concentration 2 × 10^{-7} M) in the presence of NBT (1.2 mM) for 1 hr in a CO_2 incubator. The percentage of cells stained with insoluble blue-black formazan deposits was

determined under a light microscope using a hemocytometer chamber to aid in scoring. At least 200 to 400 cells from each culture were scored.

Quantitative Spectrophotometric Assay of Total Formazan Produced. For most experiments, 900 µL of the same TPA/NBT treated cell suspensions were transferred to a microcentrifuge tube, centrifuged 13,000*g* for 1 min in a microcentrifuge, and washed once with 1 mL cold balanced salt solution (BSS: 137 mM NaCl, 5 mM KCl, 0.8 mM $MgSO_4$, 10 mM HEPES, pH 7.4) to remove unreacted NBT. For those experiments involving MOL, CAS and their corresponding RA treatments, and those described in Fig. 4, cells were microcentrifuged for 2 min and washed twice, a procedure which lowered the background further. Insoluble formazan deposits in the resulting pellet were solubilized in 1 mL of extraction solvent mixture containing 90% (v/v) dimethylsulfoxide (DMSO), 0.1% (w/v) SDS, 0.01 N NaOH with vigorous vortexing (heating at 60°C if required). After centrifugation at 13,000*g* for 1 min to remove cellular debris, the absorbance of the solubilized formazan was measured at 715 nm in a Perkin-Elmer Lambda 5 spectrophotometer against extraction solvent. Solubilized formazan was diluted in solvent mixture such that the absorbance was ≤1.5 O.D.. Data are expressed as $A_{715\,nm}$ per 10^6 cells. For comparison, human PMNs were tested using the same procedure. The molar extinction coefficient of the formazan precipitate formed by the reduction of NBT by $O_2^{\cdot-}$ generated using xanthine/xanthine oxidase was estimated as follows. 0.35 mM NBT was incubated at 37°C for 30 min with 36 µM xanthine, 71 µM EDTA, 36 mM sodium phosphate pH 7.8, 11.4 U/mL catalase, and 2 mU/mL xanthine oxidase in duplicate. After addition of more xanthine and xanthine oxidase, the reaction was further incubated at 37°C

for 30 min. The majority of the formazan precipitate was collected by centrifugation, and the residual fine precipitate was collected by filtration through a Hybond N membrane. Unreacted NBT was quantified by its absorbance at 261.6 nm. The combined precipitate was washed twice with BSS, solubilized with 90% (v/v) DMSO, 0.1% (w/v) SDS, 0.01 N NaOH and absorbance measured at 715 nm. The molar extinction coefficient of the formazan product based on the amount of NBT consumed was estimated to be approximately 18,000 $cm^{-1}Lmol^{-1}$ (absorbance per NBT concentration). To test for Cu,Zn-SOD inhibition of NBT reduction by xanthine/xanthine oxidase, similar experiments were performed in the presence or absence of 50 µg/mL SOD and 400 U/mL catalase.

Hexose Monophosphate Shunt (HMPS) Activity

HMPS activity was measured as described previously [3] with slight modifications. Ninety-six hours following treatment of U-937 cells with various inducers, 4.6×10^5 cells were transferred to 1.5 mL polypropylene microcentifuge tubes, washed by centrifugation at 600*g* (IEC Centra) in BSS, and resuspended in 300 µL of BSS containing 0.5 mM D-glucose and 0.646 µCi/mL D-[1-^{14}C]glucose (final specific activity, 1.266 µCi/µmol). HMPS activity was initiated by the addition of TPA to 2×10^{-7} M and immediately each tube was transferred to a plastic support contained within a 20 mL glass scintillation vial. A 2.5 cm diameter GF/A glass fibre filter wetted with 100 µL of 20% (w/v) KOH at the bottom of the vial, served as a CO_2 trap. Each vial was immediately sealed with a Teflon-coated silicone septum held in place with a screw-cap. Standard scintillation vial caps were modified with a small hole to allow access to the septum. The vials were

incubated at 37°C for 1 hr to allow release of [^{14}C]CO_2 from [1-^{14}C]glucose by the HMPS. Reactions were terminated and [^{14}C]CO_2 in solution was released by injecting 100 µL of 1 N HCl using a #23 needle and syringe. Vials were heated for 30 min at 80°C, then 30 min at 37°C to complete transfer of [^{14}C]CO_2 to the KOH trap. Vials were cooled at -20°C for 5 min, then opened to remove the tube of cells and the support. One mL of H_2O was added to each filter to dissolve [^{14}C]K_2CO_3 and then 10 mL of Aquasol 2 scintillation fluid was added. Each vial was mixed briskly and counted in a LKB Wallac 1219 Liquid Scintillation Counter. As a positive control, equivalent numbers of freshly isolated human PMNs were assayed for HMPS activity under similar conditions.

Northern Analysis

Isolation of cDNA Probe Fragments. Cultures for bacterial clones containing plasmid cDNA inserts for p47^{phox} (clone name p47phox-pK or clone K or p47, gene symbol NCF1), gp91^{phox} (clone name 379-10, gene symbol CYBB, also called the X-CGD gene), G6PD (clone name pGD-P-25A; gene symbol G6PD), and SOD (clone name cSOD, gene symbol SOD-1) were grown in the presence of 100 µg/mL ampicillin. A bacterial clone containing a cDNA insert for glyceraldehyde-3-phosphate dehydrogenase (clone name pGAPDH, gene symbol GADPH) was grown in the presence of 50 µg/mL tetracyclin. Plasmid DNA was isolated from these clones essentially as described in [64]. Purification of plasmid was accomplished by binding to and eluting from a glass powder suspension. The desired fragments were excised with the appropriate restriction enzyme (*EcoRI* for p47^{phox} and G6PD, *Bgl II* and *Hind III* for gp91^{phox}, *Pst I* for SOD-1 and

GAPDH [65]) and were isolated from 0.8 % agarose gels after electrophoresis in 1x TAC (40 mM Tris-HCl pH 7.8, 20 mM sodium acetate, 1 mM CDTA) using a glass powder method.

Isolation of Total RNA. Total RNA from 96 hr control and differentiated U-937 cells was extracted essentially as described in [66].

Electrophoresis and Transfer of Total RNA. Total RNA was denatured as described in [66]. 20 µg total RNA was loaded onto vertical 1.2% agarose gels containing 0.2 M formaldehyde, 2 mM CDTA, 20 mM sodium phosphate pH 6.8. Loading buffer was added to 5% (w/v) sucrose, 0.005% (w/v) bromophenol blue, and 0.2 mM CDTA. After electrophoresis in 20 mM sodium phosphate pH 6.8, 2 mM CDTA at 100 V, gels were stained with 5 µg/mL ethidium bromide for 20 min and destained for 20 min in distilled water for photography under a ultraviolet transilluminator. After soaking in 10x SSC (1.5 M NaCl, 0.15 M sodium citrate pH 6.1) for 20 min, the gel was transferred to a hydrated Hybond-N membrane using a vacuum blotting apparatus. Membranes were washed with 10x SSC for 20 min at room temperature, dried at 80°C for 20 min, and crosslinked with ultraviolet light for 3 min using a transilluminator.

Probe Labelling and Hybridization to Immobilized Total RNA. Probe fragments were labelled with [^{32}P]dCTP using an oligolabelling kit. Membranes were washed in 2x SSC containing 0.1% SDS, prehybridized with 6x SSC, 5x Denhardt's solution, 0.5% SDS, 50 mM sodium phosphate pH 6.8) containing 100 µg/mL boiled sonicated salmon sperm DNA for 1 hr at 65°C, and hybridized with 50 ng radiolabelled probe overnight at 65°C in hybridization buffer (50 µg/mL boiled sonicated salmon sperm DNA, 6x SSC, 5x

Denhardt's solution, 0.5% SDS, 5% dextran sulfate, 50 mM sodium phosphate pH 6.8). Membranes were washed twice in 2x SSC, 0.1% SDS at 65°C for 15 min, followed by two washes at 65°C in high stringency wash solution (0.16x SSC, 10 mM sodium citrate pH 6.8, 0.1% SDS) for 15 min each, and exposed to pre-flashed x-ray film. Where indicated, membranes were stripped by heating twice at 100°C in 0.25% SDS, 10 mM sodium citrate pH 6.8 for 5 min and reprobed with another probe.

Morphological Assessment

Cytospin slides of control and differentiated U-937 cells were prepared at each 24 hr time point until 96 hr. Cells were fixed with methanol for 10 min, stained with eosin and Wrights stain and examined using light microscopy.

Chemiluminescence Detection of NO· Release from Tetranitromethane

To assess whether TNM might be a NO· donor, a luminol-H_2O_2 chemiluminescence system for the detection of NO· release was employed as described in [67] with slight modifications. Briefly, a reaction mixture of 20 mM borate pH 9.4, 20 µM luminol and 150 µM desferal was freshly prepared. TNM was freshly prepared and added to the reaction mixture at concentrations ranging from 5 to 500 nM immediately before starting the reaction with 10 mM hydrogen peroxide. Integrated chemiluminescence readings were recorded every 10 seconds for 1 min using a LKB Luminometer at 25°C in a darkened room.

Fluorescamine Assay for Protein

U-937 and PMN cell extracts were prepared by resuspending 10×10^6 cells in 100 µL water and sonicating on ice using a 50-watt Microson automatic cell disruptor. Aliquots (1 to 5 µL) of the resulting cell lysates were analyzed for protein content using a fluorescamine assay for detection of amine groups as described in [68].

Statistical Analysis

Data were analyzed using one-way ANOVA followed by a post-hoc Tukey-Kramer test of significance difference between means using the computer statistical package Instat2 (GraphPad Software, Inc., 1993). A p value of ≤ 0.05 was considered to be significant.

RESULTS

Formazan Staining of Differentiating U-937 Cells

The generation of O_2^- by cells with a functional NADPH oxidase can be detected by the formation of insoluble formazan from NBT [69] in response to TPA stimulation. Undifferentiated U-937 cells do not have a functional NADPH oxidase but acquire one during the course of differentiation by RA [39-41]. The optimal concentration of RA was determined in the range 10^{-9} to 10^{-4} M over a 96 hr time course (Figure 2). RA at 10^{-5} M yielded the highest percentage of stained cells without cytotoxicity (>95% of cells excluded trypan blue after 96 hr of treatment with 10^{-9} to 10^{-5} M RA). Vehicle-treated cells (0.1%

Figure 2. ***Dose- and time-dependence of RA-induced differentiation of U-937 cells: formazan-staining.***

Control (untreated and vehicle treated) and RA-treated (10^{-9} to 10^{-4} M) U-937 cells were grown as described in *Materials and Methods*. At 24 hr intervals, cells were analyzed for their ability to reduce NBT to blue-black formazan deposits when stimulated with 200 nM TPA for 1 hr at 37°C. % Formazan-staining cells were scored microscopically. The results represent the mean ± range for 2 independent experiments (except 96 hr 10^{-7} M and 10^{-6} M RA which represent the mean ± SEM of 4 and 5 independent experiments, respectively).

Figure 2.

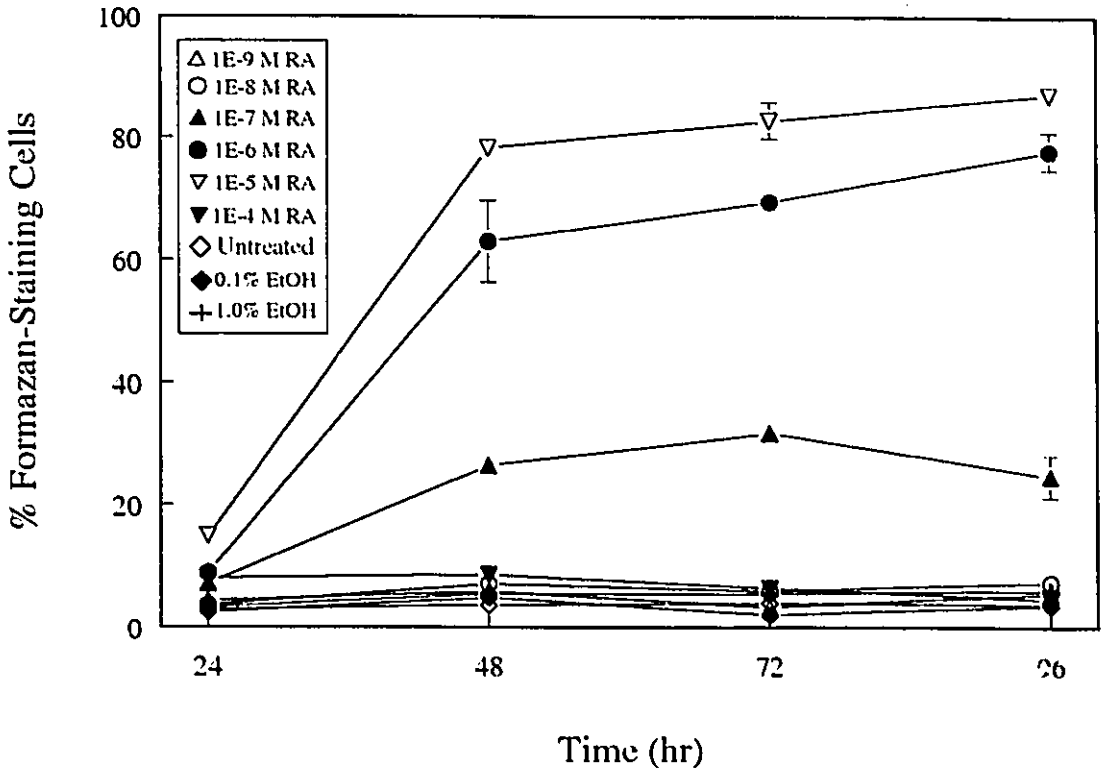
100
80
60
40
20
0
% Formazan-Staining Cells
1E-9 M RA
1E-8 M RA
1E-7 M RA
1E-6 M RA
1E-5 M RA
1E-4 M RA
Untreated
0.1% EtOH
1.0% EtOH
24
48
72
96
Time (hr)

ethanol) did not differ from untreated cells in terms of formazan staining (Figure 2) or cell viability (data not shown). Although 10^{-4} M RA treatment was found to be cytotoxic, treatment with the corresponding vehicle control (1.0% ethanol) was not (>95% viable cells).

The possibility that NO·-donating agents could potentiate the effect of RA as an inducer of U-937 cell differentiation was investigated. NO· itself is a radical species with a short half-life in oxygenated aqueous solutions but its stability and potency can be increased by complexing with transition metals and proteins to form nitrosyl complexes [70] or with thiols to form S-nitrosothiols [71-75]. Cysteine (CYS) was tested as a thiol to stabilize NO·. Combinations of CYS and GTN were cytotoxic for U-937 cells while CYS combined with TNM was not.

In the formazan staining assay, RA alone (10^{-5} M) induced significant maturation of U-937 cells compared to untreated cells (Figure 3). For RA-treated cells, an increase in percentage of stained cells was detected as early as 24 hr after initial treatment, reaching a maximum by 48-72 hr. Treatment with the other inducers in combination with RA yielded no or only small increases in the percentage of stained cells over RA alone. GTN on its own induced differentiation above control cells. Using this assay, essentially 100% of freshly isolated human PMNs stained positively for NBT reduction (data not shown).

Quantitative Measurements of Formazan Produced by Differentiating U-937 Cells

While counting formazan-staining cells microscopically scores both weakly and strongly staining cells, total formazan production can be quantitatively determined using a

Figure 3. ***Percentage of formazan-staining U-937 cells after treatments with various inducers of differentiation.***

Control (untreated) and treated U-937 cells were grown in the absence or presence of the inducing agent(s) as described in *Materials and Methods*. At 24 hr intervals, cultures were analyzed for their ability to form formazan in response to TPA, as in Figure 2. Treatment concentrations: 10^{-5} M RA, 0.1 mM GTN, 50 µM TNM, 0.3 mM CYS, 10^{-3} M MOL, 15 µM CAS. ***a.*** Shown are the mean ± SEM of 7 to 21 independent experiments. ***b.*** Mean ± SEM of 3 to 8 independent experiments. ***c.*** Mean ± SEM or range of 2 to 4 independent experiments (RA is repeated from ***a.*** for comparison). Statistically significant differences: control *vs* RA $p<0.05$ at 24 hr, $p<0.001$ for 48-96 hr; control *vs* GTN $p<0.05$ at 72 hr.

Figure 3.

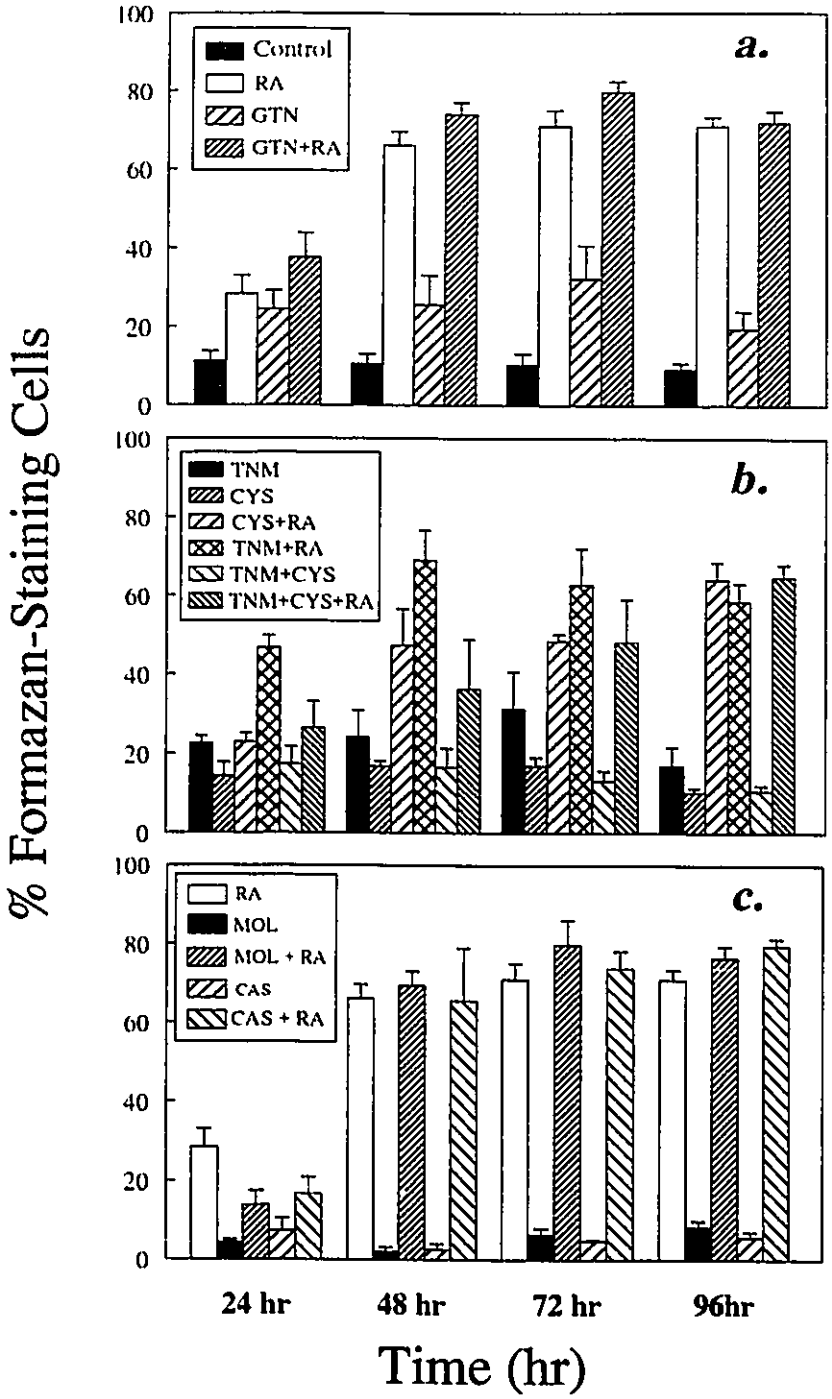
% Formazan-Staining Cells
100
80
60
40
20
0
Control
RA
GTN
GTN+RA
a.
TNM
CYS
CYS+RA
TNM+RA
TNM+CYS
TNM+CYS+RA
b.
RA
MOL
MOL + RA
CAS
CAS + RA
c.
24 hr
48 hr
72 hr
96hr
Time (hr)

spectrophotometric assay. To confirm the utility of the assay for measuring O_2^-, experiments were performed using human PMNs as well as control and RA-differentiated U-937 cells. O_2^- production by PMNs is known to be strongly stimulated by TPA. Despite this, it was observed that the reduction of NBT in PMNs was not significantly inhibited by SOD but was completely dependent upon the addition of TPA (Figure 4a); similar findings have been reported by others [69]. Even when xanthine/xanthine oxidase was used as a cell-free generator of O_2^-, NBT reduction was only inhibited on average 76% by SOD, while reduction of ferricytochrome c was completely inhibited (data not shown). Resistance to SOD inhibition may be due to the formation of an insoluble formazan precipitate which is inaccessible to SOD. Since the time course of formazan production by PMNs is: (i) similar to O_2^- production (as observed in ferricytochrome c reduction assays [4]); and (ii) is dependent on TPA, NBT reduction was used as a measure of O_2^- production. As shown in Figure 4b, NBT reduction by RA-induced U-937 cells was partially inhibited by SOD and entirely dependent upon TPA stimulation.

Figure 5 shows a time course of induction of O_2^--generating activity as determined by this procedure. As in Figure 3, the amount of formazan produced by RA-treated cells was significantly greater than by control cells as early as 24 hr, with further increases observed up to 96 hr. At 96 hr, treatment with GTN+RA resulted in a slight enhancement in formazan production (not statistically significant) compared to RA treatment alone (Figure 5a). Between 72 and 96 hr, CYS+RA and TNM+CYS+RA combinations exerted small but statistically significant increases over RA alone (Figure 5b). One million differentiated U-937 cells produced the same amount of formazan as $2.8\times10^6 \pm 0.7\times10^6$

Figure 4. ***Quantitative measurements of formazan produced by human PMNs and RA-differentiated U-937 cells. Effect of TPA and SOD.***

Cells were analyzed for formazan production in the presence or absence of 200 nM TPA (T) and/or 50 µg/mL SOD, 270 U/mL catalase (S). At the indicated times, cell-associated formazan deposits were solubilized and the absorbance at 715 nm was measured, as described in *Materials and Methods*. ***a.*** Freshly isolated human PMNs; mean ± SEM or range of 2 to 4 independent experiments. ***b.*** U-937 cells, untreated control (C) and treated for 96 hr with 10^{-5} M RA (RA); mean ± SEM of 4 to 5 independent experiments.

Figure 4.

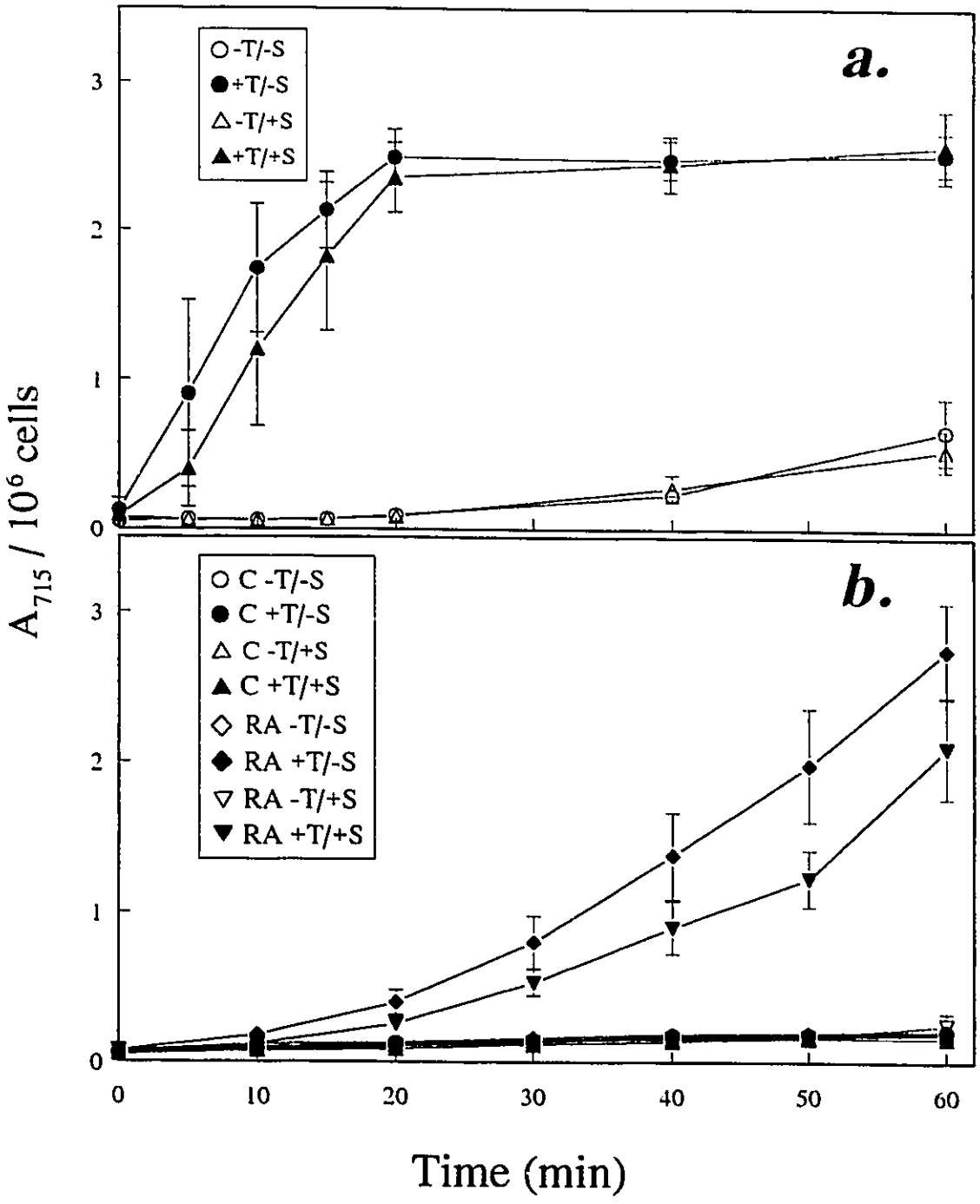
a.
-T/-S
+T/-S
-T/+S
+T/+S
b.
C -T/-S
C +T/-S
C -T/+S
C +T/+S
RA -T/-S
RA +T/-S
RA -T/+S
RA +T/+S
A_{715} / 10^6 cells
Time (min)
0
1
2
3
0
10
20
30
40
50
60

Figure 5. ***Quantitative measurements of formazan produced by differentiating U-937 cells after treatment with various combinations of inducers.***

U-937 cells were grown in the presence of various combinations of inducing agent as described in *Materials and Methods*. At 24 hr intervals, the cell number was determined and cultures were analyzed for their ability to produce formazan when stimulated with 200 nM TPA for 1 hr at 37°C. Results are expressed as $A_{715\,nm}$ per 10^6 cells. Treatment concentrations as in Figure 3. Statistically significant differences are shown in parentheses. ***a.*** Control and RA treated cells compared to GTN and GTN+RA treated cells (control *vs* RA $p<0.001$ for 24 hr). ***b.*** TNM and CYS treatments ± RA (control and RA-treated cells are replotted from ***a.*** for comparison); mean ± SEM of 3 to 7 independent experiments for both ***a.*** and ***b.*** (RA *vs* CYS+RA $p<0.05$ at 72 hr, $p<0.01$ at 96 hr. RA *vs* TNM+CYS+RA $p<0.01$ at 72 hr, $p<0.001$ at 96 hr). ***c.*** Control and RA treatments compared to MOL and CAS treatments ± RA; mean ± SEM of 4 to 5 independent experiments. In ***a.***, ***b.*** and ***c.***, $p<0.001$ for all (+) RA combinations at 48 to 96 hr relative to control.

Figure 5.

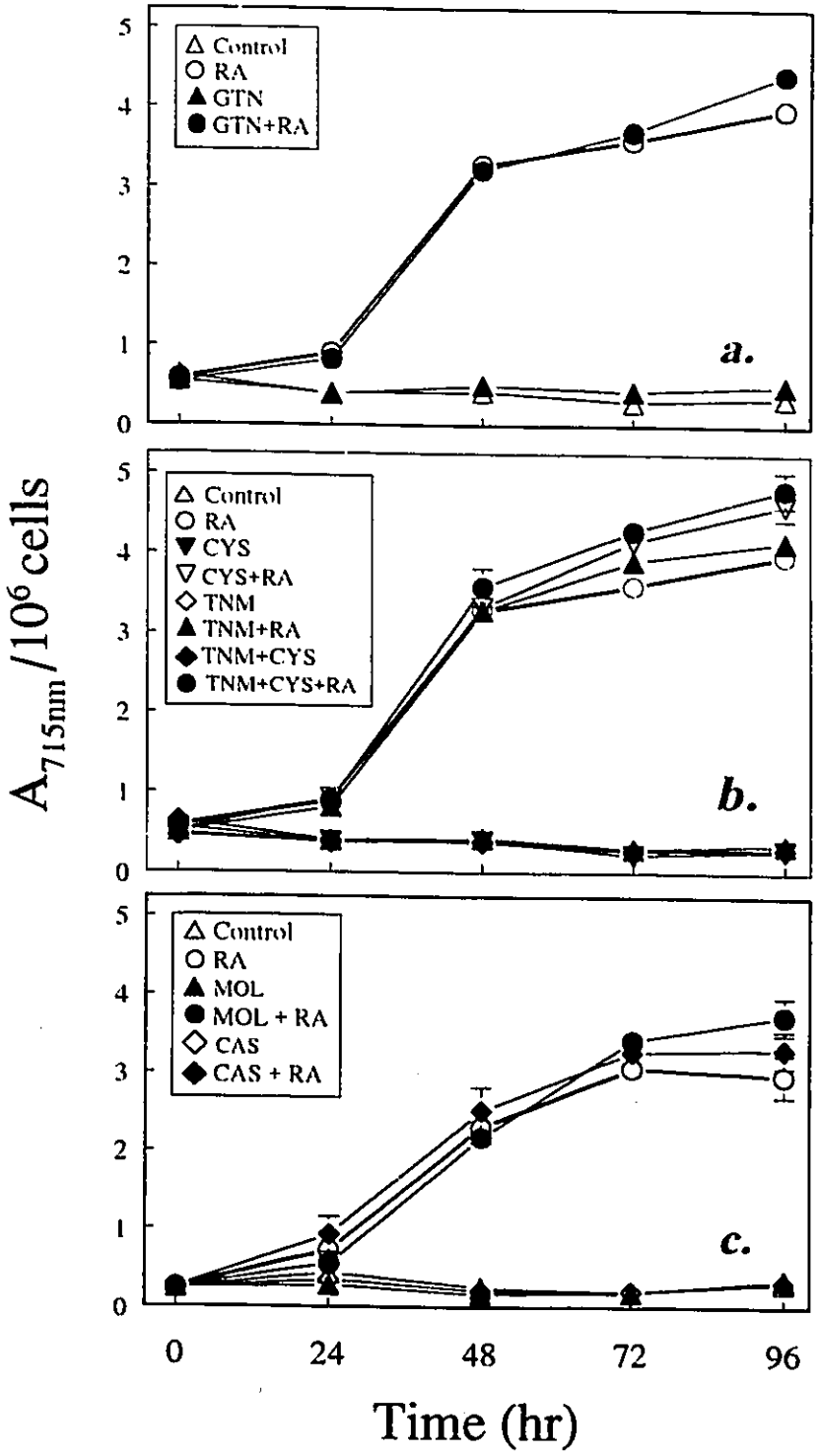
Control
RA
GTN
GTN+RA
a.
Control
RA
CYS
CYS+RA
TNM
TNM+RA
TNM+CYS
TNM+CYS+RA
b.
Control
RA
MOL
MOL + RA
CAS
CAS + RA
c.
$A_{715nm}/10^6$ cells
0
1
2
3
4
5
0
24
48
72
96
Time (hr)

freshly isolated human PMNs (mean ± range, n = 2), tested under the same conditions. MOL and CAS were slightly effective in enhancing the RA effect (not statistically significant) (Figure 5c).

Hexose Monophosphate Shunt Activity

The respiratory burst oxidase utilizes NADPH as an electron donor to reduce diatomic oxygen to $O_2^{\cdot-}$. NADPH is regenerated from $NADP^+$ by the HMPS pathway [22,34], the activity of which can be measured by quantification of $[^{14}C]CO_2$ generated from D-[1-^{14}C]glucose [35]. Therefore, as a further indicator of respiratory burst activity, TPA-initiated HMPS response was assayed at 96 hr after various treatments. All RA combinations shown in Figure 6 induced statistically significant enhancement of HMPS activity relative to control cells. Combinations of RA and GTN, CYS, TNM+CYS, or MOL were significantly more effective than RA alone. These agents exerted a much stronger potentiation of the RA effect on the HMPS (Figure 6) than on the NADPH oxidase (Figures 3 and 5). The highest observed HMPS activity of differentiated U-937 cells was >25% of the HMPS activity of human PMNs (2.44 ± 0.21 nmol $[^{14}C]CO_2/10^6$ cells/hr for MOL+RA-treated U-937 cells (Figure 6b) compared to 8.79 ± 0.40 nmol for PMNs (mean ± range for 2 independent experiments for PMNs)). GTN alone was able to induce TPA-stimulated HMPS activity (Figure 6a) while none of the other inducers alone were able to do so (not shown). The basal level (i.e., without TPA stimulation) of $[^{14}C]CO_2$ release by induced cells was not different from TPA-stimulated control cells (data not shown).

Figure 6. ***Hexose monophosphate shunt (HMPS) activity after 96 hr treatment of U-937 cells with various inducers.***

HMPS activity was determined after 96 hr treatment of U-937 cells with RA alone or in combination with GTN, TNM±CYS, MOL or CAS as described in *Materials and Methods*. Results are expressed as nmol $[^{14}C]CO_2$ released per 10^6 cells per hr incubation in response to 200 nM TPA. ***a.*** mean ± SEM of 3 to 6 independent experiments, each performed in duplicate or triplicate. ***b.*** mean ± SEM of 3 independent experiments performed in duplicate. Treatment concentrations as in Figure 3. Results after TNM and/or CYS, MOL or CAS treatments were no different from control and are not shown. The unstimulated level of $[^{14}C]CO_2$ release by induced cells was not different from TPA-stimulated uninduced cells (data not shown). * = $p<0.05$ compared to RA; ** = $p<0.01$ compared to RA; *** = $p<0.001$ compared to RA; (***) = $p<0.001$ compared to control. $p<0.001$ for all (+) RA combinations compared to control.

Figure 6.

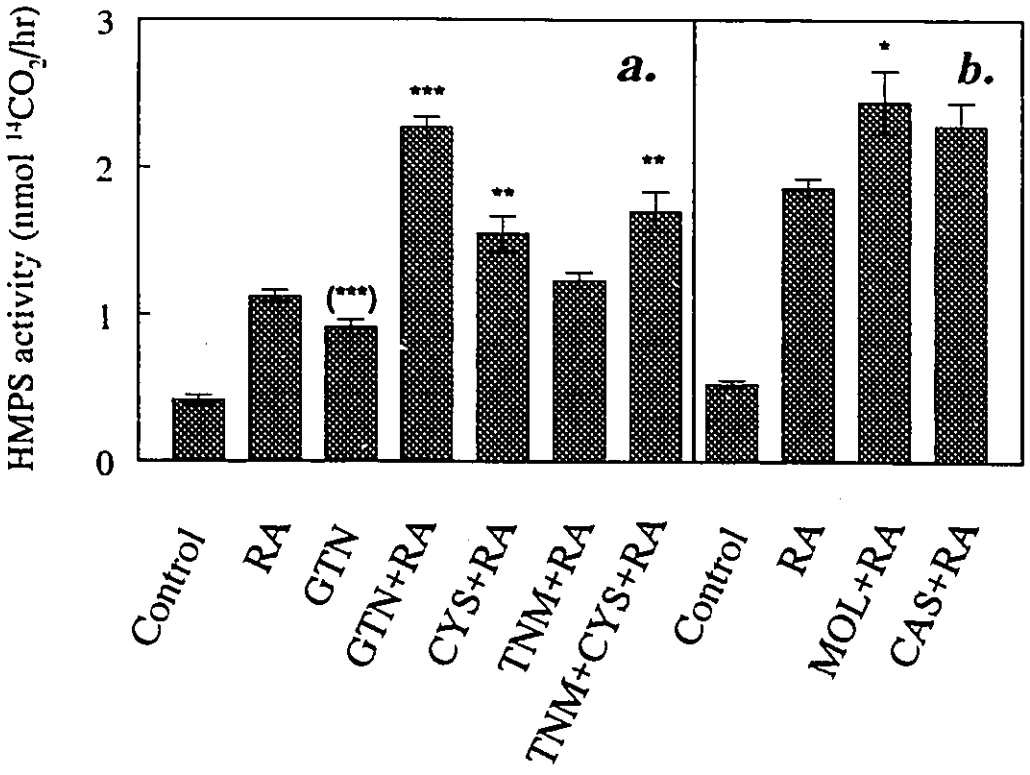
HMPS activity (nmol $^{14}CO_2$/hr)
3
2
1
0
a.
b.
***
**
(***)
**
*
Control
RA
GTN
GTN+RA
CYS+RA
TNM+RA
TNM+CYS+RA
Control
RA
MOL+RA
CAS+RA

Changes in Cell Proliferation

Reduction in the rate of cell growth is a characteristic of differentiation. Onset of growth suppression occurred between 24 and 48 hr after treatment of U-937 cells with RA (Figure 7), which coincided in time with the major increase in NADPH oxidase activity (Figures 3 and 5). GTN and, to a small extent, MOL, TNM and/or CYS also reduced cell proliferation. The combinations of GTN, MOL and TNM±CYS with RA showed greater growth suppression than RA alone. CAS treated cells grew slightly faster than control cells, likely because they were resuspended in fresh medium, a procedure not used for other treatments.

To address the possibility that cytotoxicity rather than differentiation was responsible for cessation of growth, viability studies were performed using two dye exclusion techniques. Similar results were seen using trypan blue and ethidium bromide dye exclusion techniques (data not shown). Viability was high (>92%) in all cases and for all time points up to 96 hr. Only in the case of GTN with or without RA was viability somewhat reduced (GTN alone was 88 and 79% and GTN with RA was 93 and 85%, respectively, at 72 and 96 hr).

Synergistic Effects of Low Doses of RA With Other Inducers of Differentiation

If the effects of various agents were synergistic with RA, such effects might be expected to be more apparent at lower doses of RA (10^{-7} M to 10^{-6} M). In terms of HMPS, GTN, TNM, CYS and TNM+CYS all appeared to be synergistic with RA (Figure 8a). GTN was effective, even in the absence of RA, whereas the other agents were not.

Figure 7. ***Growth suppression of U-937 cells after treatment with various inducers.***

Cell number was monitored with a Coulter counter at 24 hr intervals after initial treatment with the indicated inducers. Treatment concentrations as in Figure 3. Results represent the mean ± SEM, where n = 3 to 40 independent experiments for panel ***a.*** , 3 to 18 for panel ***b.***, and 4 to 11 for panel ***c.*** . Control (upper dotted line) and RA (lower dotted line) curves from ***a.*** are redrawn in ***b.*** and ***c.*** for reference. Statistically significant differences: control *vs* RA or GTN $p<0.001$ for 48 to 96 hr; RA *vs* GTN+RA $p<0.05$ for 48 hr, $p<0.001$ for 72 to 96 hr; RA *vs* MOL+RA $p<0.001$ at 96 hr; RA *vs* TNM+RA $p<0.05$ at 72 hr; RA *vs* TNM+CYS+RA $p<0.05$ at 72 to 96 hr.

Figure 7.

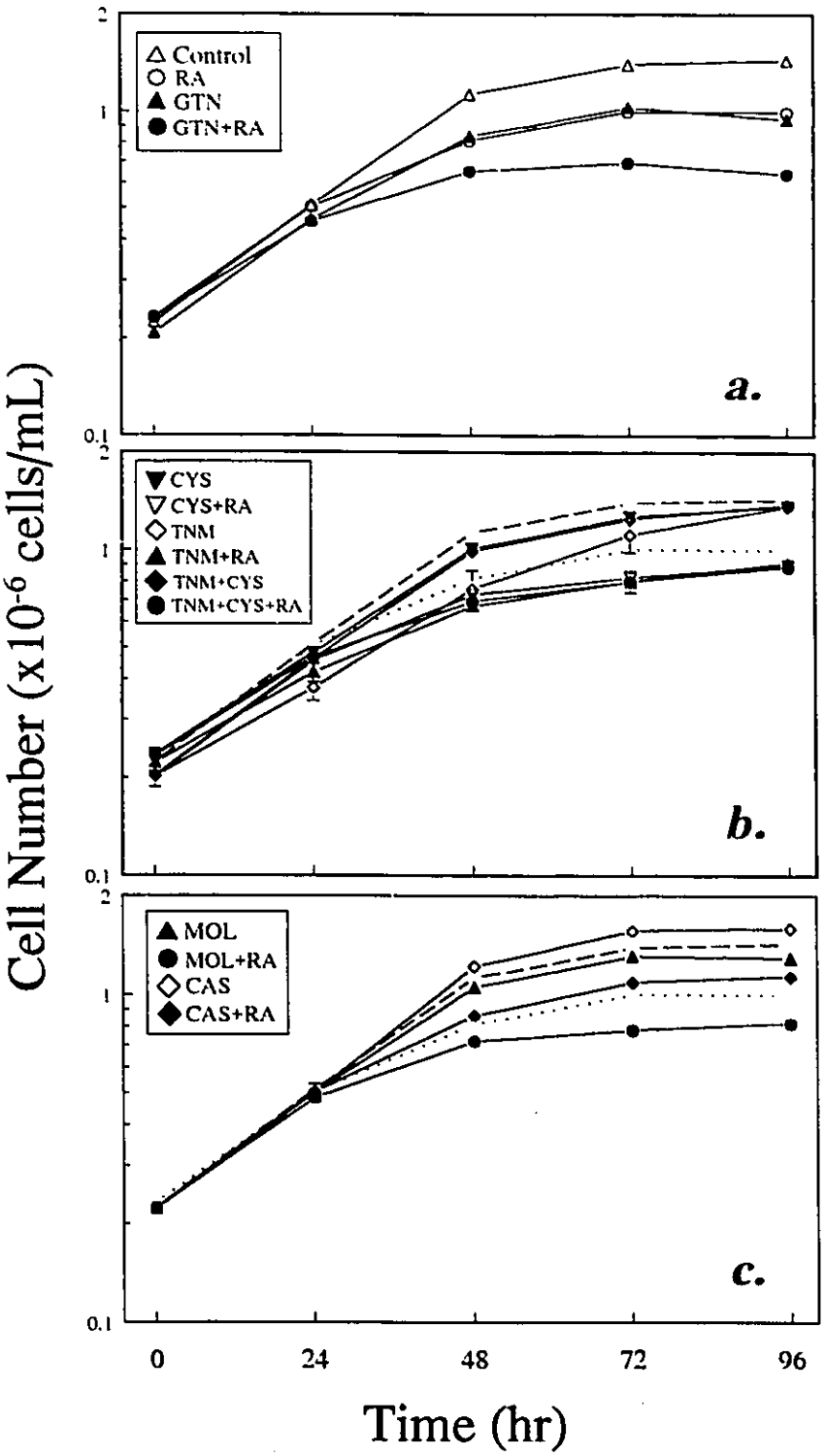
Control
RA
GTN
GTN+RA
a.
CYS
CYS+RA
TNM
TNM+RA
TNM+CYS
TNM+CYS+RA
b.
MOL
MOL+RA
CAS
CAS+RA
c.
Cell Number (x10-6 cells/mL)
2
1
0.1
0
24
48
72
96
Time (hr)

Figure 8. ***HMPS activity, formazan production, and growth suppression after 96 hr treatment with suboptimal doses of RA plus GTN, TNM and/or CYS.***

U-937 cells were grown in the presence of 0, 10^{-7} or 10^{-6} M RA, alone or in combination with GTN, TNM and/or CYS for 96 hr as described in *Materials and Methods*. Concentrations of GTN, TNM and CYS are as in Figure 3. RA concentrations are as shown. ***a.*** HMPS activity measured, as in Figure 6. For GTN with RA, the mean ± SEM of 3 independent experiments performed in duplicate or triplicate are shown; for GTN alone, 6 independent experiments were performed. For TNM and/or CYS with RA, the mean ± range of duplicates for 1 experiment are shown; for these agents alone, 3 independent experiments are shown. ***b.*** Percentage of formazan-staining cells, determined microscopically as in Figure 3; mean ± SEM (or range) of 2 to 5 independent experiments. The results for 0 RA are repeated from Figure 3. ***c.*** Quantitative measurements of formazan, measured as in Figure 5; mean ± SEM of 3 to 6 independent experiments. Results for 0 RA are repeated from Figure 5. ***d.*** Cell number, determined as in Figure 7; mean ± SEM of 4 to 7 independent experiments. Results for 0 RA are repeated from Figure 7.

Figure 8.

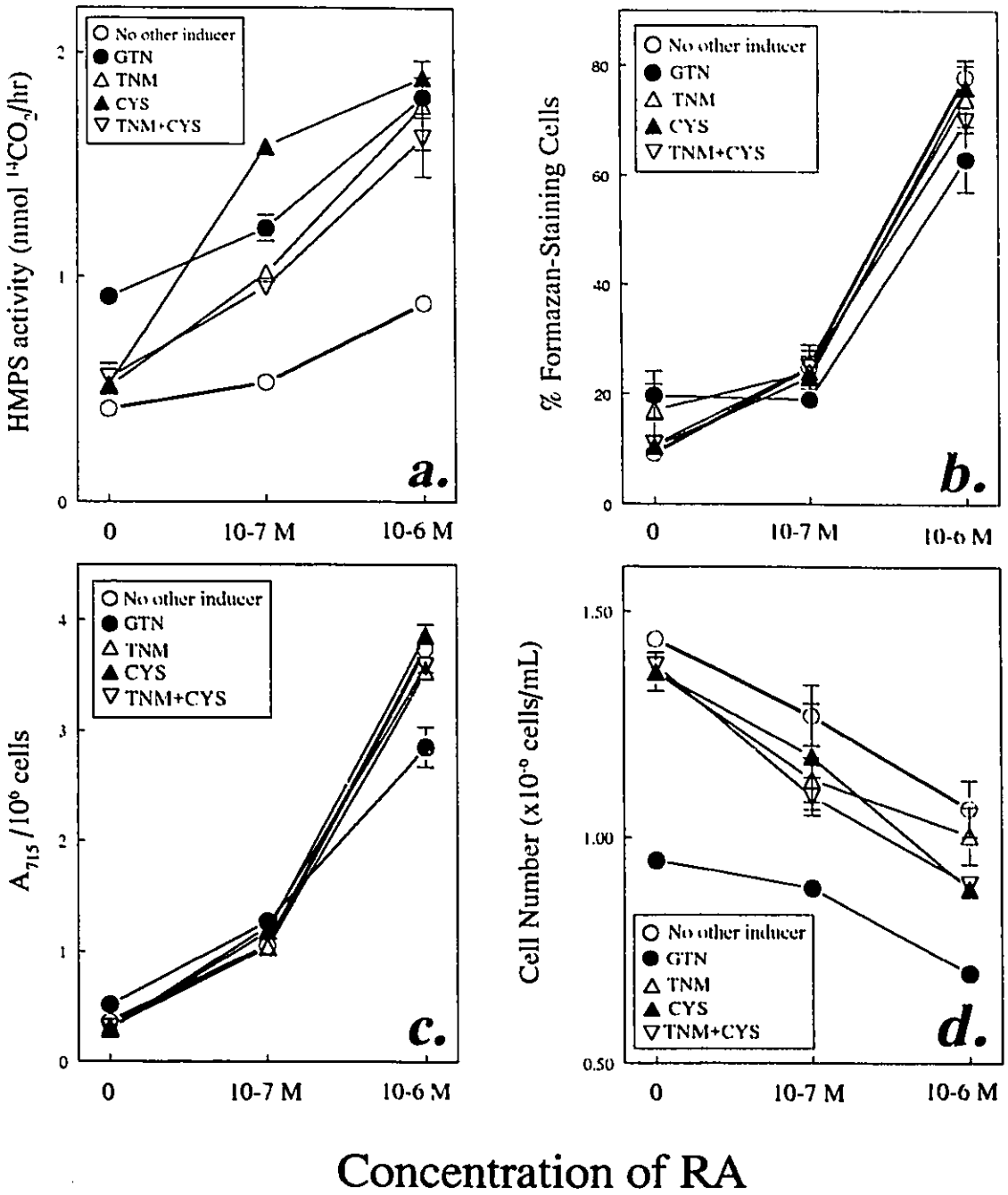
No other inducer
GTN
TNM
CYS
TNM+CYS
HMPS activity (nmol $^{14}CO_2$/hr)
a.
% Formazan-Staining Cells
b.
A_{715} /10^6 cells
c.
Cell Number (x10^{-6} cells/mL)
d.
0
10-7 M
10-6 M
Concentration of RA

In terms of the other markers of differentiation studied, none of the agents in combination with RA were appreciably different than RA alone (Figures 8b-d). Growth inhibition by GTN and RA appeared to be additive (Figure 8d).

Effects of 24 hr "Priming" of U-937 Cells With RA

In preliminary experiments, U-937 cells primed for 24 hr with RA and further incubated in its absence for 72 hr exhibited 60%, 44%, and 68% of the formazan-staining, formazan-absorbance, and HMPS activities, respectively, and 167% of the final cell number, of cells that had been continually exposed to RA for 96 hr. These data may suggest that much of the RA-inducing effect occurs in the first 24 hr. After RA priming, GTN and TNM were able to further decrease the final cell number. In the HMPS assay, while TNM and/or CYS addition did not result in any further increase after RA removal, GTN was able to enhance HMPS activity in the absence of RA. These data are consistent with other observations that GTN can act independently of RA (Figures 3, 6, 7, 8) and they suggest that GTN may act additionally along another pathway other than that of RA.

Induction of Expression of Respiratory Burst and HMPS-Related Genes

As another parameter of differentiation, the expression of two respiratory burst- and one HMPS-related genes was examined by Northern analysis. mRNA for two NADPH oxidase components, $p47^{phox}$ and $gp91^{phox}$, were induced by RA (shown in Figure 9, as well as seven other experiments for p47 and four other experiments for $gp91^{phox}$). (Note: This induction is more clearly seen in reference [76]). RA induction of these mRNAs was

Figure 9. *Changes in mRNA levels associated with differentiation of U-937 cells.*

U-937 cells were treated for 96 hr with the indicated agents (treatment concentrations as in Figure 3). mRNA was extracted from control and differentiated U-937 cells, immobilized, and probed with cDNAs for $p47^{phox}$, $gp91^{phox}$, G6PD, SOD and GAPDH as described in *Materials and Methods*. Representative Northern blots are shown here. In each panel or grouping within each panel, the same membrane has been stripped in between probings as described in *Materials and Methods*. mRNA levels for the different components are shown for control and RA-treated cells and combinations with ***a.*** GTN, ***b.*** TNM±CYS and ***c.*** MOL. GAPDH was used as a indicator of the amount of immobilized mRNA. Arrows (►) in panels *b.* and *c.* indicate the positions of the 28S and 18S rRNA. Also shown ("EtBr") are the ethidium bromide-stained RNA gels prior to transfer. Not all probes were used on membrane *b.* or *c.*; nevertheless, results from other membranes using the other probes do not show further enhancement of RA by TNM±CYS or MOL and so they are not included here.

Figure 9a.

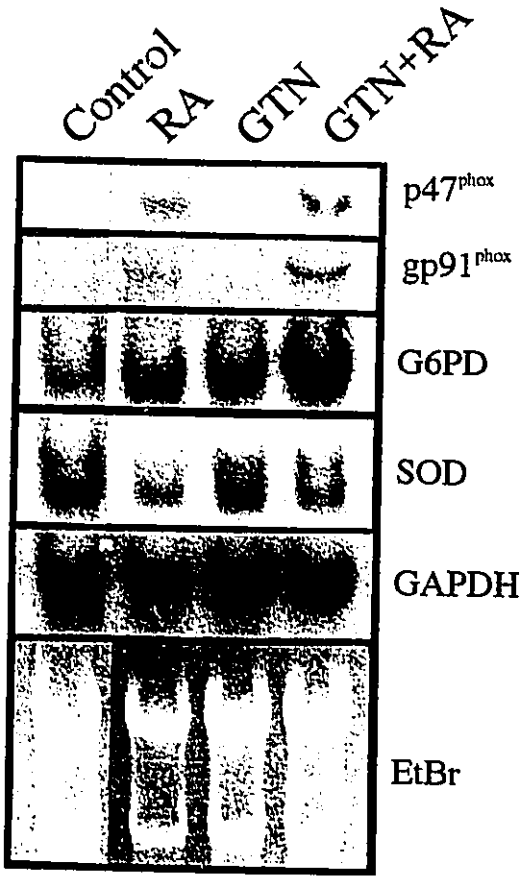

Figure 9b.

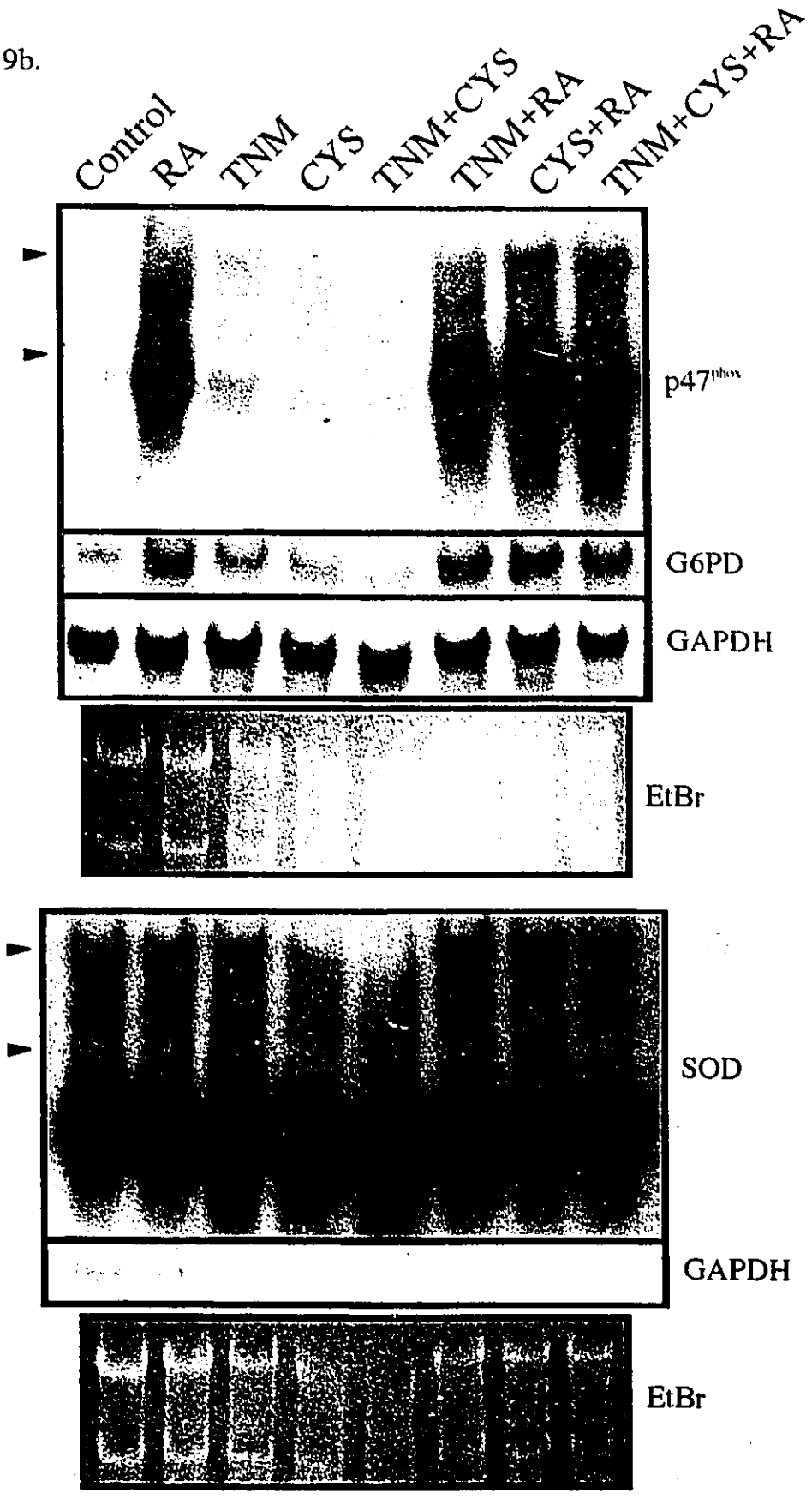
Control
RA
TNM
CYS
TNM+CYS
TNM+RA
CYS+RA
TNM+CYS+RA
p47phox
G6PD
GAPDH
EtBr
SOD
GAPDH
EtBr

Figure 9c.

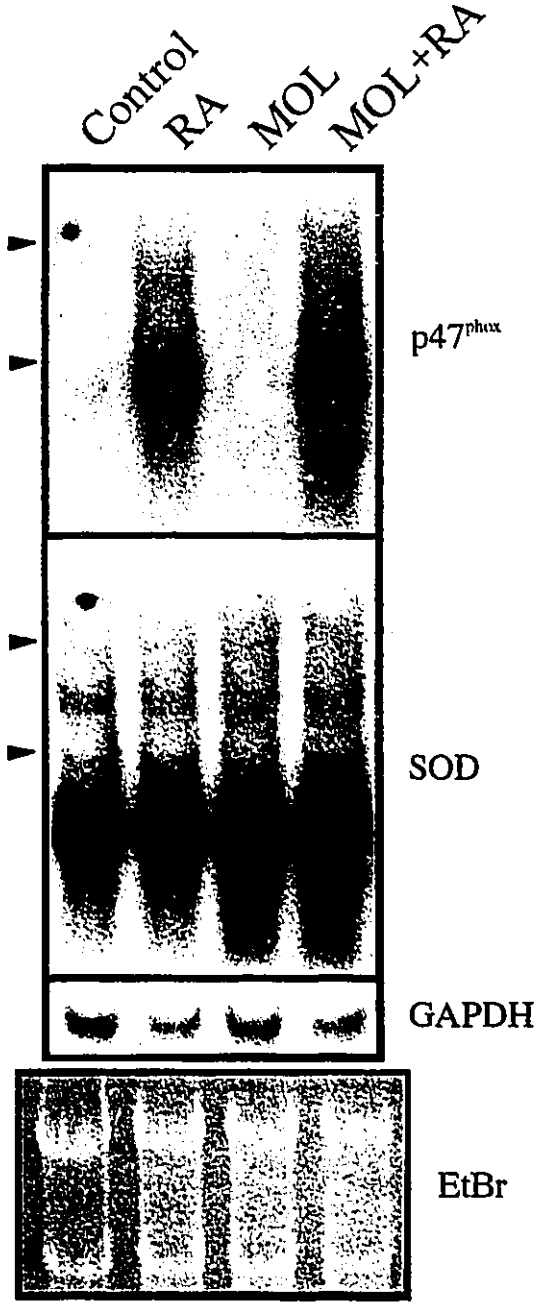

further enhanced by GTN (shown in Figure 9a, as well as one other experiment for p47 and four other experiments for $gp91^{phox}$). Expression of G6PD, the first and rate-limiting enzyme in the HMPS pathway, was enhanced by RA compared to control (Figure 9, as well as three other experiments), even more so when combined with GTN (Figure 9a, as well as four other experiments). Interestingly, GTN alone was able to slightly enhance G6PD expression relative to the control (Figure 9a, as well as three other experiments). There was no further enhancement of RA effects by the other inducers when combined with RA (Figure 9b and c). SOD mRNA levels were slightly reduced by RA (Figure 9a, as well as four other experiments but not so for the two shown in Figures 9b and c).

Morphological Changes During U-937 Differentiation

Immature U-937 cells resemble monoblastic cells [37]. During their differentiation, U-937 cell size has been reported to increase, their nuclei become more irregular and lobated, the cytoplasm becomes more vacuolated, and the cells demonstrate increased adherence (although this latter property can be the result of hydrophobic agents that alter membrane hydrophobicity and does not necessarily indicate differentiation [37]). In this study, control U-937 cells allowed to reach saturation density became slightly more adherent to tissue culture dishes and to neighbouring cells. Upon treatment with RA and its combinations, the cells became even more adherent and actually smaller in size than control cells. Cytospin slides were prepared for control and differentiated U-937 cells every 24 hr up to 96 hr. Cells cultured for 96 hr with RA displayed morphological changes associated with monocytic differentiation (Figure 10). RA-treated cells and their

Figure 10. ***Morphological changes during U-937 cell differentiation.***

Stained cytospin slides were prepared from U-937 cells treated for the indicated times with the following inducers (treatment concentrations as in Figure 3):

From top to bottom:	*Left-hand side*	*Right-hand side*
	Control, 24 hr	Control, 96 hr
	RA, 24 hr	RA, 96 hr
	GTN, 96 hr	GTN+RA, 96 hr
	TNM, 96 hr	TNM+CYS+RA, 96 hr
	MOL+RA, 96 hr	CAS+RA, 96 hr

Figure 10.

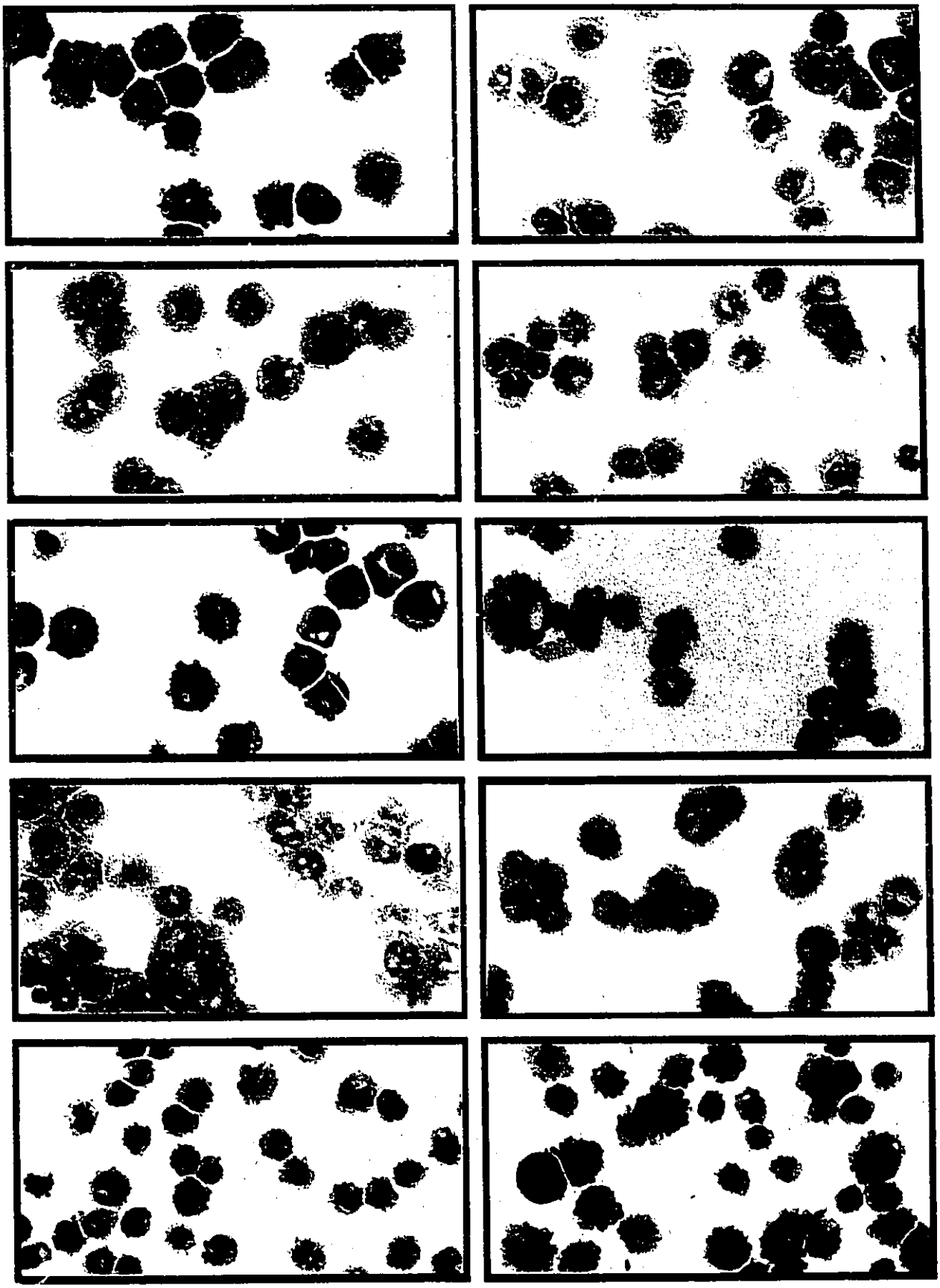

nuclei became smaller in size as the relative amount of cytoplasm generally decreased with time. While control cell nuclei were more regular, round or oval in shape, and more centrally located, RA-treated cell nuclei became irregular, with the majority horseshoe-shaped or segmented. Nucleoli became less prominent and fewer in number in a shorter time in RA-treated cells. The appearance of the cytoplasm went from fairly smooth to uneven with numerous small vacuoles. In all cultures, the proportion of mitotic cells also decreased with time as expected. Treatment with the potential NO·-donors along with RA resulted in a more heterogeneous mixture of cells in terms of size and nuclear morphology, with the occasional presence of megakaryocyte-like cells. Treatment with GTN, CYS, MOL or CAS alone more or less resulted in cells of similar morphology to control cells (unlike TNM alone which produced cells with large, extensively vacuolated cytoplasm and frequently the megakaryocyte-like appearance).

NO· Detection

To determine whether TNM possesses any NO· -like character, a luminol-H_2O_2 chemiluminescence system in which NO· is believed to react with H_2O_2 to form peroxynitrite ($ONOO^-$) which in turn reacts with luminol to generate light [67,77,78], was used. TNM gave a strong chemiluminescence signal in this system (data not shown). In the absence of H_2O_2, TNM alone gave a moderate signal suggesting that it may generate peroxynitrite.

DISCUSSION

In this part of my thesis, conditions that promote maximal differentiation of U-937 cells with respect to the respiratory burst NADPH oxidase were explored. The acquisition of a functional oxidase is commonly detected by stimulating cells with TPA and staining with NBT. Activation of a functional oxidase generates O_2^- which reduces NBT to insoluble formazan. A procedure in which the total formazan precipitate is solubilized and quantified spectrophotometrically was developed to provide a more quantitative measure of O_2^- production. RA was found to be a potent inducer of differentiation of U-937 cells with respect to the respiratory burst. The optimal concentration of RA used here (10^{-5} M; Figure 2) exceeds that used by others to differentiate U-937 cells or HL-60 cells (10^{-7} M to 10^{-6} M) [39,40,48]. In those reports, however, 10^{-5} M RA was not tested although the percentage of formazan-staining cells continued to rise with increasing RA concentration. Whether other agents could enhance differentiation induced by RA was also explored. Potential activators of guanylate cyclase were investigated since NO· donors and cGMP analogs have been shown to induce differentiation of HL-60 cells [53,59]. GTN alone was able to induce an elevated percentage of formazan-staining cells compared to control cells while TNM±CYS, MOL and CAS were not (Figure 3). In combination with RA, GTN, MOL and CAS each produced only small increases above RA alone. Similarly, only small increases in formazan production measured spectrophotometrically were seen for GTN, CYS, TNM+CYS, MOL and CAS in combination with RA compared to RA alone (Figure 5). Potentiation by these agents was not more evident at suboptimal concentrations of RA

(Figure 8b and 8c), thus, RA was clearly the major inducer of NADPH oxidase. Differentiated U-937 cells, under optimal conditions (Figure 5), can generate at least 2.8 times as much O_2^- per cell as PMNs. This may be due to the fact that U-937 cells are larger in size and contain 5 times more protein than PMNs (data not shown).

HMPS activity was assessed as another marker of differentiation since NADPH, the product of this biochemical pathway is needed for respiratory burst activity. In contrast to the relatively weak effect on the induction of NADPH oxidase, the induction of HMPS by RA was very strongly potentiated by the other agents tested (Figure 6), even at lower doses of RA (Figure 8a). GTN was able to induce HMPS, even in the absence of RA. None of the other NO--donating drugs tested could induce HMPS in the absence of RA. GTN, like MOL and CAS, is a NO--donating drug but it differs from the others in that it can induce HMPS activity on its own. This suggests that some action of GTN, other than its NO--donating ability, may be involved in the induction of HMPS activity. On the other hand, MOL and TNM and/or CYS were similar to GTN in their ability to suppress cell growth in the absence of RA (Figure 7).

Induction of NADPH oxidase and HMPS were also examined at the mRNA level (Figure 9). An increase in $p47^{phox}$ and $gp91^{phox}$ mRNA levels was observed with RA treatment. The observed increase in NADPH oxidase activity (Figures 2-5) may, in part, be attributable to the increased expression of these components. Either RA or GTN alone were able to increase G6PD expression, and their combination resulted in a further increase. These data are consistent with the observation that GTN in the absence of RA induced HMPS activity (Figure 6). Induction of NADPH oxidase mRNAs [79,80] and/or

proteins [81] by RA has been reported for HL-60 cells, which undergo granulocytic differentiation with RA, but not yet for U-937 cells, which undergo monocytic differentiation with RA. Increases in $p47^{phox}$ and $gp91^{phox}$ mRNA levels have been observed with TPA-induced monocytic differentiation of U-937 cells [79]. During tumor necrosis factor and/or interferon-γ- induced monocytic differentiation, increased $gp91^{phox}$ mRNA levels were observed for U-937 cells [82]. Co-induction of the NADPH oxidase with the HMPS in terms of mRNA levels with any agent has not yet been demonstrated until now. Levels of SOD mRNA decreased slightly with RA, less so than reported for TPA-differentiated U-937 cells [83] or THP-1 cells [84] into monocytic cells.

The morphological changes seen during U-937 cell differentiation were largely consistent with monocytic differentiation (Figure 10). Monocytic differentiation is characterized by decreased cell and nuclear size, ground glass-like basophilic cytoplasm (stains blue) with prominent vacuolization, indented, kidney-shaped or lobulated nuclei with convoluted chromatin, increased adherence, decreased number of nucleoli, and villous plasma membranes with blunt pseudopods [85]. Neutrophils, although exhibiting decreased cell and nuclear size as well as lobulated nuclei, differ in that they have a fairly acidophilic cytoplasm (stains pale pink), lack blunt pseudopods and have more prominently staining granules [85].

In summary, RA is largely responsible for the induction of the respiratory burst in terms of the NADPH oxidase and the HMPS, as well as in the reduction of cell proliferation and morphological differentiation. GTN alone displays some differentiation-inducing ability as indicated by an increase in percentage of formazan-stained cells,

increased HMPS activity, reduced cell proliferation, and induction of G6PD mRNA. When combined with RA, GTN potentiates RA-induced differentiation in all endpoints studied. The effects of GTN, MOL, CAS, and TNM±CYS appear to be largely limited by the presence and dose of RA, suggesting that either the target of GTN, TNM or CYS lies downstream of the RA target or that the stability or half-life of the RA molecule itself is increased by the other agents. Others have reported that RA may be required to prime U-937 cells for differentiation [39]. In HL-60 cells, RA-induced expression of $p67^{phox}$ was more slowly upregulated than $pp47^{phox}$ [81]. Keeping in mind that a fully active respiratory burst requires a multitude of components (reviewed in [10]) and convergence of a number of signalling pathways (reviewed in [18]), RA-induced U-937 cells might be limited in a component or pathway that the other agents might aid in overcoming. Due to the complexity of the pathways leading to acquisition of full respiratory burst activity, however, it is difficult to delineate the precise mechanisms by which GTN, MOL, CAS, and TNM±CYS are able to potentiate the action of RA in U-937 cells.

While the mechanism of GTN, MOL and CAS action may be more understood (i.e., NO·-mediated activation of cGMP pathways and other effects as reviewed in [56,86,87]), the mode of action of TNM, not previously been shown to be a NO· donor, is unclear. In this study, using a luminol-H_2O_2 chemiluminescence method for NO· detection, TNM yielded a positive signal suggesting that it may donate NO·. In addition to being a potential NO· donor, TNM may also spare endogenously produced NO· from attack by O_2^- since TNM is known to react very rapidly with O_2^- [88]. TNM is also a known nitrating agent that converts tyrosine residues to 3-nitrotyrosines [89] as does peroxynitrite

[89,90], which might also be produced by TNM. Modification of tyrosine residues in proteins by TNM could possibly inhibit signalling pathways that require tyrosine phosphorylation thereby promoting differentiation. It has been shown that inhibitors of protein tyrosine kinase activity such as genistein can induce myelomonocytic differentiation [91-93]. Lastly, TNM might be converted to other reactive oxygen species. TNM, at concentrations ≥10 μM, induces a substantial number of DNA breaks in human PMNs (unpublished observations by others in our laboratory).

SUMMARY FOR PART A

U-937 cells can be induced to differentiate into $O_2^{\cdot-}$-producing cells by RA, an effect enhanced when combined with GTN, MOL, CAS and TNM±CYS. In the absence of RA, only GTN is able to increase NADPH oxidase/HMPS activities and G6PD mRNA levels, as well as reduce cell proliferation. These data suggest that a NO·/cGMP pathway can augment RA-mediated induction of U-937 differentiation. GTN may act additionally by another pathway independent of RA. Since U-937 cells are growing prior to induction of differentiation with the conditions described above, they are amenable to genetic manipulations which are not possible in mature monocytes or granulocytes.

PART B

DEVELOPMENT OF HEPARANASE ACTIVITY ASSAYS FOR MONITORING U-937 DIFFERENTIATION AND CLONING AND CHARACTERIZING HEPARANASES

PART B: Development of Heparanase Activity Assays for Monitoring U-937 Differentiation and Cloning and Characterizing Heparanases

INTRODUCTION

Objective

Heparanase is an enzyme that specifically cleaves the glycosaminoglycan heparan sulfate (HS). My objective in this part of the thesis was to improve existing and develop new heparanase activity assays: 1) to assess whether heparanase would be useful as another U-937 differentiation marker (mature leukocytes have been shown to exhibit heparanase activity [94]); 2) to aid in cloning a cDNA for heparanase on the basis of enzymatic activity; and 3) to characterize heparanases. Since very little was known about the primary structure of heparanase, a more sensitive and easy-to-perform heparanase assay was required for use in cloning than was currently available.

Background

The extracellular matrix (ECM) is composed mainly of fibrous proteins (such as collagen, elastin, fibronectin, and laminin) and polysaccharide glycosaminoglycans (GAGs) (such as hyaluronic acid, chondroitin sulfate, dermatan sulfate, keratan sulfate and heparan sulfate). Heparan sulfate (HS) is a major GAG in basal laminae which are ECM structures that separate epithelial cell layers from underlying stroma [95,96]. Metastatic tumour cells can degrade the local ECM to gain access to the bloodstream or lymphatics and invade the endothelial wall and ECM at some distal site to establish a metastasis (Figure 11). The invasion process is believed to involve the action of both matrix proteases and

Figure 11. ***Diagrammatic representation of the tumour cell environment and metastasis.***

A cell becomes modified in a tissue, as shown in ***a.***, such that it proliferates to form a mass of localized tumour cells (or benign tumour) as shown in ***b.***. Further modifications may allow tumour cells to become invasive, permeabilizing the basal lamina and underlying stroma, as shown in ***c.***, to gain access to the bloodstream (or lymphatics) and travel to distant sites to form secondary tumours.

(adapted from reference [95], p. 957)

Figure 11.

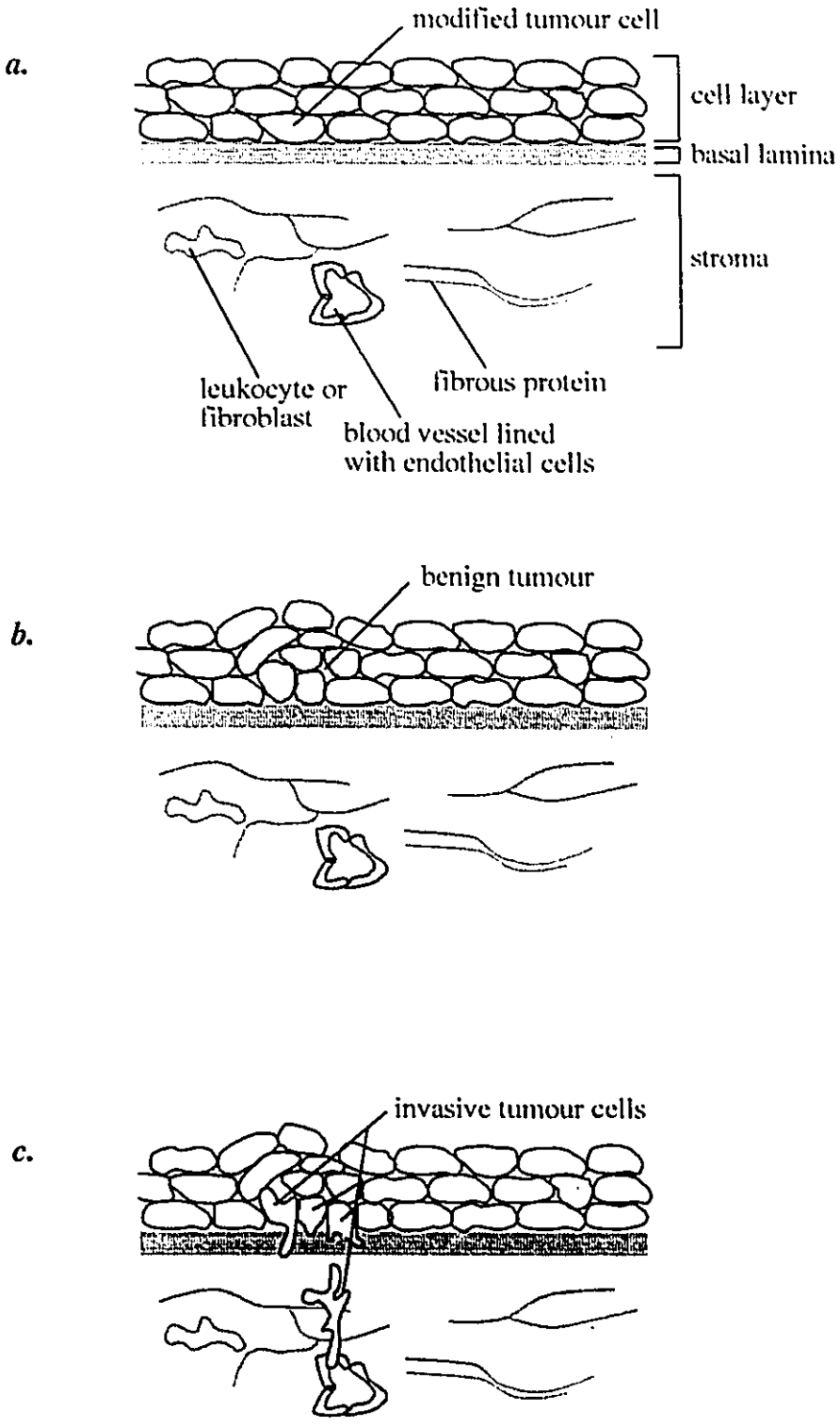
a.
modified tumour cell
cell layer
basal lamina
stroma
leukocyte or fibroblast
fibrous protein
blood vessel lined with endothelial cells
b.
benign tumour
c.
invasive tumour cells

GAG-degrading enzymes such as heparanase. While many of the matrix proteases have been cloned (including various collagenases, cathepsins, stromelysin, urokinase plasminogen activator, plasmin and elastase [96]), none of the GAG-degrading enzymes had been cloned (until very recently).

HS is a linear polysaccharide consisting of repeating disaccharide units [97]. The basic disaccharide unit consists of an amino sugar (*N*-acetylglucosamine) and an uronic acid (either D-glucuronic acid or its epimer at carbon 5, L-iduronic acid), thereby giving rise to the term glycosaminoglycan (Figure 12a). Variations in the HS molecule exist in the extent and position of substitutions (namely *N*-acetylation, *N*-sulfation, and *O*-sulfation) not only within the disaccharide unit but throughout the HS molecule as well, since segregation of specific sequences may occur [97]. There are at least ten different monosaccharides [97] and 16 types of linkages possible and it is estimated that 10^{36} types of mammalian HS are theoretically possible [98]. In addition to the heterogeneity in type of and distribution of negative charge (created by sulfate and carboxyl groups on the three basic monosaccharides), the number of residues in the chain may vary considerably even from a single source. Isolated HS preparations represent mixtures of molecules at different stages of biosynthesis, from different cells and different proteoglycans (see below). It is not even clear if the primary sequence of HS is completely defined and characteristic of a particular cell or proteoglycan to which it is attached [97]. Such diversity in composition, charge and size might dictate susceptibility to recognition and degradation by different isoforms of heparanases. This complex heterogeneity also renders HS and other GAGs rather difficult to study.

Figure 12. ***Heparan sulfate glycosaminoglycans and proteoglycans.***

a. Basic disaccharide unit structure of heparan sulfate glycosaminoglycans.

The basic disaccharide unit consists of *N*-acetylglucosamine and either D-glucuronic acid or its epimer at carbon 5, L-iduronic acid. Glycosidic linkages between adjacent *N*-acetylglucosamine and uronic acid residues are α(1->4) and those between the uronic acid and *N*-acetylglucosamine residues are either β(1->4) or α(1->4) if the uronic acid is D-glucuronic acid or L-iduronic acid respectively. On average, 50% of the glucosamine residues are *N*-sulfated and 50% are *N*-acetylated. *O*-sulfation occurs on *N*-sulfoglucosamine residues and/or on the uronic acid residues adjacent to *N*-sulfoglucosamine residues. As noted in the figure (middle panel), on average, there are 25 to 75 disaccharide units in each HS chain, with 0.2 to 2.0 sulfates per disaccharide unit, giving M_r ranging from 10,000 to 30,000.

b. Trisaccharide linkage to serine residues on protein core of proteoglycans.

HS chains are attached to core proteins to form proteoglycans. A D-glucuronic acid from the GAG chain is attached to a galactose-galactose-xylose trisaccharide linker region which is *O*-linked to specific serine residues of the core protein. In more detail, the linker region is as follows: -(1->4)-β-D-glucuronic acid-(1->3)-β-D-galactose-(1->3)-β-D-galactose-(1->4)-β-D-xylose-(1->3)-L-serine. While there are generally more HS chains in ECM HSPGs than membrane HSPGs, the number of HS chains on HSPGs is typically 3 to 8 but can reach up to 40. It is possible that HS chains are clustered at specific regions in the protein core containing serine-glycine repeats.

(Reference: [97])

Figure 12.

a.

STRUCTURE OF HEPARAN SULFATE

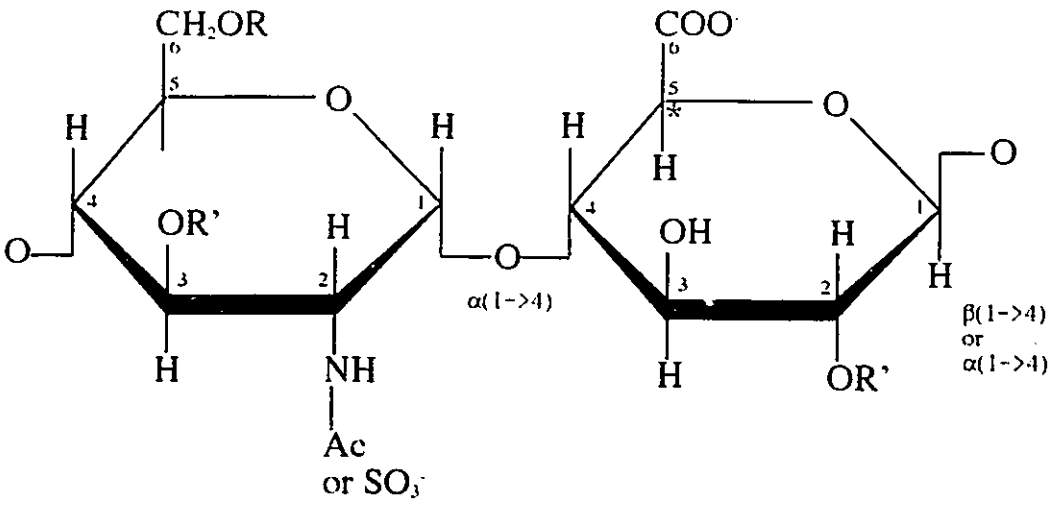

Glucosamine

D-Glucuronic acid

NOTE: (*) Epimer at C5 is L-Iduronic acid if the first residue is *N*-sulfated
(R=H or SO_3^-)
(R'=H or SO_3^-)(latter can occur if the adjacent residue is *N*-sulfated)
(Ac=acetyl; $COCH_3$)

- Long unbranched chain of repeating disaccharide units (25 to 75)
- *M*, 10,000 to 30,000 on average; can be up to 60,000 or 70,000
- 0.2 to 2.0 sulfates per disaccharide unit on average
- Covalently *O*- linked to core proteins on SER via trisaccharide linker (Gal-Gal-Xyl) to form heparan sulfate proteoglycans, HSPG (see ***b.***)
- Distribution: cell surfaces, extracellular matrix
- Heparanase = endo-β-D-glucuronidase (cleaves β-D-glucuronosyl-N-acetylglucosaminyl linkages; thus, only a few hits per molecule)

b.

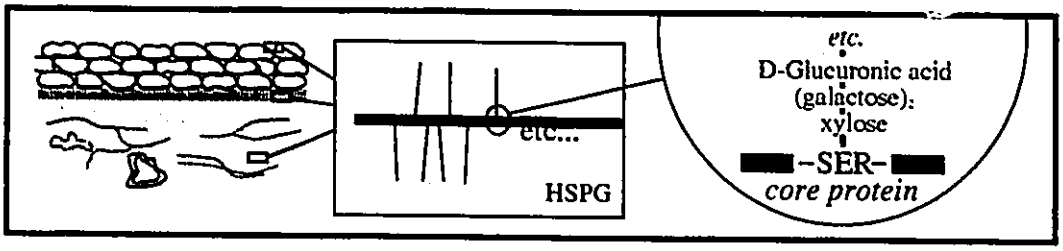

HS exists primarily in the ECM and at cell surfaces covalently linked to a core protein in the form of a proteoglycan (HSPG, heparan sulfate proteoglycan), connected via a galactose-galactose-xylose trisaccharide linker region which is *O*-linked to serine (Figure 12b) [99]. In the ECM, particularly in basement membranes, HS chains on HSPGs (such as perlecan [100]) repulse one another and extend outward to form a highly hydrated gel-like matrix that, depending on the magnitude of negative charge or hydrophilicity and the number of HS chains, confers either rigidity or flexibility to the local environment. This matrix serves to embed and to specifically bind structural (eg. collagen I, III, IV) and adhesive (eg. fibronectin and laminin) ECM proteins [97,100] and to sequester ions (eg. Ca^{2+}). The matrix also acts a molecular sieve to allow selective passage of water, ions, nutrients and metabolites and serves as a physical barrier to inhibit cell migration [101]. HSPGs are also found associated with cell membranes of most mammalian cells whether by insertion into the plasma membrane as integral proteins or by a phosphatidylinositol lipid anchor or interaction with a cell-surface receptor [97,100,102]. Cell surface HSPGs (such as fibroglycan, syndecan and glypican) have been shown to bind matrix proteins (eg. collagen type I, III, IV, fibronectin, thrombospondin, tenascin, cell adhesion molecules) [99-101]. Such HSPGs are believed to mediate cell-matrix and cell-cell interactions.

The role of HS has more recently been proposed to be much more diverse as it is believed to specifically bind a number of molecules including growth factors (eg. basic and acidic fibroblast growth factor, transforming growth factor-beta), hormones, neurotransmitters, vascular enzymes (eg. blood coagulation enzymes, lipoprotein lipase, elastase, and extracellular superoxide dismutase), cytokines (eg. granulocyte-macrophage

colony stimulating factor, interleukin 3), antithrombin III and thrombin, apolipoproteins, DNA polymerase and transcription factors [97,100-103]. The protein core of HSPG itself may bind molecules (eg. transferrin and hyaluronate) [97]. Although some of the above are *in vitro* observations, HS has been implicated to serve as a molecular reservoir and means of regulation of diverse cellular and/or tissue functions such as cell adhesion, cell proliferation and differentiation, leukocyte migration into tissues during inflammation, blood coagulation, angiogenesis, morphogenesis, platelet aggregation, wound healing, antigen presentation, and gene regulation [97,101,102]. Current research has focused on identification of the putative molecular binding sites on HS and the mechanisms controlling their binding such as proteoglycan expression or degradation. Plasma membrane HSPG turnover may occur by endocytosis followed by intracellular breakdown by proteolytic, endoglycosidic and exoglycosidic cleavage or by shedding into growth medium while ECM HSPGs may be degraded by secreted or membrane-associated heparanases [97,104] acting in concert with proteases [96,100,102,105,106].

Heparanases are endoglycosidases. Most have been found to be endo-β-D-glucuronidases, which hydrolyze β(1->4) linkages between D-glucuronic acids and *N*-acetylglucosamine residues [96]. Heparanases release oligosaccharides of between one-third to one-thirteenth the original size yielding fragments of M_r about 5 to 10 kDa [104,107,108]. Therefore, there are only a few hits per HS molecule. Most heparanases have been shown to have pH optima between pH 5 and 7.5 [94,96,109-112]. Because the structure of HS bears close resemblance to the anti-coagulant heparin (also a GAG stored intracellularly in and released from mast cells) differing mainly in higher glucuronic acid,

lower *N*- and *O*-sulfate and higher *N*-acetyl content [101], some heparanases digest heparin. At least three types of mammalian heparanases have been identified [96,104]: 1) those that digest HS but not heparin (eg. melanoma, fibrosarcoma, liver, neutrophil, macrophage, lymphocyte [108,109,113-117]); 2) those that degrade both HS and heparin (eg. human platelet [110,112]); and 3) those that degrade heparin preferentially (eg. mouse mastocytoma [96]). Specificity also arises depending on the source of the substrate, as HS from different tissues vary in size and composition [100,118].

Because HS has been implicated as a molecular reservoir and regulator of many processes especially those affected by cell-matrix and cell-cell interactions (as discussed above), heparanase is believed to be an important regulator of the biological activities of HS [96]. Altered heparanase expression or activity may contribute to diseased states, including tumour metastasis. The importance of cloning and characterization of heparanase is clear.

The Heparanase Cloning Project and The Problem at Hand

As mentioned earlier, there was little amino acid sequence information available on heparanase. This is due to the considerable difficulty that other workers have encountered in purifying heparanase sufficiently to permit for sequencing of the protein. Until very recently [110], no group has been successful in purifying heparanase to homogeneity. Our collaborator and a prominent researcher in the field, Dr. I. Vlodavsky, has experienced great difficulty in obtaining pure heparanase (personal communication). Protein sequencing has repeatedly revealed contaminating proteins in his enzyme preparations. Jin *et al.*

reported that they had raised antibodies to an *N*-terminal peptide fragment of B16 mouse melanoma heparanase [119] which they used to clone the cDNA for human heparanase from a λgt11 library (as reported in an abstract in 1992 [120] but the sequence of which they have not yet published). We raised antibodies to a synthetic peptide corresponding to their published peptide sequence and screened our λgt11 cDNA expression library using mRNA from KNRK (*K*irsten murine-sarcoma-virus-transformed *n*ormal *r*at *k*idney cells) cells which we had identified to have strong heparanase activity in our standard PAGE assay (described below). A pure clone was obtained based on specific immunoreactivity of the protein product towards the antibody and was subjected to nucleotide sequencing. We found that the published sequence corresponded to a 94 kDa glucose-regulated protein (GRP94) or endoplasmin, a molecular chaperone that may have co-purified with their heparanase [68]. Furthermore, the expressed protein failed to exhibit heparanase activity as had been reported by the original authors [120].

Because of the potential difficulty in purifying heparanase ourselves, we decided to screen a cDNA expression library on the basis of heparanase activity rather than sequence information. Using the process of "sib selection", the library (prepared from cells exhibiting heparanase activity) would be divided into pools of clones, grown, then extracts would be prepared from a portion of each pool and examined for heparanase activity, while the remainder of each pool is stored. A "heparanase-positive" pool would then be further subdivided, grown and a portion tested for heparanase activity until a pure clone for heparanase is obtained. Several heparanase activity assays have been described in the literature (see below). While each has its advantages and disadvantages, none seem suited

for the proposed "sib selection" screening of our expression library. An optimal assay should allow rapid and facile processing of large numbers of samples and should be sensitive enough to detect small levels of heparanase activity in pooled cell extracts. Thus, it was my objective here to improve our existing heparanase assay (Chapter I) and to develop a more sensitive and quantitative assay suitable for screening purposes (Chapter III) and for characterization of heparanase in KNRK cells (cells that had not previously been characterized in terms of heparanase activity) in addition to assessing heparanase activity in differentiating U-937 cells for its possible use as another differentiation marker (Chapter II).

Synopsis of Existing Heparanase Assays

One type of heparanase assay involves *in vivo* labelling with $[^{35}S]SO_4^{2-}$ of subendothelial matrix GAGs produced and deposited by endothelial cells onto polystyrene plates [107,114,121]. The cell layer is dissolved away with detergent and ammonium hydroxide leaving intact ECM with the bulk of the label incorporated into HS. Test extracts are added to the plates and heparanase activity is measured as the release of ^{35}S label into the supernatant. Although the described assay is easy to perform, it suffers from the disadvantage that proteolytic activity may contribute significantly to the release of radiolabel, since HS is immobilized to the polystyrene via proteins. This would lead to a large number of false positives for heparanase activity. Furthermore, the substrate is labelled at relatively low specific activity.

A variation on the above assay involves more extensive proteolytic digestion [114]

or cleavage by β-elimination [110], thereby releasing intact [^{35}S]-HS chains for use in a soluble assay. Chondroitin sulfates and hyaluronic acids are digested away by chondroitinase and hyaluronidase, respectively [114]. After purification of the HS, test extracts are incubated with the soluble substrate and HS product fragments are separated by size using gel filtration chromatography. The elution profiles of pre- and post-digestion samples are compared to assess heparanase activity. Although less prone to interference by proteolytic degradation, this method is rather cumbersome in that it involves running multiple columns per analysis and collecting multiple fractions per test sample.

Separation of HS fragments on the basis of size and charge can also be achieved using polyacrylamide gel electrophoresis (PAGE). This method forms the basis of our present assay which I refined as part of my project (refer to Figure 14). Size fractionation of commercially available HS substrate is performed to obtain the highest molecular weight fraction to increase the chances of detecting digestion. After digestion of the soluble substrate and separation of products on PAGE, the gel is stained with methylene blue, a basic dye which binds to acidic macromolecules such as HS. Because HS is heterogeneous with respect to size and charge, undigested HS appears as a smear in the gel when stained. Digestion of HS is indicated by a shift from lower to higher electrophoretic mobility. This assay is subject to interference by other polyanionic molecules such as nucleic acids or acidic proteins which, therefore, must be routinely removed with extensive micrococcal nuclease and proteinase K digestion prior to PAGE separation. While this assay may be sensitive enough to perform sib selection screening of an expression library (it can detect activity in 5 µg of cell extract which may represent 0.5 ng heparanase), this

assay is not as rapid and easy-to-perform as is desired for screening purposes. For general purposes, this heparanase assay is reliable; however, the information gained from this type of analysis is qualitative. Even if densitometry of stained gel is to be performed, the shift is often subtle particularly in cases where heparanase activity is low. Since there are only a few hits per molecule, only strong heparanase activity results in the characteristic shift. Furthermore, relatively large amounts of HS (1 to 2 μg) are needed to be visible on the gel when using methylene blue dye. Although other cationic dyes such as alcian blue [122] provide more sensitive detection of HS, these dyes also stain nucleic acids and acidic proteins which, again, must be removed. Thus, it is clear that a simpler and quantitative heparanase assay is most desirable.

Nicolson *et al.* employed a solid-phase substrate approach [123]. HS is labelled by *N*-desulfation of *N*-sulfo-*D*-glucosamine residues using DMSO solvolysis (Chapter III) and introduction of [^{14}C]acetyl groups to the newly formed amino groups on *D*-glucosamine using [^{14}C]acetic anhydride. The substrate is immobilized by reductive amination of the reducing terminus to introduce a terminal amino group (Chapter III) which is covalently coupled to amine-reactive Affigel 15 beads. Heparanase activity is detected as release of [^{14}C]-labelled HS fragments into the supernatant. The advantages of this assay are that separation of reactants and products is relatively easy and fast, and protein or nucleic acid removal is unnecessary. With such an assay, even one hit per molecule could be detected. The disadvantages are that large amounts of [^{14}C]-acetic anhydride are needed to label HS with enough specific activity, loss of negative charge upon *N*-desulfation may affect recognition and digestion by heparanase, and, more importantly, immobilization of the

substrate to a bulky agarose bead might sterically hinder the access of heparanase to HS.

Proposed Approach to the Problem

In developing a more sensitive, easy-to-perform and quantitative heparanase assay, we followed some steps of the solid-phase [^{14}C]HS assay with several modifications (Figure 13). To relieve steric hindrance imposed by the large bead, biotin can substituted onto a terminal amino group introduced by reductive amination (Figure 13a) or, alternatively, directly onto the terminal aldehyde in the native HS molecule (Figure 13b). Instead of [^{14}C]acetyl labels, fluorescent tags can be introduced onto *N*-desulfated glucosamine residues (Figure 13a and 13b), thereby increasing the sensitivity of detection, reducing the amount of substrate required and eliminating the use of radiolabel altogether. This system would allow for less restricted digestion since it would be performed in the soluble phase. Subsequent binding of the biotin-containing fragments to a biotin-capture system (such as streptavidin or avidin) and measurement of the fluorescence of the non-bound fraction in a fluorometer would provide a quantitative measure of heparanase activity (Figure 13c). Besides the initial substrate preparation, the assay itself would be rapid and easy-to-perform and would thus be suitable for screening purposes. The only potential problem with this assay might be impaired recognition and/or digestion of the substrate due to loss of charge upon *N*-desulfation (as in the [^{14}C]HS assay) or introduction of the hydrophobic and bulky fluorescent probe. These are not likely to interfere to a large extent since mammalian endoglucuronidases are believed to cleave linkages between D-glucuronic and *N*-acetylglucosamine residues in regions of low *N*- (and *O*-) sulfation

Figure 13. *Substrate and assay design for the proposed fluorescence-based heparanase assay.*

a. After reductive amination of the reducing end of the native substrate with sodium cyanoborohydride ($NaBH_3CN$) and ammonia (NH_3), a biotin can be introduced to the newly formed amino group using the amine-reactive succinimidyl ester analog of biotin (shown here with a spacer arm for extension, biotin-XX-succinimidyl ester). Partial DMSO solvolysis liberates *N*-sulfates from *N*-sulfo-*D*-glucosamine residues leaving behind amino groups to which fluorescein can be attached using FITC.

b. As an alternative method for preparing the substrate, the terminal aldehyde at the reducing end of native HS can be directly coupled to biotin using biotin hydrazide. DMSO solvolysis and fluorescein labelling would be carried out as in *a.*

c. One configuration for the proposed fluorescence-based assay would involve digestion of the fluoresceinated, biotinylated substrate with heparanase, binding of the digests to immobilized avidin or streptavidin to capture biotinylated fragments, and collection of the unbound fragments to be quantified using a fluorometer.

Figure 13.

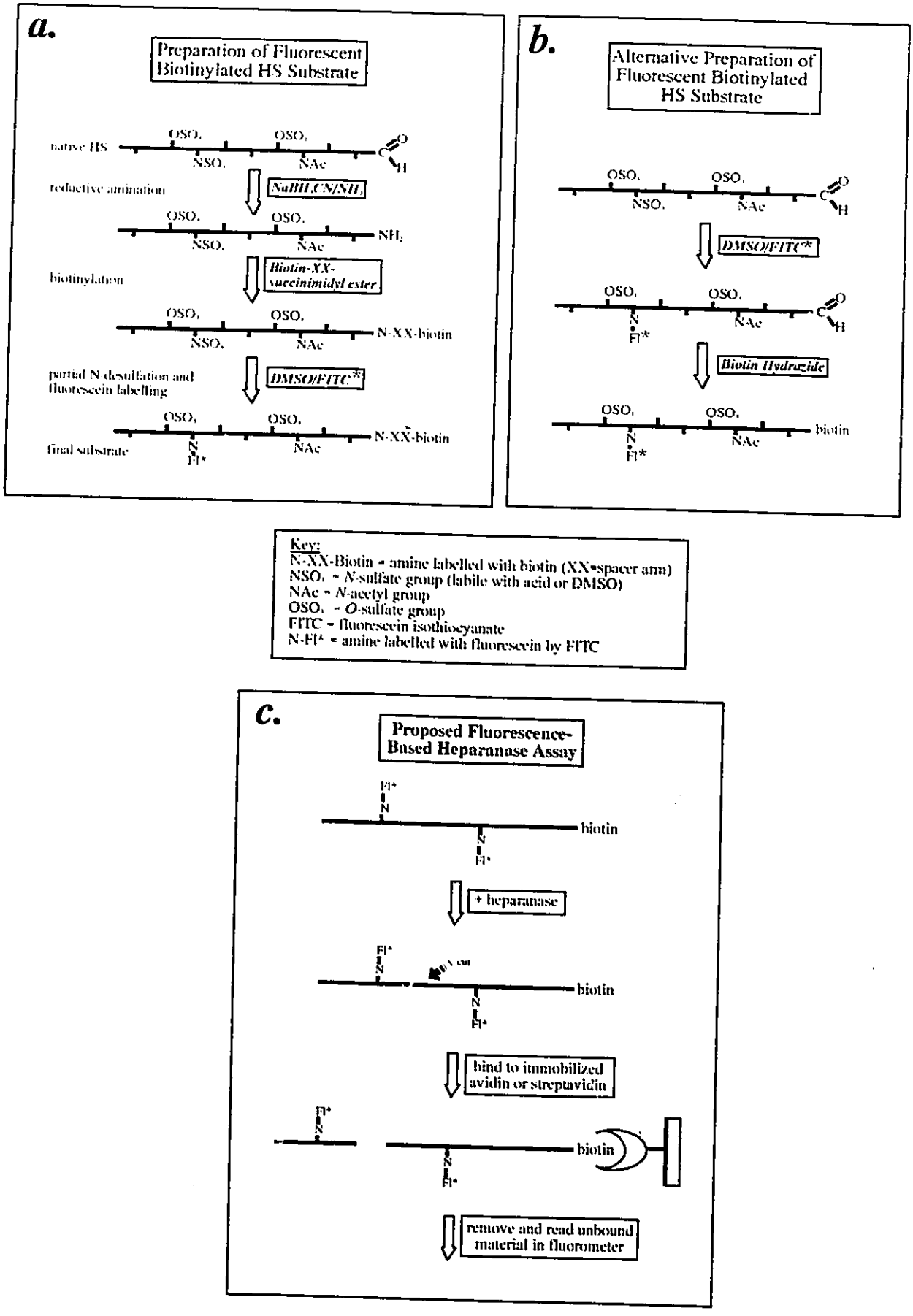
a.
Preparation of Fluorescent Biotinylated HS Substrate
native HS
reductive amination
NaBH3CN/NH4
biotinylation
Biotin-XX-succinimidyl ester
N-XX-biotin
partial N-desulfation and fluorescein labelling
DMSO/FITC*
final substrate
b.
Alternative Preparation of Fluorescent Biotinylated HS Substrate
DMSO/FITC*
Biotin Hydrazide
biotin
Key:
N-XX-Biotin = amine labelled with biotin (XX=spacer arm)
NSO3 = N-sulfate group (labile with acid or DMSO)
NAc = N-acetyl group
OSO3 = O-sulfate group
FITC = fluorescein isothiocyanate
N-Fl* = amine labelled with fluorescein by FITC
c.
Proposed Fluorescence-Based Heparanase Assay
biotin
+ heparanase
bind to immobilized avidin or streptavidin
remove and read unbound material in fluorometer

[97] and the presence of *N*-sulfate and *O*-sulfate groups are not essential for full activity [124].

Such a sensitive, rapid and easy-to-perform fluorescence-based assay would greatly facilitate the sib selection screening process. Furthermore, the proposed assay would provide quantitative measurements of heparanase activity useful for characterization of various heparanases and assessment of heparanase activity during the course of U-937 cell differentiation.

CHAPTER I. REFINEMENT OF THE PAGE ASSAY

Our standard heparanase assay consisted of PAGE separation and methylene blue staining of HS degradation products. The PAGE assay is useful for qualitative analysis of heparanase activity (Chapter II) as well as a reference assay to monitor the integrity and digestibility of HS after chemical modifications (such as in Chapter III). The PAGE assay was modelled after one reported by Nakajima *et al.* [94] to which modifications were made to optimize conditions for detecting heparanase activity.

An outline of the steps and a representative result of the refined PAGE assay is shown in Figure 14. The final procedure for the PAGE assay is provided in detail in the figure legend. The presence of heparanase activity is indicated by a decrease in staining in the upper area of the HS smear (such as above the arrows shown) rather than an increase in staining in the lower area (out of which lower molecular weight HS fragments tend to diffuse during electrophoresis or soaking, and in which background staining due to the extract tends to be most prominent). For every test reaction (usually denoted as "16 hr"), three controls are typically set up for incubation in the presence of reaction buffer to be processed similarly as the test reaction: 1) HS alone (usually denoted as "HS") to assess the mobility of undigested HS; 2) incubated extract to which HS is added after the incubation ("0 hr" co-incubation) to determine whether cell extract components interfere with HS staining or mobility; and 3) extract alone (usually denoted as "ext") to assess the contribution of the cell extract towards background staining by methylene blue. The "0 hr" control is sufficient as the only control; however, the other controls facilitate interpretation

Figure 14. *Refined standard PAGE assay and a representative result.*

The finalized refined PAGE assay is described in detail below.

Confluent monolayer cultured cells (typically 5 to 10 x 10^6 cells) are washed with Ca^{2+} and Mg^{2+}-free phosphate buffered saline (PBS) and removed from tissue culture plates by incubation at 37°C in a CO_2 incubator for 5-10 min with PBS containing 2 mM EDTA. Cells are pelleted by centrifugation at 700*g* for 10 min at 4°C in a Centra-7R refrigerated centrifuge (International Equipment Co.). The cell pellet is resuspended in 10 mL PBS, centrifuged again, resuspended in 1 mL PBS, transferred to a microcentrifuge tube and spun for 1 min room temperature (RT) at low speed in a desktop microcentrifuge. Suspension cells are removed from culture medium by centrifugation at 700*g* at 4°C for 10 min and washed twice in PBS by centrifugation. Whole cell extracts are prepared by sonication in working heparanase extraction buffer (50 mM MOPS pH 7.5, 1 mM PMSF (freshly added from 20x stock in methanol), 5 mM NEM, 0.05% (w/v) sodium azide, 0.1 mM CDTA, 50 µM chymostatin (freshly added from 1:10 dilution in water of a 10 mM stock in DMSO), and 2 µg/mL aprotinin (freshly added from 1:50 dilution in water of a 2 mg/mL stock in water)) on low setting (power 1 setting of a 50-watt Microson automatic cell disrupter) twice for 5 seconds on ice (cooling in between pulses), and glycerol addition to a final concentration of 20-30% (v/v). Protein concentration of extracts is determined using a fluorescamine assay for protein [68]. Extracts are stored at -20°C.

HS is size-fractionated using gel filtration chromatography. Sephadex G-75 resin is hydrated by boiling in CT (10 mM Tris-HCl, pH 7.5, 1 mM CDTA). A 9 mm x 11.5 cm column is prepared and equilibrated with CT. Typically, 100 to 200 µL of 10 mg/mL bovine kidney HS in water is added to the column and eluted with CT at a flow rate of approximately 10-12 drops per minute. After about 45 drops have emerged, two to three drop fractions are collected into small glass test tubes. 1 µL aliquots from each HS elution fraction are spotted on a Hybond-N membrane, air-dried and tested for the presence of HS by staining with 0.1% (w/v) methylene blue in 50% ethanol/water (v/v) for 10 min, and destaining in water. Every three to four consecutive HS-containing fractions are pooled to obtain three pooled fractions (each about 500 µL of 1 µg/µL HS). The first high molecular weight pooled fraction (HMW#1) is routinely used in the PAGE assay.

Extract (typically 50 µg/10 µL reaction) is incubated without (shown as "ext") or with (shown as "16 hr") 2 µg HMW#1 HS in 20 mM cacodylate pH 6.1 at 37°C overnight. A "0 hr" control consists of extract incubated in the absence of HS. A HS alone control ("HS") consists of HS incubated in the absence of extract. After incubation, reactions are treated with 0.1 U micrococcal nuclease (MNase) per 10 µL reaction in 1x MNase buffer (1 mM $CaCl_2$, 10 mM Tris-HCl pH 9.5) at 37°C for 1 to 2 hr. 2 µg HS is added to 0 hr controls and reactions are further treated with 5 µg/10 µL proteinase K/0.1% SDS at 60°C for 1 to 2 hr. Loading buffer is added to the samples to 16% glycerol containing 1 mM CDTA.

7.5% PAGE gels in 1x TAC (40 mM Tris/20 mM sodium acetate, pH 7.8, 1 mM CDTA) containing 0.025% (w/v) ammonium persulfate and 0.1% (v/v) TEMED are prepared from a 30% acrylamide/bisacrylamide (19:1) mix. Samples are run in 1x TAC for 30 to 40 min at 100 V using the Bio-Rad Mini Protean II apparatus. Gels are soaked for 20 min in running water, stained with 0.1% (w/v) methylene blue in 50% (v/v) ethanol/water for 20 min and destained in running water for 50 to 60 min. Gels are dried under vacuum between layers of pre-moistened BioGel Wrap, with 3M paper as an underlying support, using a Bio-Rad Model 583 gel dryer at 60°C for 45 min.

In the representative gel shown, 60 µg KNRK (Kirsten murine-sarcoma-virus-transformed normal rat kidney cells) or B16F10 (murine melanoma cells) extracts were incubated at 37°C overnight with 2 µg bovine kidney HS. Heparanase activity is indicated as a decrease in staining in the upper portion of the HS smear (such as above the indicated arrows (→,←)).

Figure 14.

STANDARD PAGE ASSAY
OUTLINE OF STEPS

size fractionate HS

prepare cell extract

incubate HS with extract
(controls: HS alone, 0 hr, extract alone)

treat reactions with micrococcal nuclease

treat reactions with proteinase K/SDS

separate on PAGE gel

soak, stain and dry gel

Representative Result

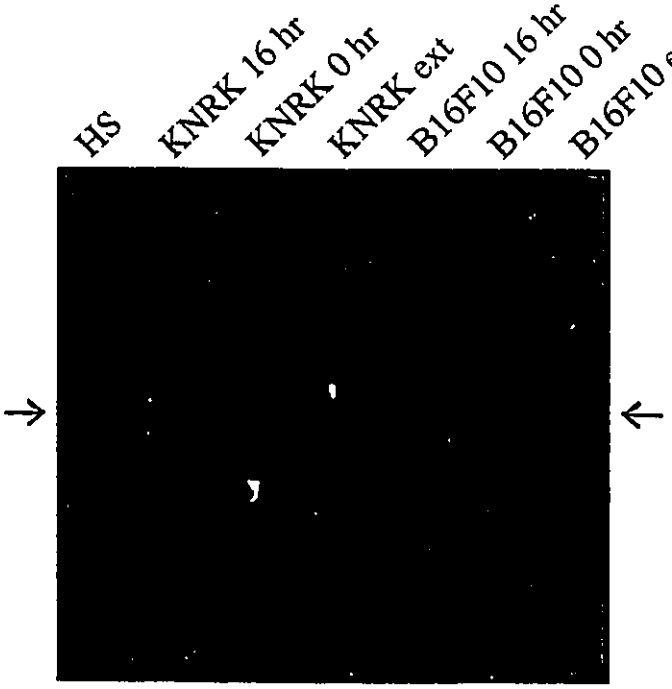

and identification of the major contributors to background staining if present.

The following chapter outlines the modifications that were made to the original protocol to arrive at the refined PAGE assay as described in Figure 14.

I.1. *Size Fractionation of HS and Polyacrylamide Gel Electrophoresis Conditions*

HS was fractionated by gel filtration chromatography to isolate the high molecular weight (HMW) fraction from the heterogeneous starting material. The rationale behind performing the fractionation was that the longer the HS molecule used in the digest, the greater the probability of digestion and the number of cuts. This would result in greater size differences between starting material and degradation products and therefore easier visualization of the differences when separated (eg. by PAGE).

Among various chromatographic systems tested (including cellulose-acetate electrophoresis and thin layer chromatography (TLC)), a PAGE-based method was found to be best suited to good separation and resolution. Nakajima et al. [94] had described the use of toluidine blue to stain HS on polyacrylamide gels. The basic dye, methylene blue, was chosen for our purposes since greater sensitivity of detection was achieved with methylene blue in comparison to toluidine blue (not shown).

Results and Discussion:

A methylene blue stained membrane of elution fractions from a typical size fractionation of bovine kidney HS by gel filtration is shown in Figure 15a. Elution using buffer at pH 7.5 was optimal for the separation, while at higher pH (8.0 or above), the elution peak became too broad (not shown). In the latter case, residual HS was retained on

Figure 15. *Typical elution profile of HS size fractionation and PAGE separation of pooled fractions.*

Sephadex G-75 resin was hydrated by boiling in CT (10 mM Tris-HCl, pH 7.5, 1 mM CDTA). A 9 mm x 11.5 cm column was prepared and equilibrated with CT. 140 µL of 10 mg/mL bovine kidney HS in water was applied to the column and eluted with CT at a flow rate of approximately 10-12 drops per minute. Two drop fractions were collected after 45 drops had emerged.

a. Methylene blue staining of elution fractions to test for the presence of HS. In the sample fractionation shown, 1 µL aliquots from each HS elution fraction were spotted on a Hybond-N membrane, air-dried, stained with 0.1% (w/v) methylene blue in 50% ethanol/water (v/v) for 10 min, and destained in water.

b. PAGE separation of pooled HS fractions. In the sample fractionation shown in *a.*, fractions 3 to 6 were pooled to form HMW#1 (HMW = high molecular weight), fractions 7 to 10 were pooled to form HMW#2, and fractions 11 to 14 were pooled to form HMW#3. Each pool (about 500 µL) contained approximately 1 µg/µL HS. 7.5% polyacrylamide gels in 1x TAC containing 0.025% (w/v) ammonium persulfate and 0.1% (v/v) TEMED were prepared from a 30% acrylamide/bisacrylamide (19:1) stock. 2 µL of each pooled fraction or unfractionated HS (shown as "TOTAL") was electrophoresed on 7.5% PAGE for 30 min, stained for 20 min with 0.1% (w/v) methylene blue in 50% (v/v) ethanol/water, destained for 60 min with water and dried in under vacuum between one upper and two lower layers of pre-moistened BioGel Wrap, with 3M paper as an underlying support, using a Bio-Rad Model 583 gel dryer at 60°C for 45 min.

Figure 15.

a.

b.

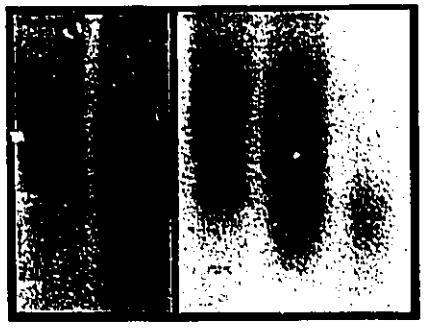

the column even with extra addition of buffer, suggesting increased non-specific binding to resin. Typically, three or four consecutive HS-containing fractions were pooled to obtain three HMW fractions (Figure 15b), the first (HMW#1) of which was chosen for use in PAGE assays. (For a comparison of digestion of total versus fractionated bovine kidney HS in the PAGE assay, refer to Figure 23a.) The HMW#1 fraction contains enough substrate for at least 250 determinations.

In testing conditions for PAGE separation, electrophoresis in 1x TAC buffer (40 mM Tris/20 mM sodium acetate, pH 7.8, 1 mM CDTA) gave better separation than barium acetate buffer (not shown). Due to the heterogeneous size and charge distribution of HS, HS produced a broad smear in the gel when stained. The initial 30 min run (Figure 15b for example) was later extended to 40 min (Figure 14 for example) for better separation and easier visualization of changes in mobility. To prevent transfer of methylene blue to the 3M paper support when drying with a gel dryer, two layers of BioGel Wrap were used underneath the gel instead of one. Background staining by methylene blue of SDS in SDS-containing samples (SDS would be remaining after the proteinase K digestion of reactions as described later in section I.3; for an example, refer to Figure 23b) was eliminated by soaking gels in running water for 10 to 20 min prior to staining, allowing SDS to diffuse out of the gel. With prolonged soaking (>1 hr), lower molecular weight material tended to diffuse out of the gel.

I.2. *Preparation of Cell Extracts*

The following experiments were performed to establish the optimal method for

preparing cell extracts for obtaining maximal heparanase activity and least interference due to background staining in the PAGE assay. Being the most promising in terms of heparanase activity, most studies were performed using KNRK extracts.

Cells were harvested and washed as described in the legend of Figure 14. To each washed cell pellet was added 100 µL working heparanase extraction buffer composed of: 50 mM MOPS pH 7.5, 1 mM PMSF (freshly added from 20x stock in methanol), 5 mM NEM, 0.05% (w/v) sodium azide, ± 0.5% (v/v) Triton X-100, ± 0.1% (w/v) CHAPS, ± 0.1 mM CDTA, ± 50 µM chymostatin (freshly added from 1:10 dilution in water of a 10 mM stock in DMSO), ± 2 µg/mL aprotinin (freshly added from 1:50 dilution in water of a 2 mg/mL stock in water). Cells were subsequently processed in either one of two ways: 1) mixed briskly by vortexing, incubated at 0°C for 1 hr, centrifuged at 17,300*g* in a Sorvall RC-5B Superspeed Centrifuge (Dupont Instruments) at 4°C for 20 min to pellet out insoluble material (nuclei, membranes, etc.) and the supernatant or the "soluble" extract was treated with 0.02 units micrococcal nuclease (MNase) for 20 min at 37°C (to remove DNA and RNA) and stored at 0°C; or 2) subject to rapid freezing/thawing and/or sonicating on power 1 setting of a 50-watt Microson automatic cell disrupter twice for 5 seconds on ice with cooling between pulses, with or without glycerol addition to the lysate to a final concentration of 20-30% (v/v), and storage at -20°C. Protein concentration of cell extracts was assessed using a fluorescamine assay for protein as described in [68].

Results and Discussion:

The heparanase extraction buffer, modelled after Jin et al. [119], was essentially the same with the exception of MOPS, pH 7.5 being used in place of Tris-HCl, pH 7.5 and the

addition of more protease inhibitors. There seems to be no requirement for detergents such as Triton X-100 or CHAPS in the extraction buffer for extracting heparanase activity in KNRK cells (data not shown).

MNase-treated soluble cell extracts (i.e., nuclei, membranes removed) were originally prepared to reduce the amount of contaminating nucleic acids that would contribute to background staining by methylene blue in the gel. Addition of CDTA to extracts to chelate Ca^{2+} remaining after MNase treatment prior to heparanase digestion very slightly improved heparanase activity in KNRK and NRK (*n*ormal *r*at *k*idney) cells (Figure 16a). This may indicate that heparanase does not require and/or is inhibited by Ca^{2+} (or other divalent cations) or that CDTA addition may inhibit divalent cation-dependent proteinases that would normally degrade heparanases or other required protein factors.

The low heparanase activities represented in Figure 16a were obtained from 40 hr incubations of soluble KNRK or NRK extract with HS. Digestion was more apparent with longer incubation (72 hr as in Figure 17a). Whole cell extracts, rather than soluble extracts, yielded stronger heparanase activity in a shorter time (less than 16 hr for KNRK as seen in Figure 17b) and more reproducible results over time. This might suggest heparanase may require the presence of or it itself is associated with the insoluble membrane fraction. Tumour cell heparanase activity has been detected in intact cells as well as with cell homogenates [94,109,125] suggesting a plasma membrane association or secretion of heparanase from the cell. Thus, whole cell extracts were subsequently used in digests rather than soluble extracts. The use of whole cell extracts, however, demanded that MNase and proteinase K treatments be increased accordingly (see Section I.3. below).

Figure 16a. ***Addition of CDTA to soluble extracts after MNase treatment prior to the PAGE assay.***

Soluble (i.e., minus nuclei, membranes) extracts from confluent KNRK and NRK cells were prepared (with Triton X-100, and without CHAPS, chymostatin, or aprotinin in the extraction buffer) and MNase treated (0.02 U MNase for 20 min at 37°C) as described in Section I.2. 2 µL of each extract was incubated with approximately 2 µg of HMW#1 fraction of bovine kidney HS in 20 mM cacodylate buffer pH 6.1 at 37°C for 40 hror 0 hr in the presence or absence of 50 µM CDTA. In parallel, equivalent amount of extract was incubated in the absence of HS ("0 hr" control) at 37°C for 40 hr after which 2 µg HS was added and separately, 2 µg HS alone was incubated at 37°C for 40 hr. Reactions were added to lyophilized proteinase K/urea (5 µg proteinase K/5.8 µL of 10 M stock urea), incubated at 60°C for 1 hr and electrophoresed 30 min on 7.5% PAGE, stained, destained and dried as described in Section I.1. Heparanase activity (here it is slight) is indicated as a decreased staining in the upper portion of the HS smear in 40 hr digests compared to controls (0 hr and HS lanes).

Figure 16b. ***Determination of optimal MNase concentration for treatment of whole cell extracts.***

Whole cell extract was prepared from confluent KNRK cells using heparanase extraction buffer without Triton X-100 or CHAPS and with chymostatin, aprotinin, and CDTA as described in Section I.2. The lysate was sonicated and stored at 0°C until needed. 50 µg protein equivalent aliquot of KNRK extract in 20 mM cacodylate pH 6.1 and 1x MNase buffer (1 mM $CaCl_2$, 10 mM Tris-HCl pH 9.5) was incubated for 1 hr at 37°C with 0 to 0.2 U MNase. Samples were added to lyophilized proteinase K/urea (5 µg proteinase K/5.8 µL of 10 M stock urea), incubated at 60°C for 1 hr and electrophoresed 40 min on 7.5% PAGE, stained, destained and dried as described in Section I.1. MNase is effective in removing higher molecular weight nucleic acids indicated here as a decrease in staining of the slower migrating material (found in the upper portion of the gel).

Figure 16.

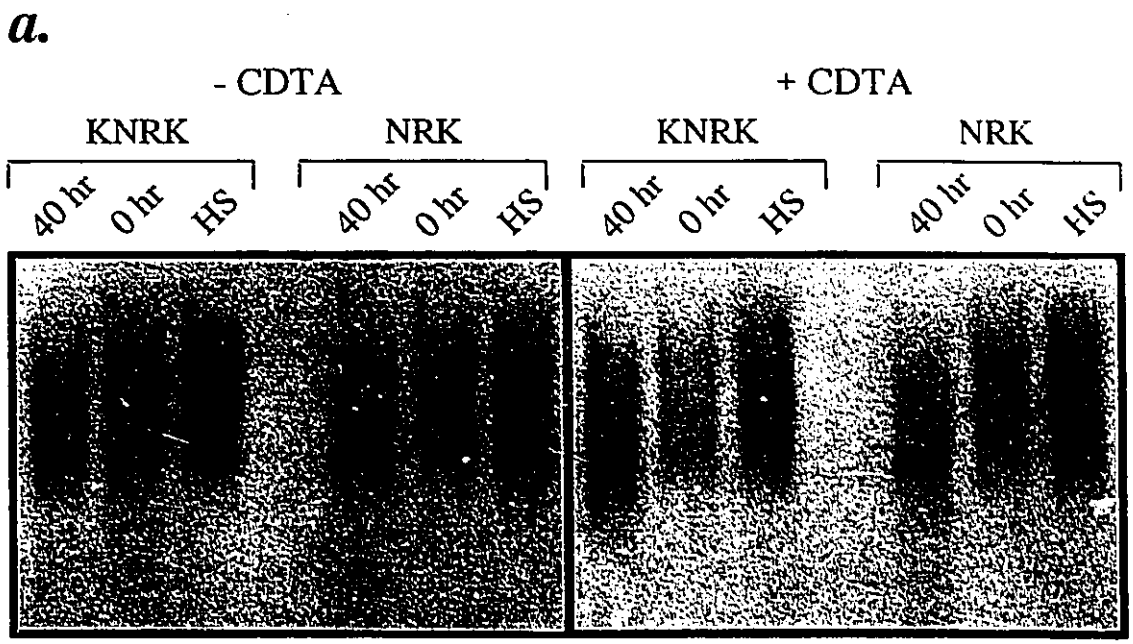
a.
- CDTA
+ CDTA
KNRK
NRK
KNRK
NRK
40 hr
0 hr
HS
40 hr
0 hr
HS
40 hr
0 hr
HS
40 hr
0 hr
HS

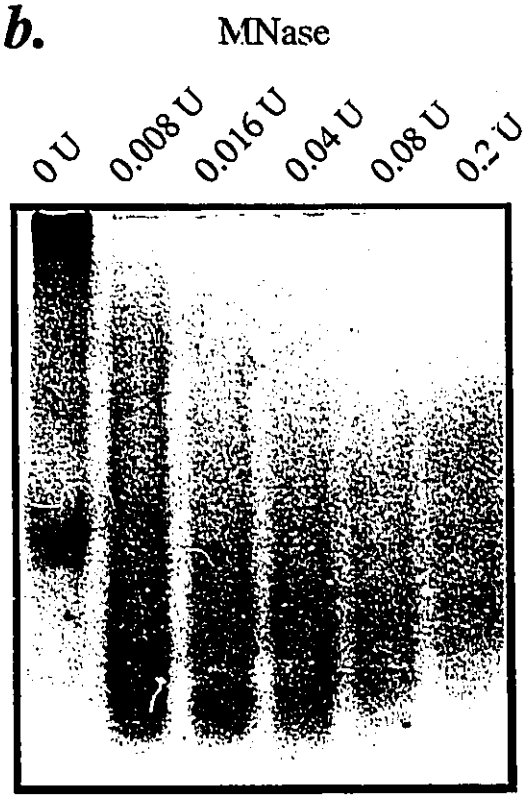
b.
MNase
0 U
0.008 U
0.016 U
0.04 U
0.08 U
0.2 U

Furthermore, to avoid possible proteolytic degradation of heparanase prior to assaying for its activity, MNase treatment should be performed after incubation with HS rather than before. Due to this change in procedure, CDTA was added to the extraction buffer rather than after the MNase treatment.

Sonication was found to be as or more effective in disrupting cells than vortexing or freeze/thawing without compromising heparanase activity. This was indicated by complete cell permeability to ethidium bromide upon visualization of lysed cells under a fluorescence microscope.

Glycerol was later routinely added to protect the extract from repeated freezing and thawing for assays. The extracts prepared in this way were very stable (at least for KNRK cell extracts) and could be stored at -20°C for several months without significant loss of activity even after repeated freezing and thawing (even after 6 months). Interestingly, Ledbetter *et al.* has also reported that storage increased the amount of active heparanase [110].

I.3. *Background Removal*

In the paper by Nakajima *et al.* [94], incubation mixtures were centrifuged to remove cell debris and a portion of the supernatant was applied to a gel. However, since nucleic acids and acidic proteins also stain with methylene blue, complete removal of these interfering components was desired before PAGE separation to minimize background.

Background removal after incubation with HS was accomplished using MNase and proteinase K treatments. Incubations with MNase were carried out at 37°C in 1x MNase

reaction buffer. Incubations with proteinase K were carried out at 60°C with or without denaturating agent (urea or SDS).

Results and Discussion:

Originally, MNase treatment of extracts was performed in bulk before incubation with HS (described above in Section I.2). To prevent any loss of heparanase activity due to proteolysis that might also occur during the MNase incubation, MNase treatments were subsequently performed after incubation with HS. As stated earlier, whole cell lysates yielded stronger heparanase activity and more reproducible results compared with that obtained with soluble extracts. With subsequent use of whole cell extracts, MNase treatment was to be modified accordingly. One hr incubation at 37°C with 0.04 to 0.08 U MNase for 50 µg protein in the KNRK extract was sufficient to remove interfering nucleic acids that stained in the upper area of the gel (where high molecular weight HS is expected to stain) (Figure 16b). The standard MNase treatment was therefore increased from 0.02 U per 100 µL extract (i.e. 0.2 mU/µL) at 37°C for 20 min to 0.1 U per 10 µL reaction (= 10 mU/µL) at 37°C for 1 to 2 hr. It should be noted that MNase treatment could also be performed at 45 or 55°C. After HS digestion using soluble cell extracts, proteinase K treatment originally consisted of 2 µg/10 µL proteinase K at 60°C for 1 hr. With the use of whole cell extracts, this was increased to 5 µg/10 µL reaction (60°C for 1 hr). Combined proteinase K/urea treatment (addition of reaction to lyophilized sample of 5 µg proteinase K and 5.8 µL of 10 M stock urea) at 60°C for 1 hr was effective in removing protein; however, the presence of urea often resulted in aberrant lanes in the PAGE gel, characterized by very intense staining along lane edges and lighter staining in lane centres

(refer to Figures 17b-d, 18, or 19 for examples). As an alternative, proteinase K digestion was performed in the presence of 0.1% SDS. This was equally effective; however, because the anionic SDS also stained strongly by methylene blue in the gel (eg. Figure 23b), an additional 10 to 20 min soaking step in water was incorporated into the protocol as described earlier in Section I.1.

I.4. *Conditions for Heparanase Digestion Reaction and Appropriate Controls*

In the original paper [94], digestion of 50 µg HS with 40 µg cell extract (± boiling) was performed in 0.1 M sodium phosphate, 0.2% Triton X-100, 0.15 M NaCl, pH 6.0 at 37°C after which 2 µL supernatant of a 70 µL centrifuged digest was applied to a gel. For our studies, reactions were carried out at 37°C in 20 mM sodium cacodylate pH 6.1. Triton X-100 was not added to the reaction buffer since it was not found to be necessary for activity (Section I.2.). Heparanase activity has been characterized to be a relatively slow enzyme [94]. We had found that digestion of HS by B16F10 was evident after 4 to 8 hr. Thus, an overnight (typically 16 hr) digestion was routinely performed.

Equivalent protein amounts of whole cell extract (typically 50 µg per 10 µL reaction) were added to HS (1 to 2 µg per 10 µL reaction) and incubated in 20 mM sodium cacodylate buffer pH 6.1 at 37°C overnight. After the incubation, the reactions were treated with MNase and proteinase K and subjected to PAGE analysis (described in Figure 14 legend).

Results and Discussion:

20 mM cacodylate buffer pH 6.1 was chosen as the reaction buffer, although

digestion also occurred equally well in sodium acetate pH 6.0 (Figure 24).

Unlike the 50 µg HS that were required in the original assay [94], we were able to detect heparanase activity with 1 or 2 µg HS given a similar amount of extract. Thus, our PAGE assay consumes less substrate.

Initially, as a "0 hr" control, a reaction containing HS and extract was held at 0°C for the same time as the test reaction (instead of boiling the extract). However, it was found that heparanase activity could be detected in this control (not shown) indicating that heparanase may be active at 0°C. To correct this, the "0 hr" control was modified such that the extract was incubated with the reaction buffer for the equivalent amount of time as the test samples, treated with MNase at 37°C as for the test samples after which HS was added prior to or during the proteinase K treatment at 55 to 60°C (a temperature at which heparanase would be inactive).

I.5. *Summary for Chapter I*

After various modification steps, the PAGE assay was finalized as shown in Figure 14. The entire process from the setting up the reactions to PAGE takes about 22 hours. Preparation of extracts takes less than an hour. Size fractionation of HS is performed in bulk and therefore is only necessary when substrate is needed.

The most notable change in the procedure is the use of whole cell extracts rather than post-membrane fractions for incubation with HS. With whole cell extracts, heparanase activity appears to be much more active and stable suggesting heparanase is largely associated with the insoluble fraction. MNase and proteinase K treatments

effectively remove background staining material that might obscure results.

The PAGE assay, although not quantitative nor highly sensitive, does yield consistent results and it is suitable for qualitative analyses in the characterization of heparanases and HS substrates. For the proposed fluorescence-based assay, it is useful for monitoring the intactness and digestibility of HS substrates after chemical modification.

CHAPTER II. APPLICATION OF THE PAGE ASSAY IN THE ATTEMPTED CLONING AND CHARACTERIZATION OF HEPARANASE AND IN ASSESSING THE USEFULNESS OF HEPARANASE AS A U-937 DIFFERENTIATION MARKER

The PAGE assay described in Chapter I was applied to various aspects of the cloning project (Section II.1. and II.2.). This included identification of cells with the strongest heparanase activity from which a cDNA expression library would be constructed, verification of the specificity of a putative anti-heparanase antibody, and "sib selection" screening of an expression library for heparanase activity. The PAGE assay was further used to characterize and compare heparanases in a variety of cell types in terms of level of heparanase activity, substrate preference, and sensitivity to inhibitors (Section II.3.). Among the cells compared in the PAGE assay were U-937 control and differentiated cells (Section II.4.). This chapter outlines the application of the PAGE assay in these studies.

II.1. *Survey of Different Cell Types for Heparanase Activity and Testing of Purified HS Endoglycosidases*

PAGE assays were performed on a survey of cell lines to find: 1) the cell line having strongest heparanase activity from which a cDNA library would be constructed, and 2) the cell line having minimal or undetectable heparanase activity to serve as an appropriate host for a mammalian expression vector system. Two purified HS endoglycosidase enzymes, a commercial source of bacterial Heparinase III (Hep III) and human placental heparanase (α,MM) from our collaborator Dr. I. Vlodavsky, were also tested in the PAGE assay for their potential use as positive controls for use in the development of the new fluorescence-based heparanase assay. Hep III is different from

heparanase in that it is a heparin α-lyase, rather than a hydrolase, cleaving between 6-*O*-sulfated *N*-sulfoglucosamine and 2-*O*-sulfated iduronic acid residues by an elimination reaction [97] rather than a hydrolysis reaction.

Results and Discussion:

Of the cells tested, most were negative with respect to heparanase activity when bovine kidney HS was used as a substrate with the exception of KNRK, B16F10 (Figure 14), NRK (Figure 17a), and freshly isolated human lymphocytes (Figure 17c).

Of the positive cell lines, KNRK exhibited the strongest heparanase activity (eg. Figure 14, 17a and 17b). Based upon this result, mRNA was extracted from KNRK cells and used to generate a cDNA library [68]. B16F10 (Figure 14) and NRK (Figure 17a) cells possessed heparanase activity, although weaker. Interestingly, B16F10 heparanase activity was greater when cells were harvested from confluent cells that were on the verge of lifting off the culture plates. The significance of this observation is not clear. NIH 3T3, HL-60, U-937, and TK6 cells lacked heparanase activity while HSC 93 cells were marginally active (Figure 17b). TK6 cells were later found to be appropriate hosts for a mammalian expression library (Section II.2.5.). (Note: Primary rat embryo fibroblast cells, Rec, and a derived line, RecRas (both prepared by S. Bennett), were also found to be negative with respect to heparanase activity (not shown)). Human lymphocytes possessed heparanase activity while mature granulocytes (PMNs) did not (Figure 17c).

Others have also found that fibroblast cells are negative with respect to heparanase activity [96,109]. However, in this study, human leukemia or lymphoma cell lines (U-937, HL-60, HSC 93, and TK6) and fresh PMNs were not active, contrary to the reports of

Figure 17. *Heparanase activity in various cell lines and purified enzyme preparations.*

Cell lines, other than U-937, were maintained in DMEM containing 10% fetal calf serum (FCS) for up to four weeks. U-937 cells were cultured in RPMI 1640 containing 10% FCS for up to four weeks. At confluency, monolayer cultures (including B16F10 in Figure 14), NRK, KNRK, NIH 3T3, Rec (not shown) and RecRas (not shown) cells) were passaged by first washing in PBS, lifting in PBS containing 0.05% trypsin, and diluting into fresh medium. Suspension cells (HL-60, HSC 93, TK6, and U-937 cells) were maintained by dilution into fresh medium. Human PMNs were freshly isolated from healthy donors as described in [6] at which time lymphocytes were also recovered from the density gradient and washed in balanced salt solution (BSS). Whole cell extracts from confluent cells or late log cells were prepared as described in Figure 14 (except for soluble KNRK and NRK extracts used in *a.* which is described in Chapter I, Section I.2.). Digests with purified bacterial HS lyase Heparinase III (Hep III) were performed in 1x Hep III reaction buffer (0.25 M sodium acetate pH 8, 2.5 mM $CaCl_2$). Digests with cell extracts or purified human placental heparanase (α,MM) were performed in 20 mM cacodylate pH 6.1. Extracts and purified enzymes were subjected to the PAGE assay, as described in Figure 14, using bovine kidney HS as a substrate.

a. ~ 40 µg KNRK or NRK soluble extracts were incubated at 37°C for 72 hr or 0 hr with 1 µg bovine kidney HS. KNRK and NRK heparanase activities at 72 hr are indicated as decreases in the staining of slower migrating material (in the upper portion of the gel) compared to 0 hr and HS controls.

b. 56 µg KNRK, NIH 3T3 (murine fibroblastic cell line), HL-60 or U-937, or 50 µg HSC 93 (human lymphoma cell line), or 60 µg TK6 (human lymphoblastic cell line) extracts were incubated at 37°C for 16 hr or 0 hr with 2 µg bovine kidney HS. KNRK heparanase activity at 16 hr is indicated as a decrease in staining of slower migrating material (in the upper portion of the gel) compared to 0 hr and HS controls. Similarly, marginal activity is seen with 16 hr HSC 93.

c. 67 µg PMN and 35 µg lymphocyte extracts were incubated at 37°C for 16 hr or 0 hr with 2 µg bovine kidney HS. Lymphocyte heparanase activity at 16 hr is indicated as a decrease in staining of slower migrating material (in the upper portion of the gel) compared to the 0 hr control.

d. 5 mU Hep III, 133 µg α,MM, 267 or 533 µg α,MM or were incubated at 37°C for 16 hr with 2 µg bovine kidney HS. (HS alone control lane for 133 µg α,MM is found in Figure 14. HS control lane for 267 and 533 µg α,MM is found in Figure 27 right-hand side). Hep III strongly digests HS as indicated as a marked decrease in the staining of slower migrating material (in the upper portion of the gel) compared to HS alone control. Similarly, α,MM heparanase appears to be active at 133 µg and slightly active at 267 µg.

Figure 17.

a.
KNRK 72 hr
KNRK 0 hr
HS
KNRK ext
NRK 72 hr
NRK 0 hr
HS
NRK ext
b.
HS
KNRK 16 hr
KNRK 0 hr
3T3 16 hr
3T3 0 hr
HL60 16 hr
HL60 0 hr
U937 16 hr
U937 0 hr
HSC93 16 hr
HSC93 0 hr
TK6 16 hr
TK6 0 hr
c.
PMN 16 hr
PMN 0 hr
Lymphocyte 16 hr
Lymphocyte 0 hr
d.
HS+ Hep III
HS alone
α,MM 133 ug 16 hr
α,MM 133 ug 0 hr
α,MM 267 ug 16 hr
α,MM 533 ug 16 hr

others [94,111,114,115,126,127]. It has been noted that PMN heparanase activity is very low compared to B16 murine melanoma heparanase [127]. Those cells that I found to be negative for heparanase activity may have heparanases that have different substrate preferences other than bovine kidney HS. It is therefore not be surprising that the two kidney cell lines, KNRK and NRK, were able to digest bovine kidney HS relatively well. Invasive cells such as B16F10 murine melanoma cells may lack substrate specificity and therefore be able to digest different sources of HS with greater ease. It is tempting to speculate that the stronger heparanase activity observed in KNRK cells relative to NRK cells is due to transformation by Kirsten-*ras* since heparanase activity is elevated in highly metastatic cells [94,96,109,119].

Two purified HS-degrading enzymes were tested in the PAGE assay to investigate their potential use as positive controls in the development of the new assay. Hep III (Figure 17d; Figure 21d) was found to extensively digest bovine kidney HS (here 5 mU; minimum about 0.3 mU as in Figure 23e). α,MM was not active at several concentrations ranging from 1.3 to 53 µg protein/10 µL reaction (not shown). It was, however, slightly active at 133 µg or 267 µg but not at higher concentrations (such as 533 µg/10 µL reaction) (Figure 17d). (This inactivity may have been due to the higher concentration of salt as greater amounts of enzyme were added.) Therefore, Hep III was chosen as a more suitable positive control.

II.2. *Application of the PAGE Assay To the Heparanase Cloning Project*

A λgt11 bacteriophage library was constructed from the mRNA of KNRK cells (described in [68]), a cell line that we had confirmed to exhibit heparanase activity using our standard PAGE assay (Section II.1.) and that Dr. Vlodavsky had shown to be active using both ^{35}S-ECM and gel chromatography assays. Initial screening of the library for heparanase was performed using primary antibodies raised to a synthetic keyhole limpet hemocyanin-peptide conjugate corresponding to the *N*-terminal sequence of a putative heparanase [68] as published by Jin *et al.* [119]. Several experiments were performed to characterize the specificity of these antibodies.

II.2.1. *Testing for Inhibition of Heparanase by Primary Antibodies to the N-Terminal Peptide Fragment of the Putative Heparanase*

Others in our lab prepared and used antibodies to detect the presence of the putative heparanase peptide sequence in KNRK cells by immunoblot analysis [68]. Immune serum R8IS5 yielded particularly strong immunoreactivity to a 98 kDa protein from our heparanase-positive cell lines, KNRK and B16F10. This corresponded to the molecular weight of the original melanoma heparanase reported by Jin *et al.* (96 to 97 kDa) [96,119]. Immune serum R8IS5 also detected a 210 kDa protein found in positive clones from the λgt11 library. This corresponded to the predicted molecular weight of the β-galactosidase fusion protein. Furthermore, the observed immunoreactivities described above were competed out by excess peptide, indicating that the antibodies were specific for the peptide. However, immune serum R8IS5 also detected (equally strong) a 98 kDa protein in U-937, HL-60, Rec and NIH 3T3 (not shown), cell lines that were all shown to be negative with respect to heparanase activity in the PAGE assay (Section II.1.). This

would suggest that either the antibody was not specific for heparanase or that the conditions of the heparanase assay were not optimal to detect activity in these cells. Therefore, as a test of the specificity of the antibodies towards heparanase, the possibility of inhibition of heparanase activity by the antibodies was investigated using the PAGE assay.

Results and Discussion:

Neither pre-immune (PreS1R8) nor immune sera (R8IS5) inhibited KNRK heparanase (Figure 18a). The same was true for immune sera from eight other rabbits (Figure 18b). In the event that heparanase activity was present in the sera itself (in which case KNRK heparanase may falsely appear active although inhibited by the antibody), pre-immune and immune sera were incubated with HS (in the absence of KNRK extract). Heparanase activity was not found in any of the sera (data not shown). Together, these results suggest either that the antibodies recognize an epitope different from the active site or that they do not recognize heparanase at all.

II.2.2. *Heparanase or heat shock protein?*

While the antibody screening of the λgt11 library was being carried out in our laboratory, there were unpublished reports that the original published heparanase peptide sequence was actually that of a heat shock protein that had co-purified with heparanase rather than heparanase itself. This would suggest that heparanase may normally be complexed to or its folding may be mediated by such heat shock proteins. This prompted an investigation into the effect of heat shock on KNRK cells. Using conditions of heat shock that were sufficient to induce heat shock protein (hsp) 70 transcription, others in our

Figure 18. *Absence of inhibition of KNRK heparanase by putative anti-heparanase peptide antibodies.*

a. To test for possible inhibition of heparanase activity by the antibodies, 50 µg KNRK extract was incubated either 16 hr or 0 hr at 37°C with 2 µg bovine kidney HS in the presence or absence of 0.5 µL immune sera sample R8IS5 ("IS") or pre-immune sera sample PreS1 R8 ("Pre") and subjected to the PAGE assay as described in Figure 14. (Note: Proteinase K/urea treatment and 30 min electrophoresis were performed in the experiment shown). KNRK heparanase activity at 16 hr, indicated by a decrease in the staining of slower migrating material (in the upper portion of the gel) compared to 0 hr or HS controls, is neither inhibited by immune nor pre-immune sera.

b. Immune sera from eight different rabbits were tested for possible inhibitory effects on heparanase activity. 45 µg KNRK was incubated with 2 µg bovine kidney HS in the presence or absence of 0.05 µL equivalent of immune sera samples obtained from rabbits 1 to 8 ("R1" to "R8") for 16 hr or 0 hr at 37°C and subjected to the PAGE assay as in Figure 14. KNRK heparanase activity at 16 hr, indicated by a decrease in the staining of slower migrating material (in the upper portion of the gel) compared to 0 hr or HS controls, is not inhibited by immune sera from the eight rabbits.

Figure 18.

a.
16 hr
0 hr
HS
extract
16 hr+IS
0 hr+IS
HS+IS
extract+IS
16 hr+Pre
0 hr+Pre
HS+Pre
extract+Pre
b.
16 hr
0 hr
HS
extract
16 hr R1
0 hr R1
16 hr R2
0 hr R2
16 hr R3
0 hr R3
16 hr R4
0 hr R4
16 hr R5
0 hr R5
16 hr R6
0 hr R6
16 hr R7
0 hr R7
16 hr R8
0 hr R8

laboratory found no induction of the putative heparanase sequence by Northern analysis and no increased expression of the protein by Western analysis (not shown). This initially suggested that the published sequence was probably not of a heat shock-induced protein. To complement this study, extracts prepared from control and heat shocked KNRK cells and tested in the PAGE assay to determine whether heat shock induced heparanase activity. Increased heparanase activity might result due to increased stability of the protein when complexed with induced heat shock proteins, rather than increased heparanase transcription or translation.

Results and Discussion:

Heat shock did not appear to alter KNRK heparanase activity (Figure 19). This would suggest that heparanase activity was not enhanced by induction of heat shock proteins. Thus, neither the expression nor activity of heparanase was found to be heat shock-inducible.

II.2.3. *Immunoselection of λgt11 Clones Containing the Putative N-Terminal Heparanase Sequence and Testing for Heparanase Activity Using the PAGE Assay*

Bacterial lysogens from the λgt11 library were grown and immunoselected on the basis of reactivity towards the putative anti-heparanase antibody by M. DeVouge [68]. Competition by excess peptide was used to verify the specificity of the antibody-antigen reaction in positive clones. A single such clone was isolated and purified. Bacterial lysates were prepared from the positive clone and subjected to the PAGE-based heparanase assay to determine whether the clone exhibited heparanase activity (assuming that heparanase expressed in bacteria was active, as it has been reported in an abstract [120] but never published).

Figure 19. ***Heparanase activity is not induced by heat shock.***

KNRK cells were heat shocked for 1 hr at 43°C (5% CO_2 in air) and further incubated at 37°C for 90 min to allow for heat shock response to occur. Cell viability was not altered by this treatment (as assessed by trypan blue staining). 50 µg whole cell extracts were prepared and incubated with 2 µg bovine kidney HS in 20 mM cacodylate pH 6.1 for 16 hr or 0 hr. Reactions were added to lyophilized proteinase K/urea, incubated at 60°C for 1 hr, electrophoresed 40 min on 7.5% PAGE, stained, destained and dried as described in Figure 14. KNRK heparanase activity at 16 hr, indicated by a decrease in the staining of slower migrating material (in the upper portion of the gel) compared to 0 hr or HS controls, is not induced by heat shock.

Figure 20. ***Absence of heparanase activity in immunoselected λgt11 clones.***

Bacterial lysates were prepared as described in [68]. Briefly, cells were pelleted at 1000*g* for 5 min at RT, resuspended in 0.02 volumes of original culture of 10 mM Tris-HCl, pH 8.0, 150 mM NaCl, 0.1 mM CDTA, frozen quickly in liquid nitrogen, and stored at -100°C until needed. Once thawed, PMSF was added to 2 mM and lysozyme to 0.25 mg/mL. The suspension was incubated at 0°C for at least 1 hr to lyse the cells. To reduce viscosity, the lysates were sonicated twice for 15 seconds at power setting 5 on a 50-watt Microson automatic cell disrupter, cooling on ice in between pulses. Protein content of lysates was measured using the fluorescamine assay for protein. 50 µg of KNRK extract or bacterial lysate were incubated with 2 µg bovine kidney HS at 37°C for 16 hr or 0 hr in 20 mM cacodylate pH 6.1 and subjected to the PAGE assay as described in Figure 14. "λ" and "10-4" refer to the non-recombinant and recombinant clone respectively. "-IPTG" and "+IPTG" refer to uninduced and induced bacterial cultures respectively. Induced recombinant bacterial clones immunoselected by the putative anti-heparanase antibodies do not display any heparanase activity at 16 hr as indicated by the absence of a decrease in the staining of slower migrating material (in the upper portion of the gel) compared to 0 hr or HS controls (as seen with KNRK heparanase at 16 hr).

Figure 19.

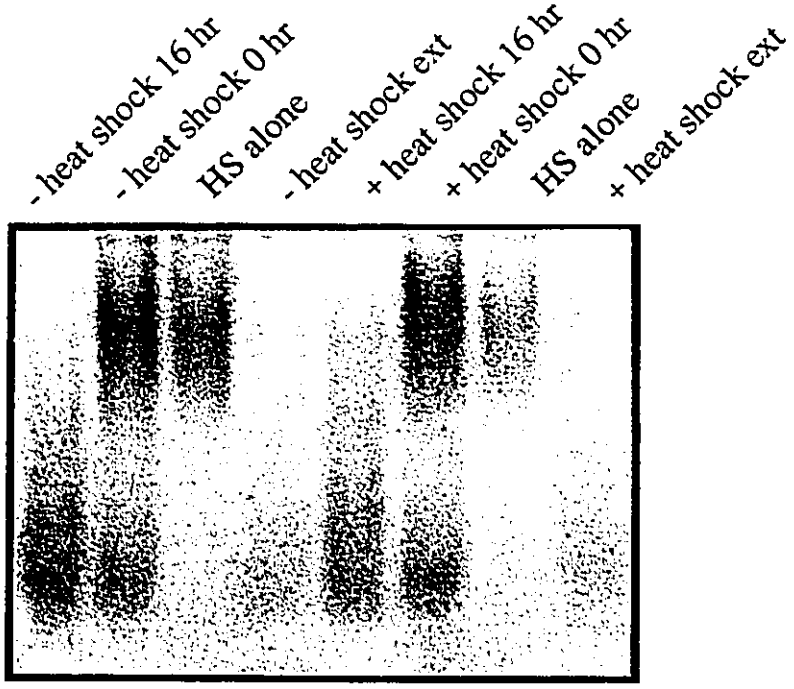

Figure 20.

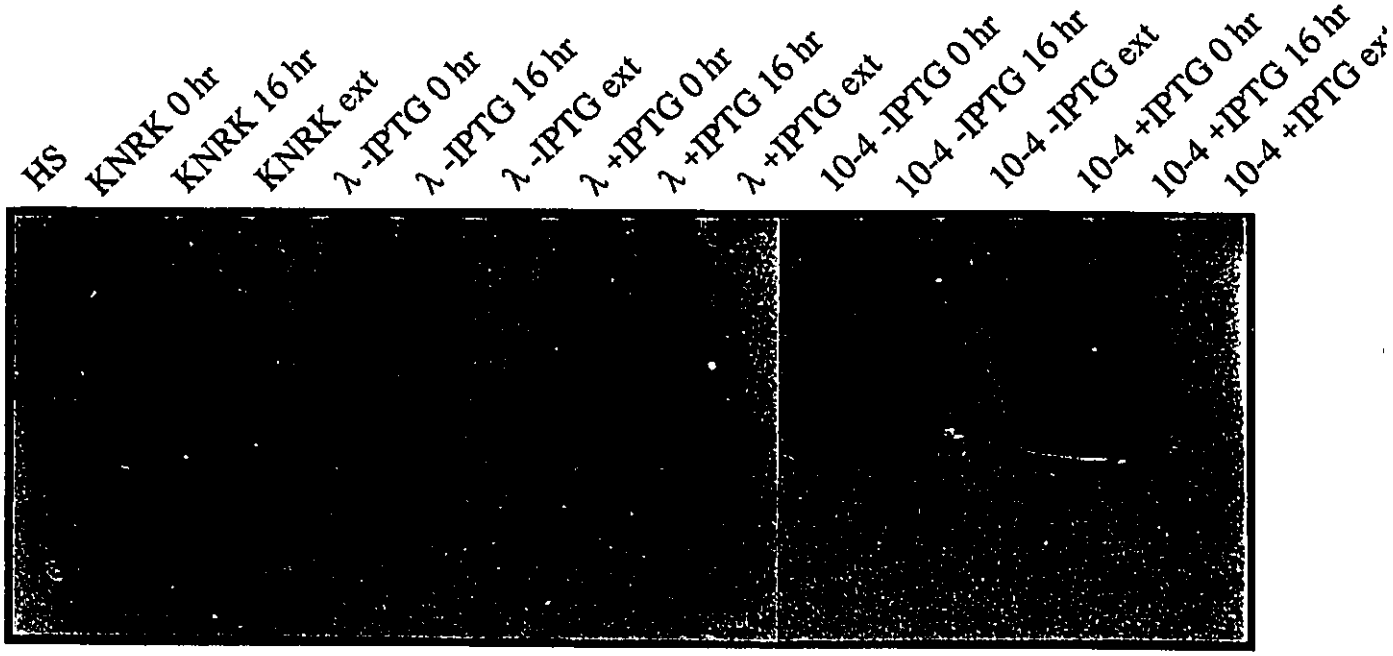

Results and Discussion:

The bacterial clone positive for specific reaction to the putative anti-heparanase antibody was negative with respect to heparanase activity using the PAGE assay (Figure 20). This could be due to inappropriate expression, insolubility and/or absence of required processing of the protein in bacteria rendering the enzyme non-functional. However, taken together with the above findings, it is also possible that the original peptide sequence was not part of a heparanase. In the same paper, we have shown that the published N-terminal sequence used to generate the putative anti-heparanase antibody rather encodes for endoplasmin (GRP94, glucose-regulated protein of 94 kDa), a molecular chaperone [68]. This would suggest that GRP94 had been co-purified with heparanase (although we cannot rule out that heparanase may contain part of the same sequence as found in GRP94). GRP94 is a stress-related protein having significant homology to the heat shock proteins, hsp70 and hsp90 [128]. This finding is not necessarily inconsistent with our heat-shock experiments since GRP94 is induced under stress conditions such as glucose deprivation [94] rather than heat-shock.

II.2.4. *Sib Selection Screening of the λgt11 Library Using the PAGE Assay*

As an alternative screening strategy, the λgt11 library could also be screened on the basis of heparanase activity using the PAGE assay and a sib selection approach.

Results and Discussion:

To calculate the number of cells in a pool and the number of pools of cells to be screened, it was first necessary to determine the minimum amount of KNRK extract that would be needed to detect heparanase activity in the PAGE assay. Using bovine lung HS

as a substrate, this minimum amount was determined to be approximately 5 µg extract protein (Figure 21) (less than 10 µg for bovine kidney HS (not shown)). 5 µg extract protein corresponds to about 0.5 ng heparanase (a conservative estimate based on Dr. Vlodavsky's 10,000 fold purification of placental heparanase). Assuming that heparanase may account for roughly 5% of the protein of an extract from a pure clone of induced, heparanase-expressing bacterial cells, at least 2.5 µg of 50 µg protein typically used in a PAGE assay would be heparanase itself. Diluting a pure clone 300x with non-heparanase-expressing cells would mean that 50 µg bacterial extract would contain only about 8 ng heparanase, which should be readily detectable using the PAGE assay. Thus, our 90,000 clone library was divided into 300 pools of 300 cells. After culturing, half of each pool was stored and the other half was used to prepare lysates that were subjected to the PAGE assay (work by H. Song in our laboratory). With this procedure, even after a second round of screening, none of the pools tested positive for heparanase activity (data not shown). These results suggest that heparanase may be non-functional or inappropriately expressed in bacteria or this library did not contain the full-length cDNA for heparanase. The latter is less likely since the mRNA used to construct the library contained high-molecular weight mRNA suggesting the presence of full-length messages.

II.2.5. *Proposed Sib Selection Screening of Mammalian Expression Library Using the PAGE Assay: Mixing Experiments with TK6 and KNRK*

In parallel with the bacterial expression library screening, a mammalian expression library from KNRK mRNA was being prepared. Since it is more likely that heparanase would be properly expressed in this system, such a library is more appropriate for screening on the basis of heparanase activity. TK6 cells, shown to be negative with

Figure 21. ***Minimum amount of KNRK extract needed to observe digestion of HS in the PAGE assay.***

1, 5, 25 or 50 µg of KNRK extract was incubated with 2 µg bovine lung HS at 37°C for 16 hr in 20 mM cacodylate pH 6.1 and subjected to the PAGE assay as described in Figure 14. Heparanase activity at 16 hr with 5 to 50 µg KNRK extract is indicated as a decrease in the staining of slower migrating material (in the upper portion of the gel) compared to the HS and respective 0 hr controls.

Figure 22. ***KNRK heparanase activity is not inhibited by TK6 extract.***

2 µg bovine lung HS was incubated for 16 hr at 37°C alone or with either 25 µg of KNRK extract, 25 µg KNRK extract plus 25 µg TK6 extract, or 25 µg TK6 extract in 20 mM cacodylate pH 6.1 and subjected to the PAGE assay as described in Figure 14. KNRK heparanase activity, indicated as a decrease in the staining of slower migrating material in the "+ KNRK" lane (in the upper portion of the gel) compared to the HS control, is not inhibited by TK6 extract (as seen in the "+ KNRK + TK6" lane).

Figure 21.

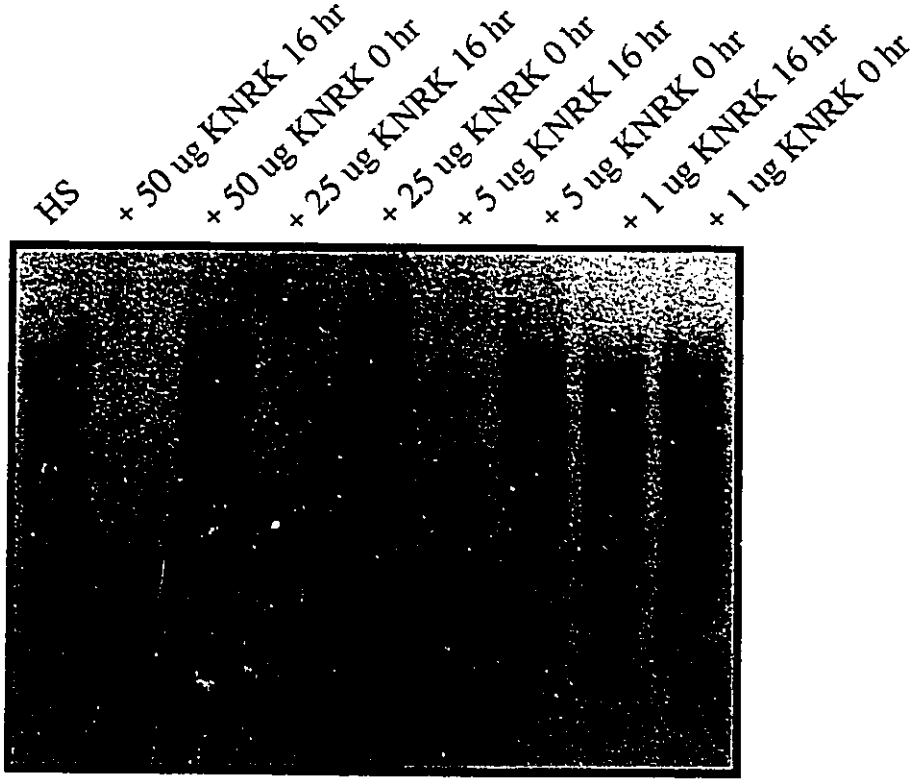

Figure 22.

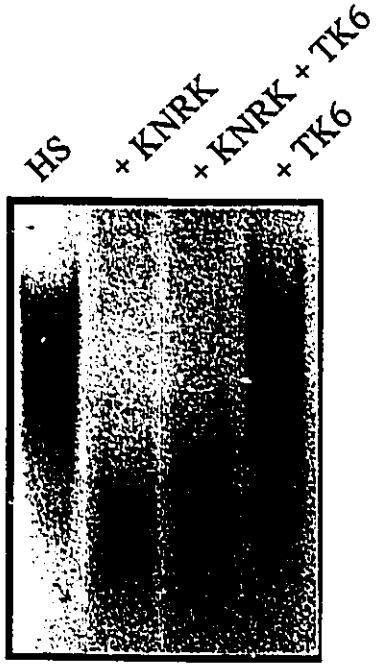

respect to heparanase activity (Figure 17b), were chosen as mammalian host cells for transfection with a KNRK cDNA library packaged in a mammalian expression vector system. It was therefore necessary to establish whether components in TK6 cell extracts could potentially inhibit KNRK heparanase. This was tested using PAGE analysis by co-incubating KNRK and TK6 extracts with HS.

Results and Discussion:

TK6 extract alone did not exhibit heparanase activity while KNRK was very active (Figure 22). Co-incubation of KNRK and TK6 extracts did not alter KNRK heparanase activity suggesting that the TK6 extract was not inhibitory to KNRK heparanase. (In retrospect, "extract only" controls should have been performed to confirm that the slight darkening of the "+KNRK+TK6" lane was due to the presence of the TK6 extract and not slight inhibition of KNRK heparanase by TK6 extract.) Therefore, it appeared that TK6 cells were suitable hosts for the mammalian expression library.

II.2.6. *Summary of Section II.1. and II.2. and Recent Developments in the Cloning Project*

Purified Hep III has been found to be a suitable positive control for HS digestion in the PAGE assay. Of the cells tested in our laboratory using the PAGE assay, only KNRK, B16F10, NRK and lymphocytes exhibited heparanase activity (Figures 14 and 17). Among these heparanase-positive cells, KNRK cells were identified to have the strongest activity.

We constructed a bacterial λgt11 expression library from mRNA of KNRK cells. Using antibodies raised toward the published putative heparanase *N*-terminal peptide sequence, we specifically immunoselected a clone from this library, whose sequence corresponds to GRP94/endoplasmin and whose expressed protein product does not exhibit

heparanase activity (Figure 20). Failure of the antibodies to inhibit KNRK heparanase activity (Figure 18) taken together with the above findings casts doubt on the specificity of the peptide sequence for heparanase (although it may also be that the antibodies do not recognize the active site). Either heparanase activity is not properly expressed in bacteria or heparanase does indeed contain the same peptide sequence as found in GRP94. The former is possible since sib selection screening of the λgt11 library using the PAGE assay has not revealed an active heparanase-positive clone. Sib selection screening based on enzyme activity of the newer mammalian expression library in TK6 cells (cells shown to lack heparanase activity (Figures 17 and 22)) should solve this question. In terms of the latter, while homology of the *N*-terminal peptide sequence to the hsp90 family of molecular chaperones and cell-surface tumour glycoprotein rejection antigens has been noted by others [128-130], it is agreed that the conclusion that heparanase shares the same sequence must be approached with caution [130] since it is possible that the published peptide sequence belongs to a contaminating molecular chaperone that had co-purified with heparanase.

Recently, human platelet heparanase has been purified, sequenced and identified to be part of the previously cloned platelet basic protein (PBP). Heparanase activity is associated with two *N*-truncated products PBP known as connective tissue activating peptide-III (CTAP-III) and neutrophil activating peptide-2, both of which are chemokines [110]. Although platelet heparanase, an endoglucosaminidase which digests both heparin and HS, is different from KNRK heparanase (which digests only HS (Section II.3.4.)), the two presumably belong to a family of heparanases. Both share a pH optimum of close to

pH 6 (Section II.3.2.). Platelet heparanase is a small enzyme of 8 to 10 kDa; if KNRK heparanase is also small, it may explain its apparent stability to freeze/thawing. The authors believe that post-translational modifications activate the platelet enzyme; this may explain our inability to detect heparanase activity in bacterial extracts during attempts to clone KNRK heparanase.

II.3. *Characterization of KNRK and Other Heparanases Using the PAGE Assay*

Prior to our studies, KNRK cells had never been shown to exhibit heparanase activity and thus characterization of the enzyme was of interest. Characterization of KNRK and other heparanases with respect to substrate specificity, pH optimum, sensitivity to the heparanase inhibitor heparin and exo-β-glucuronidase inhibitor saccharic acid 1,4-lactone (SAL), was performed on a qualitative basis using the PAGE assay. From analysis of substrate specificity, a suitable HS substrate and starting material for the PAGE as well as the new fluorescent assay could also be chosen.

II.3.1. *Comparison of Bovine Intestine, Kidney and Lung HS Digestibility by Various Heparanases*

HS starting material was chosen such that it was of the highest average molecular weight. The higher the molecular weight, the greater the probability of endoglycosidic cleavage occurring, and furthermore, the greater separation between starting material and products when separated using PAGE. Among the commercially available sources (of which there are very few), bovine intestine and bovine kidney were initially compared. Later in our studies, we acquired bovine lung HS from Dr. Vlodavsky to compare its digestibility with our existing bovine kidney HS substrate.

Results and Discussion:

Because bovine intestine HS was found to be of lower average molecular weight (greater mobility) compared to the substrate we had been using, HS "pbs", digestion by KNRK was difficult to detect (Figure 23a). Figure 23a also exemplifies the greater contrast that is achieved between 16 hr and 0 hr digests with higher molecular weight fractions of substrate (HMW#1 compared to HMW#3) thus allowing easier detection of heparanase activity. Another substrate, HS "pfs", ran faster in the gel and its digestion by KNRK was also less apparent than with HS "pbs" (Figure 23b). HL-60 cells did not digest either bovine kidney HS substrate. Because of its higher molecular weight and greater susceptibility to digestion, bovine kidney HS (pbs) was chosen for subsequent chemical modifications for the new assay.

Bovine lung HS which, although it migrated faster in the gel than bovine kidney HS, was found to be much more digestible by KNRK, B16F10 (Figure 23c as compared to Figure 14) and lymphocytes (Figure 23d as compared to Figure 17c). For B16F10, this is not very surprising since the cell line has been characterized to be highly invasive and metastatic with high potential for lung colonization [94]. It can be speculated that the differences in digestibility may be due to the composition of the HS substrates as it has been shown that, among other differences, bovine lung HS has a greater proportion of 6-*O*-sulfated glucosamine residues than bovine kidney HS [118] and that more highly metastatic tumours have basement membranes with more highly sulfated HS (especially sulfation as 6-*O*-sulfated glucosamine) [131].

The differences between digestibility of bovine kidney and lung HS as substrates

Figure 23. *Comparison of bovine intestine, kidney, and lung HS in terms of electrophoretic mobility and susceptibility to digestion by heparanases.*

Bovine intestine (Sigma) and bovine kidney ("pbs" or prepared by Sigma) HS samples were size fractionated (as described in Section I.1.). For comparison, another bovine kidney HS substrate ("pfs" or prepared for Sigma) and bovine lung HS substrate (gift from Dr. I. Vlodavsky) were tested. To conserve material, size fractionation of bovine lung HS was not performed. The concentration of bovine lung HS stock was determined to be ~ 30 µg/µL in the dimethylmethylene blue (DMMB) assay (Appendix II.1.) using unfractionated bovine kidney HS (pbs) as the standard.

KNRK, HL-60 and B16F10 cells were maintained and PMNs and lymphocytes were freshly isolated as described in the legend for Figure 17.

a. 2 µg unfractionated ("total") or fractionated (HMW#1, HMW#2 or HMW#3) HS from bovine intestine ("bi") and bovine kidney ("bk") (prepared by Sigma) were incubated with 40 µg KNRK extract in 20 mM cacodylate buffer pH 6.1 for 16 hr or 0 hr at 37°C and subjected to PAGE analysis as described in Figure 14. KNRK heparanase activity at 16 hr, indicated as a decrease in the staining of slower migrating material (in the upper portion of the gel) compared to 0 hr or HS alone controls, is most clearly seen with bovine kidney HS, particularly with higher molecular weight fractions (HMW#1 and 2).

b. 2 µg unfractionated bovine kidney HS ("pbs" or prepared by Sigma) or HS ("pfs" or prepared for Sigma) were incubated with 20 µg KNRK or HL-60 extract in 20 mM cacodylate buffer pH 6.1 for 16 hr at 37°C and subjected to the PAGE assay as described in Figure 14. (Note: This gel was not soaked in water prior to staining with methylene blue therefore SDS has stained in the lower portion of the gel.) KNRK heparanase activity is seen using both HS preparations obtained from Sigma, indicated as a decrease in the staining of slower migrating material in "+KNRK" lanes compared to HS alone controls.

c. 2 µg unfractionated bovine lung ("bl") HS were incubated with 60 µg KNRK or B16F10 extract or 130 µg α,MM in 20 mM cacodylate buffer pH 6.1 for 16 hr or 0 hr at 37°C and subjected to the PAGE assay as described in Figure 14. Strong KNRK and B16F10 heparanase activity at 16 hr is indicated as a marked decrease in the staining of slower migrating material compared to 0 hr or HS controls. α,MM heparanase is slightly active.

d. 2 µg unfractionated bovine lung HS ("bl") was incubated with 67 µg PMN or 35 µg lymphocyte extract in 20 mM cacodylate buffer pH 6.1 for 16 hr or 0 hr at 37°C and subjected to the PAGE assay as described in Figure 14. Lymphocyte heparanase activity is seen at 16 hr as indicated by a decrease in the staining of slower migrating material compared to 0 hr control.

e. 2 µg fractionated (HMW#1) bovine kidney ("bk") or unfractionated lung HS ("bl") were incubated with 0.3 mU Hep III in 1x Hep III reaction buffer (0.25 M sodium acetate pH 8, 2.5 mM $CaCl_2$) for 16 hr or 0 hr at 37°C and subjected to the PAGE assay as described in Figure 14. Hep III digests both substrates as indicated by decreases in the staining of slower migrating material compared to 0 hr or HS controls.

Figure 23.

c
bl alone
bl+KNRK 16 hr
bl+KNRK 0 hr
KNRK ext
bl+B16F10 16 hr
B16F10 ext
bl+α,MM 16 hr
bl+α,MM 0 hr
d
bl+pMN 16 hr
bl+pMN 0 hr
bl+Lymphocyte 16 hr
bk+Lymphocyte 0 hr
e
bk
bk+Hep III 16 hr
bk+Hep III 0 hr
bl
bl+Hep III 16 hr
bl+Hep III 0 hr
f
bk(pbs)
bk(pfs)
bk(pbs)+KNRK
bk(pfs)+KNRK
bk(pbs)+HL60
bk(pfs)+HL60
KNRK ext
HL60 ext
g
bl(total)
16 hr bl(total)
0 hr bl(total)
bl/HMWW#1
16 hr bl/(HMWW#1)
0 hr bl/(HMWW#1)
16 hr bk(total)
0 hr bk(total)
16 hr bk(HMWW#1)
0 hr bk(HMWW#1)
16 hr bk(HMWW#2)
0 hr bk(HMWW#2)
16 hr bk(HMWW#3)
0 hr bk(HMWW#3)
ext alone

were more subtle with PMNs (Figure 23d as compared to Figure 17c), α,MM (Figure 23c as compared to Figure 17d) and Hep III (Figure 23e). Unlike KNRK and B16F10 cells, Hep III and α,MM usually appeared to digest bovine kidney HS more effectively than bovine lung HS.

Although most chemical modification studies for the proposed assay were carried out using the higher molecular weight bovine kidney HS, the more digestible bovine lung HS was later found to be more suitable for chemical modification for reasons described later (Section III.6.).

II.3.2. *pH Optimum for KNRK Heparanase and Its Possible Requirement for Calcium*

The pH optimum for heparanase has been reported to be between pH 5 and 6 [94,96,109,110]. However, heparanase assays have routinely been performed at pH 6 to prevent protein precipitation [94]. Others have reported pH optima of 6.2 to 7.5 and higher [111-113,116] depending on the cell type. pH optimum for KNRK heparanase was determined using the PAGE assay. Also, in order to establish a requirement of calcium or reducing conditions by heparanase, digests were carried in the presence or absence of calcium, with or without reducing agent, at a pH at which heparanase activity was lower and analyzed using the PAGE assay. Dithiothreitol (DTT) was used as a reducing agent under similar conditions used by Dr. Vlodavsky with his human placental heparanase (α,MM) (personal communication).

Results and Discussion:

In the range of pH 6 to 8, KNRK heparanase was only active at pH 6 (very active) to 6.5 (partially active) (Figure 24a and 24b). At pH 7 or greater, enzyme activity was

virtually undetectable. (Although protein precipitation might occur at lower pH as described by others [94], a reaction could have been carried out at pH less than 6 to see if KNRK heparanase was more active at lower pH.) The narrow range of activity around pH 6 is consistent with other heparanases [96,108-110,112] and may suggest lysosomal origin [104,108,109].

Addition of calcium at pH 7 did not improve KNRK heparanase activity (Figure 24b). Incubation in the presence of calcium and reducing agent (DTT) at pH 6.1 did not improve KNRK or α,MM activity but rather appeared to slightly reduce activity (Figure 24c) (whether this was due to reduced activity or reduced efficiency of background removal is unclear since 0 hr controls were not performed). KNRK activity was the same using either acetate buffer pH 6 (Figure 24b) or cacodylate buffer pH 6.1 (Figure 24c). Therefore, it appeared that KNRK heparanase was maximally active at pH 6 and did not require calcium or DTT for activity.

II.3.3. *Boiling or Treatment of KNRK Extract With β-Mercaptoethanol or SDS Prior to the PAGE Assay*

Boiling or treatment with reducing agent, β-mercaptoethanol, or detergent, SDS, of KNRK extract was employed as means to inactivate enzymatic activity to confirm the protein-like nature of heparanase and to serve as potential negative controls in the new fluorescence-based heparanase assay.

Results and Discussion:

From Figure 25a, KNRK heparanase activity was abolished with 10 min boiling or treatment with 47 mM β-mercaptoethanol, conditions under which typical protein enzymes would be inactivated. From Figure 25b, KNRK heparanase was partially inhibited by

Figure 24. ***Determination of pH optimum of KNRK heparanase and requirement for calcium or reducing agent by KNRK and α,MM heparanases.***

a. 25 µg of KNRK extract was incubated with 2 µg bovine lung HS at 37°C for 16 hr or 0 hr in 250 mM sodium acetate pH 6, 7 or 8 and subjected to the PAGE assay as described in Figure 14. Note: "HS" was incubated in 20 mM cacodylate pH 6.1 rather than sodium acetate buffer.

b. 2 µg bovine lung HS was incubated alone or with 25 µg of KNRK extract at 37°C for 16 hr or 0 hr in 250 mM sodium acetate pH 6, 6.5 or 7 and subjected to the PAGE assay as described in Figure 14. For pH 7, incubations were performed either in the presence or absence of 2.5 mM $CaCl_2$.

c. 200 µg α,MM or 25 µg KNRK was incubated with 2 µg bovine lung HS in 20 mM cacodylate buffer pH 6.1 in the presence or absence of 1 mM $CaCl_2$/1 mM DTT at 37°C for 16 hr and subjected to the PAGE assay as described in Figure 14.

In this figure, KNRK heparanase activity at 16 hr is strongest at pH 6, as indicated by the greatest decrease in the staining of slower migrating material (in the upper portion of the gel) compared to 0 hr or HS controls. KNRK and α,MM heparanase activity do not appear to require but rather may be slightly inhibited by calcium and/or DTT, as indicated by a slightly greater staining in the upper portion of "+Ca^{2+}/DTT" lanes compared to "+α,MM" or "+KNRK" lanes.

Figure 24.

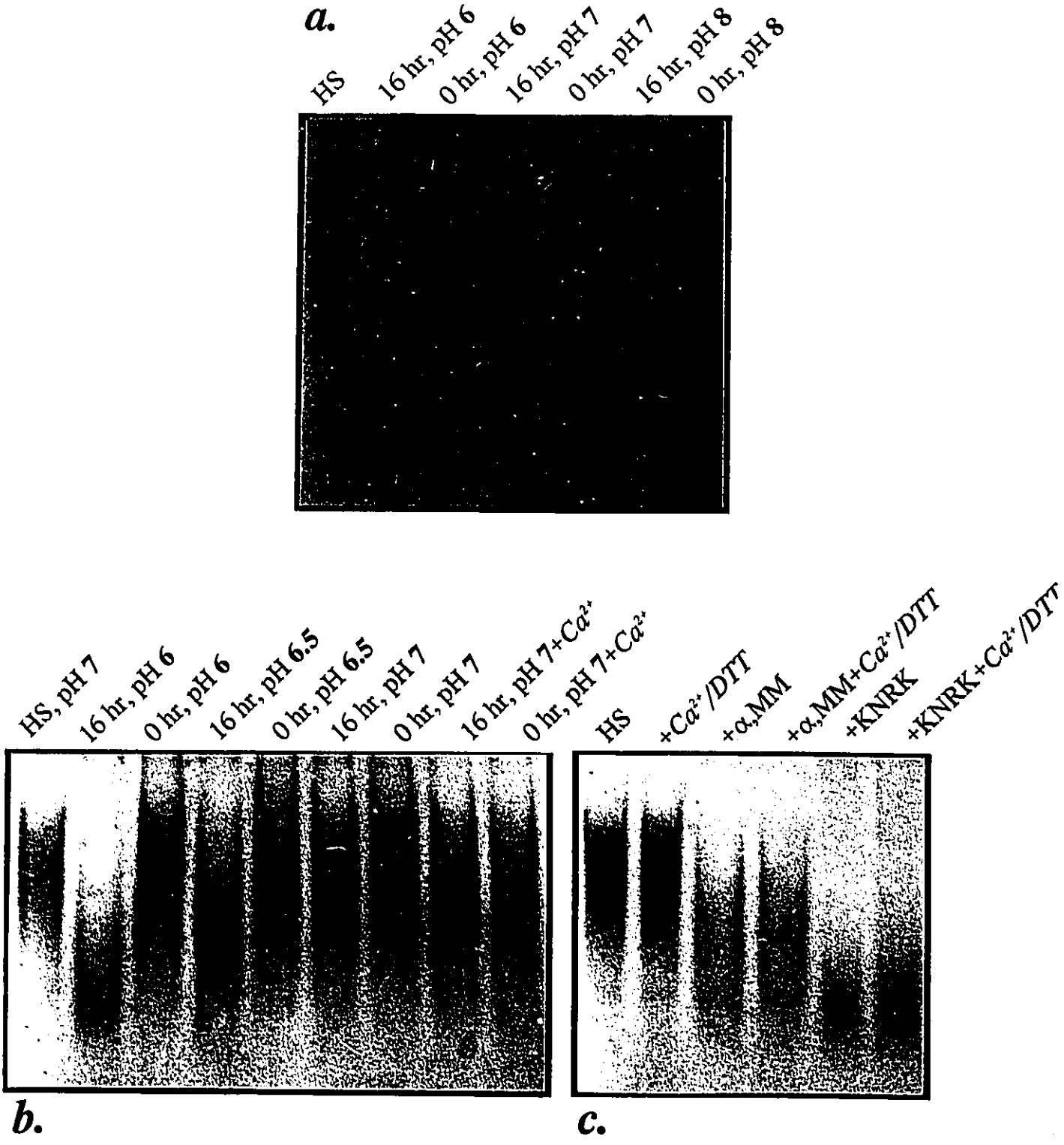
a.
HS
16 hr, pH 6
0 hr, pH 6
16 hr, pH 7
0 hr, pH 7
16 hr, pH 8
0 hr, pH 8
HS, pH 7
16 hr, pH 6
0 hr, pH 6
16 hr, pH 6.5
0 hr, pH 6.5
16 hr, pH 7
0 hr, pH 7
16 hr, pH 7+Ca2+
0 hr, pH 7+Ca2+
b.
HS
+Ca2+/DTT
+α,MM
+α,MM+Ca2+/DTT
+KNRK
+KNRK+Ca2+/DTT
c.

Figure 25. ***Boiling or treatment of KNRK extract with β-mercaptoethanol or SDS prior to the PAGE assay.***

a. 50 µg of KNRK extract, with or without 10 min boiling ("boiled") or treatment with 47 mM β-mercaptoethanol ("β-ME"), was incubated with 2 µg of bovine lung HS at 37°C for 16 hr or 0 hr and subjected to the PAGE assay as described in Figure 14. KNRK heparanase activity at 16 hr, indicated as a decrease in the staining of slower migrating material (in the upper portion of the gel) compared to 0 hr or HS controls, is fully inhibited by boiling or treatment with β-mercaptoethanol.

b. To find a SDS concentration that was inhibitory to KNRK heparanase, 55 µg KNRK was incubated 16 hr or 0 hr with 2 µg bovine kidney HS at 37°C in the presence of 0, 0.02, 0.05 and 0.1% SDS and subjected to the PAGE assay as described in Figure 14. (Note: Rather than the usual proteinase K/SDS treatment, these digests were added to lyophilized proteinase K/urea (Section I.3.) and were incubated at 60°C for 1 hr. Also, this gel was not soaked in water prior to staining which resulted in background staining.) KNRK heparanase activity at 16 hr ("- SDS"), indicated as a decrease in the staining of slower migrating material (in the upper portion of the gel) compared to 0 hr or HS controls, is fully inhibited by 0.1% SDS.

Figure 25.

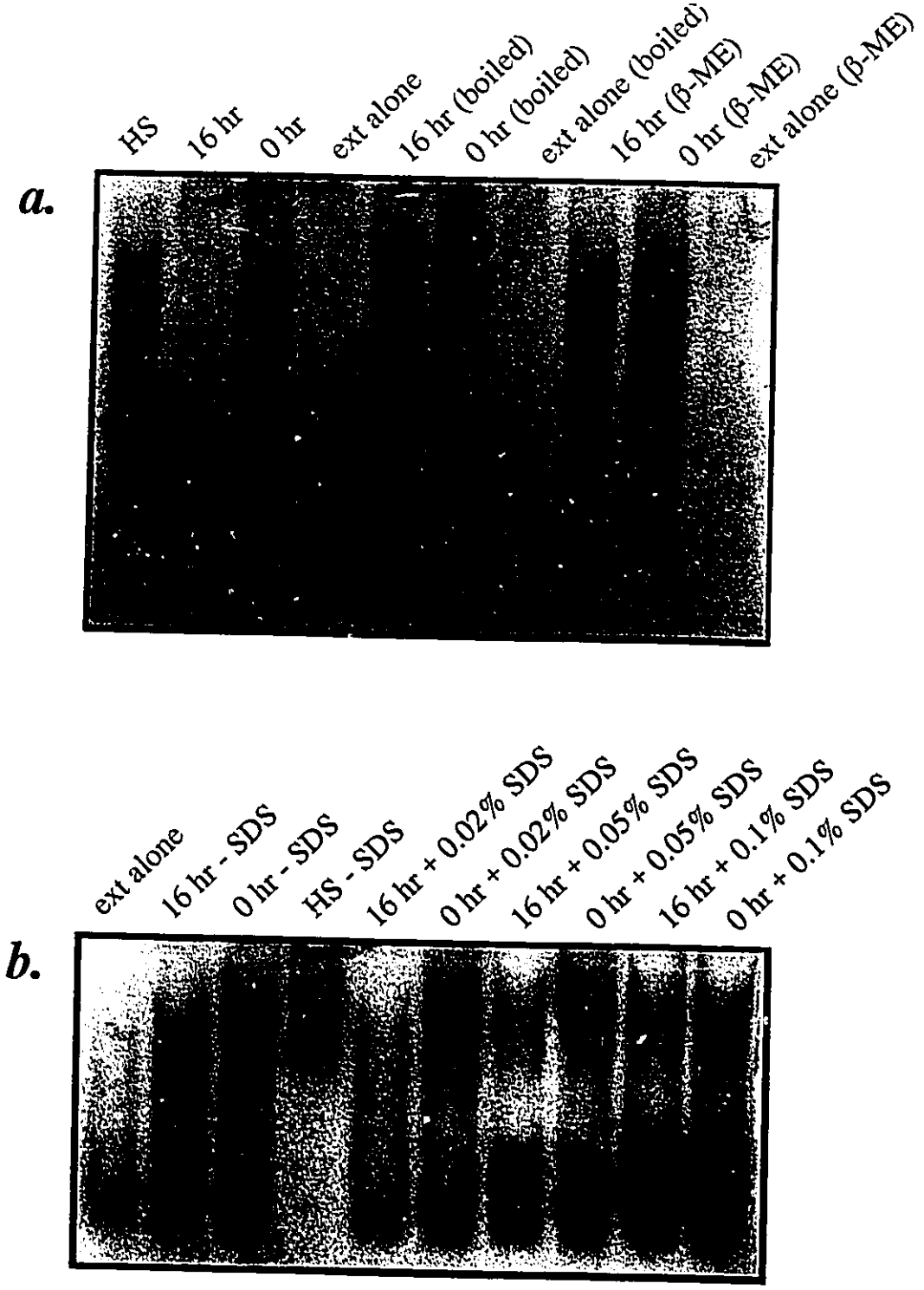
a.
HS
16 hr
0 hr
ext alone
16 hr (boiled)
0 hr (boiled)
ext alone (boiled)
16 hr (β-ME)
0 hr (β-ME)
ext alone (β-ME)
b.
ext alone
16 hr - SDS
0 hr - SDS
HS - SDS
16 hr + 0.02% SDS
0 hr + 0.02% SDS
16 hr + 0.05% SDS
0 hr + 0.05% SDS
16 hr + 0.1% SDS
0 hr + 0.1% SDS

0.05% SDS and completely inhibited by 0.1% SDS. Thus, HS-degrading activity appears to be attributed to a protein enzyme. These conditions may be useful for negative controls.

II.3.4. *Inhibition of KNRK Heparanase by Heparin*

Heparin has been reported to be a potent inhibitor of heparanases that exclusively degrade HS (e.g. melanoma, endothelial cell, lymphocyte, macrophage and neutrophil heparanases [108,114-117,132]). Two other types of heparanases characterized to date either digest both HS and heparin or heparin alone [96]. Inhibition of KNRK heparanase activity by heparin was investigated using the PAGE assay.

Results and Discussion:

Heparin (from Fisher) migrated with higher mobility in the gel than HS (Figure 26a and 26b). At 0.1 μg/μL, this heparin source did not inhibit KNRK heparanase digestion of bovine kidney HS (Figure 26a). Heparin itself was slightly digested by KNRK (Figure 26a) but not by Hep III (Figure 26b). (Inhibition of KNRK digestion of bovine lung HS by this heparin source was not performed.)

For comparison, bovine lung heparin (active as an inhibitor in Dr. Vlodavsky's assays) was also tested as an inhibitor of KNRK heparanase (Figure 26c). Bovine lung heparin also ran lower in the gel than kidney and lung HS. It was not, however, digested by KNRK as observed with Fisher heparin in Figure 26a. Bovine lung heparin was able to fully inhibit KNRK digestion of bovine kidney HS but only partially inhibit KNRK digestion of bovine lung HS. This might suggest that KNRK extract may possess two types of HS-degrading activities depending on the substrate used, one inhibitable and another not inhibitable by heparin. (One might speculate that this might be due to multiple

Figure 26. *Inhibition of KNRK heparanase by heparin.*

Heparin (sodium salt, Fisher) was co-incubated with KNRK extract or Hep III and subjected to the PAGE assay as described in Figure 14. For comparison, a higher quality bovine lung heparin (gift from Dr. Vlodavsky) was also tested.

a. 1 µg unfractionated bovine kidney HS and/or 1 µg heparin (Fisher) was incubated with 45 µg KNRK in 20 mM cacodylate buffer pH 6.1 for 16 hr or 0 hr at 37°C and subjected to the PAGE assay. KNRK heparanase activity at 16 hr, indicated as a decrease in the staining of slower migrating material in the "HS + KNRK 16 hr" lane (in the upper portion of the gel) compared to 0 hr or HS controls, is not inhibited by heparin ("HS + heparin + KNRK 16 hr" compared to "HS + heparin" or "HS + heparin + KNRK 0 hr" lanes). Heparin is slightly digested by KNRK, as indicated by a slight decrease in the staining of the upper portion of the heparin smear ("heparin + KNRK 16 hr" compared to "heparin" or "heparin + KNRK 0 hr" controls).

b. 2 µg heparin (Fisher) was incubated at 37°C for 16 hr in the presence or absence of 5 mU Hep III in 0.25 M sodium acetate pH 7.0 and 2.5 mM $CaCl_2$ and subjected to the PAGE assay. Hep III digestion of HS is not affected by heparin as indicated by the absence of alteration in HS staining.

c. 2 µg bovine lung ("bl") heparin was incubated alone or with either 2 µg bovine kidney ("bk") HS or 2 µg bovine lung HS in 20 mM cacodylate buffer pH 6.1 for 16 hr or 0 hr at 37°C in the presence or absence of 60 µg KNRK extract and subjected to the PAGE assay. KNRK digestion of bovine kidney HS at 16 hr, indicated as a decrease in the staining of slower migrating material (in the upper portion of the gel) compared to 0 hr or HS controls (in Figure 14), is inhibited by bovine lung heparin ("bk HS + bl heparin + KNRK 16 hr" shows no change from "bk HS + bl heparin" or "bk HS + bl heparin + KNRK 0 hr" lanes). KNRK digestion of bovine lung HS at 16 hr, indicated as a decrease in the staining of slower migrating material compared to 0 hr or HS controls (in Figure 23c), is partially inhibited by bovine lung heparin (as indicated by decreased staining in the upper portion of the "bl HS + bl heparin + KNRK 16 hr" lane compared to "bl HS + bl heparin + KNRK 0 hr" or "bl HS + bl heparin" lanes).

Figure 26.

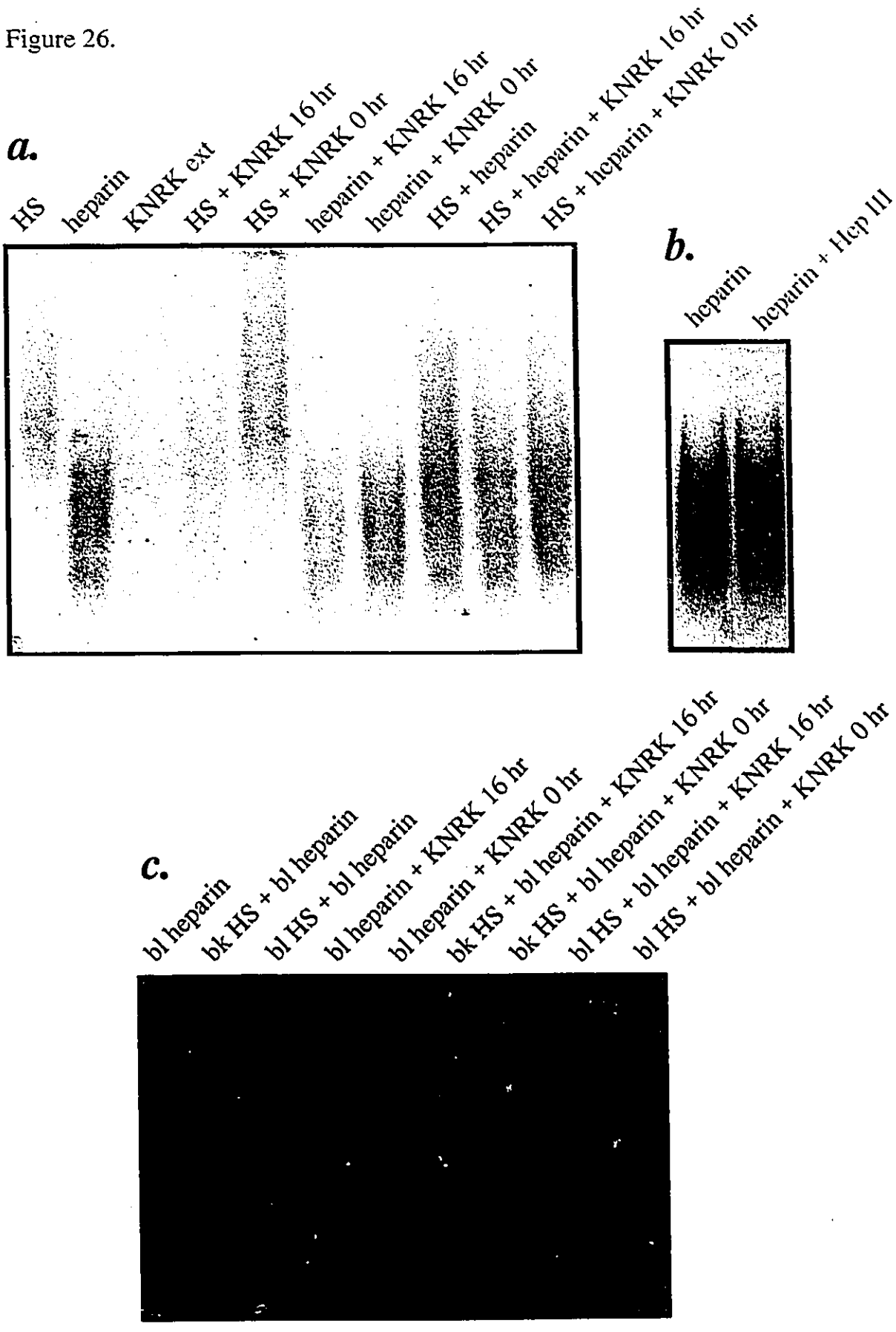
a.
HS
heparin
KNRK ext
HS + KNRK 16 hr
HS + KNRK 0 hr
heparin + KNRK 16 hr
heparin + KNRK 0 hr
HS + heparin
HS + heparin + KNRK 16 hr
HS + heparin + KNRK 0 hr
b.
heparin
heparin + Hep III
c.
bl heparin
bk HS + bl heparin
bl HS + bl heparin
bl heparin + KNRK 16 hr
bl heparin + KNRK 0 hr
bk HS + bl heparin + KNRK 16 hr
bk HS + bl heparin + KNRK 0 hr
bl HS + bl heparin + KNRK 16 hr
bl HS + bl heparin + KNRK 0 hr

endoglycosidase activities perhaps arising from different cell compartments [104,133] or that the two HS substrates differ in the proportion of cleavage sites that are inhibitable by heparin.) Thus, depending on the heparin source used, it appears that KNRK extract largely contains a heparin-inhibitable heparanase which is consistent with the HS-degrading heparanases and possibly another heparin-degrading heparanase.

II.3.5. *Inhibition of HS Exoglycosidase Activity by SAL*

Saccharic acid 1,4-lactone (SAL) has been used as a lysosomal exo-β-glucuronidase inhibitor [94,108,110]. To confirm that KNRK HS-degrading activity represented an endoglycosidase, digestion of bovine kidney HS with KNRK in the presence or absence of SAL was performed and subjected to the PAGE assay.

Results and Discussion:

Since SAL was found to be very acidic (~ pH 1.5), the pH of SAL was adjusted to pH 6.1. The concentration of Tris was increased ten fold for the MNase treatment to overcome the additional buffering at pH 6.1 by SAL. From Figure 27, SAL did not inhibit KNRK HS-degrading activity suggesting that KNRK extract exhibits HS endoglycosidase rather than exoglycosidase activity when bovine kidney HS is used as a substrate. Furthermore, whereas endoglycosidase activity yields oligosaccharides which produce the characteristic shift in the PAGE assay, exoglycosidase activities would have eventually yielded di- or monosaccharides [104] which would diffuse out of the gel. It may be speculated that KNRK digestion of bovine lung HS may be partially due to exoglycosidase activity although experiments with SAL were not performed using bovine lung HS as a substrate.

Figure 27. ***Inhibition of HS exoglycosidase activity by SAL.***

60 µg KNRK extract was incubated with 2 µg bovine kidney HS in the presence of 20 mM cacodylate buffer ± 20 mM SAL pH 6.1 for 16 hr at 37°C and subjected to the PAGE assay as described in Figure 14. Where indicated by "+T", the concentration of Tris-HCl pH 9.5 was increased ten fold for the MNase treatment. KNRK heparanase activity at 16 hr, indicated as a decrease in the staining of slower migrating material (in the upper portion of the gel) compared to 0 hr or HS controls, is not inhibited by SAL.

Figure 27.

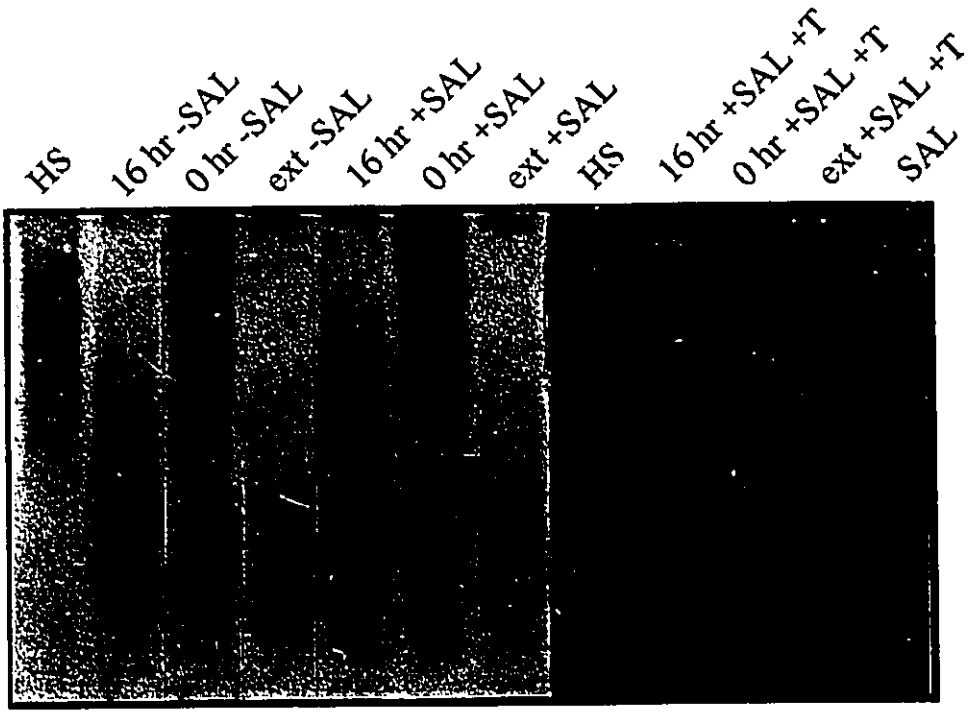
HS
16 hr -SAL
0 hr -SAL
ext -SAL
16 hr +SAL
0 hr +SAL
ext +SAL
HS
16 hr +SAL +T
0 hr +SAL +T
ext +SAL +T
SAL

II.3.6. *Comparison of PAGE Assay to ^{35}S-ECM Assay: Sensitivities to SAL and Heparin*

Dr. Vlodavsky later provided us with an ^{35}S-ECM plate prepared by his laboratory, essentially as described in [107]. As noted earlier in the *Introduction*, this assay, although easy to perform, is subject to interference by proteinases that release ^{35}S-labelled HS from remnant ECM proteins. However, with this assay, we were able to compare the results of the PAGE assays on the effects of SAL and heparin on KNRK heparanase activity as well as obtain a more quantitative measure of activity.

Results and Discussion:

KNRK heparanase was able to digest the ^{35}S-ECM substrate (Figure 28a). Unlike the inactivity typically seen in the PAGE assay (Figure 17d or 23c), α,MM heparanase was also very active in the ^{35}S-ECM assay (Figure 28a). It displayed a dose-dependent increase in ^{35}S release (in a very similar manner to Dr. Vlodavsky's results (personal communication)). Degradation was extensive and virtually complete with Hep III. Proteinase K resulted in marked release of label from remaining ^{35}S-HS attached to ECM proteins (Figure 28b). Because the contribution to ^{35}S release by proteolytic activity can potentially be large, this assay suffers from lack of specificity for solely detecting heparanase activity. However, in the case of KNRK, contribution by proteolysis was probably low since the addition of protease inhibitors did not alter ^{35}S release (Figure 28b).

When SAL and/or heparin (Fisher) were incubated with KNRK in the ^{35}S-ECM assay, KNRK was only slightly inhibited by their combination (Figure 28b) (the significance of this is not clear). KNRK activity was actually enhanced by SAL possibly due to the increased buffering at pH 6.1 by SAL (the pH optimum for the enzyme).

Figure 28. ***^{35}S-ECM digestion by cell extracts and purified endoglycosidases, and effects of SAL and/or heparin on KNRK heparanase.***

The 96 well plate coated with ^{35}S-labelled subendothelial ECM was prepared as described in [107,121]. Essentially, bovine corneal endothelial cells were cultured in the presence of $Na_2[^{35}S]SO_4$ for sufficient time to allow incorporation into HS. Cells were lysed with Triton X-100 and cellular debris was removed with NH_4OH treatment with washing. For my studies, wells were rehydrated and washed in PBS. 50 µL reactions with KNRK extract and purified α,MM enzyme were performed in 20 mM cacodylate buffer pH 6.1. Hep III digests were performed in 1x Hep III buffer (0.25 M sodium acetate pH 8, 2.5 mM $CaCl_2$). The plate was incubated at 37°C for the times indicated. After cooling, the well contents (50 µL) were removed and saved, wells washed with 50 µL PBS and pooled with the first fraction. 900 µL of Aquasol-2 was added, the mixtures were vortexed for 10 seconds and counted in a LKB Wallac 1219 Liquid Scintillation Counter.

a. Wells were incubated with 60 µg KNRK or α,MM (shown as a,MM from 4 to 320 µg) or Hep III (5 to 25 mU) for 1 hr and 40 min at 37°C. Error bars shown represent the range of duplicate wells; all other wells were treated in single trials.

b. Wells were incubated with 60 µg KNRK ± 20 mM SAL pH 6.1 (denoted as "S") ± 0.1 µg/µL heparin (Fisher). Error bars represent the range of duplicate wells. In single wells, 60 µg KNRK with protease inhibitors (shown as "+prot. inh.") (1 mM PMSF, 2 µg/mL aprotinin, 50 µM chymostatin) or 0.1 µg/µL proteinase K alone were incubated in cacodylate buffer. All incubations were performed at 37°C for 1 hr and 40 min.

c. Wells were incubated with 180 µg KNRK, 180 µg B16F10 or 320 µg α,MM in the absence ("-S") or presence ("+S") of 18 mM SAL pH 6.1. α,MM was also tested for inhibition by 0.1 µg/µL heparin (Fisher). 5 mU Hep III was as a positive control. Each of these experiments were carried out as single trials. All incubations were performed at 37°C for 1 hr.

Figure 28.

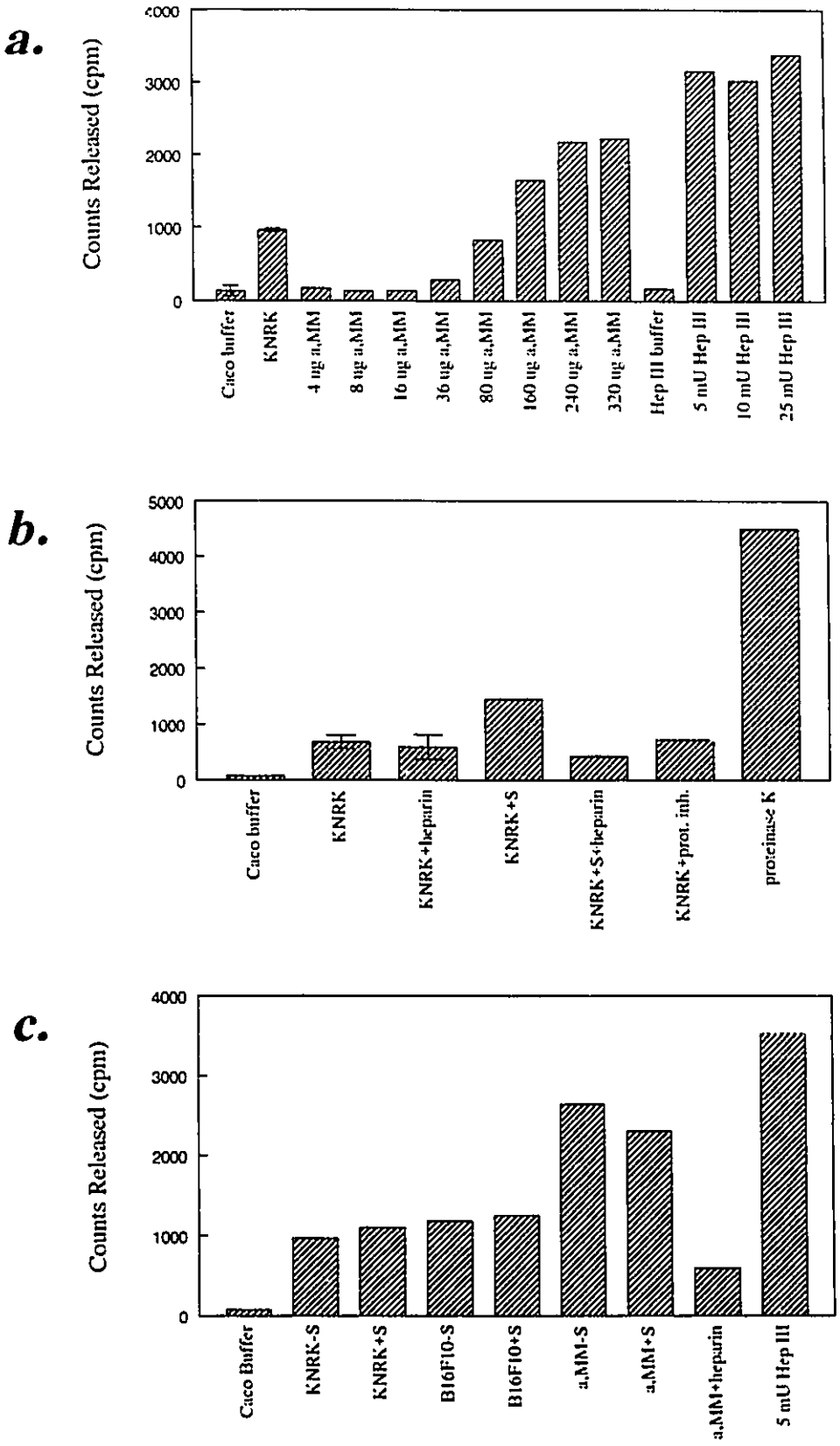
a.
Counts Released (cpm)
4000
3000
2000
1000
0
Caco buffer
KNRK
4 ug aMM
8 ug aMM
16 ug aMM
36 ug aMM
80 ug aMM
160 ug aMM
240 ug aMM
320 ug aMM
Hep III buffer
5 mU Hep III
10 mU Hep III
25 mU Hep III
b.
Counts Released (cpm)
5000
4000
3000
2000
1000
0
Caco buffer
KNRK
KNRK+heparin
KNRK+S
KNRK+S+heparin
KNRK+prot. inh.
proteinase K
c.
Counts Released (cpm)
4000
3000
2000
1000
0
Caco Buffer
KNRK-S
KNRK+S
B16F10-S
B16F10+S
aMM-S
aMM+S
aMM+heparin
5 mU Hep III

Insensitivity to this source of heparin in the ^{35}S-ECM assay as well as in the PAGE assay (Section II.3.4.) suggested that either this heparin was inactive as an inhibitor or that this heparin does not inhibit KNRK digestion of this particular substrate. (Unfortunately, bovine lung heparin was not yet available to us at this point for comparison).

In another experiment, B16F10 displayed activity comparable to KNRK with or without SAL (Figure 28c). Again, activity was slightly enhanced by SAL in both cases. α,MM was slightly inhibited by SAL (~ 13%) and strongly inhibited by heparin (~77%). This would suggest that this source of heparin (Fisher) was indeed active and its inhibition of HS-degrading activities depended on the enzyme and substrate used. The difference in sensitivity to heparin further suggests that KNRK heparanase is of a different type than α,MM heparanase.

Although a number of steps is required to generate such an immobilized substrate, this assay is simple to perform and rapid (1 hr) and quantification is reliable. However, the presence of residual protein associated with ^{35}S-HS may result in falsely positive results if proteolytic activity is also present. Nevertheless, such a convenient configuration would be an attractive alternative for the proposed fluorescent assay (although a soluble substrate is preferred over an immobilized one to permit better access of heparanase to the substrate).

II.4. *Induction of Heparanase Activity During Differentiation of U-937 Cells by RA as Measured by the PAGE and ^{35}S-ECM Assays*

Cells that normally have the capacity to invade vascular walls and extracellular matrices such as blood leukocytes are believed to possess heparanase activity [94,102]. As a complement to the differentiation project (Part A), extracts from control and differentiated U-937 cells were tested in the PAGE and ^{35}S-ECM assays to determine whether heparanase activity was induced during their differentiation into monocyte-like cells. Although heparanase activity was not detected earlier in PMNs (Figure 17c and 23d), it might be present in monocytes (which were not tested since they are hard to isolate in sufficient numbers). If heparanase activity could be shown to be enhanced in differentiated cells, it could be used as another marker for U-937 cell differentiation.

Results and Discussion:

Using the PAGE assay, a small increase in heparanase activity was observed in extracts of retinoic acid (RA)-differentiated U-937 cells compared to control cells (Figure 29a). Although subtle, this prompted further investigation. When comparing bovine lung or kidney HS as substrates, there was little difference in their digestibility by control and RA-induced U-937 cell extracts, including combinations with glyceryl trinitrate (GTN) and molsidomine (MOL) (not shown). However, when using bovine lung HS as a substrate, TNM+RA±CYS (TNM, tetranitromethane; CYS, L-cysteine) inducers were more effective than RA alone in inducing heparanase activity while GTN+RA and MOL+RA were comparable to RA alone (Figure 29b). This may suggest that TNM might induce a heparanase that has greater preference for the lung HS substrate. It should be noted that with time, heparanase activity diminished greatly with the age of the U-937 extracts, unlike

Figure 29. ***Modest induction of heparanase activity during differentiation of U-937 cells by RA±TNM±CYS.***

U-937 cells (2 x 10^5 cells/mL) were treated 96 hr in the continued presence of either no inducer or 10^{-5} M RA, alone or in combination with 0.1 mM GTN, 50 µM TNM ± 0.3 mM CYS, or 10^{-3} M MOL (see *Materials and Methods* in Part A for further details). Human PMNs and lymphocytes were freshly isolated as described in Figure 17. Whole cell extracts were prepared and subjected to either the PAGE assay as described in Figure 14 or the ^{35}S-ECM assay as described in Figure 28.

a. 60 µg of cell extract was incubated for 16 hr at 37°C with 2 µg bovine kidney HS in 20 mM cacodylate pH 6.1 and subjected to the PAGE assay. RA induces heparanase activity in U-937 cells, as indicated by a greater decrease in the staining of slower migrating material (upper portion of the gel) in the "RA 16 hr" lane compared to the "Control 16 hr" lane.

b. 60 µg of cell extract was incubated for 16 hr at 37°C with 2 µg bovine lung HS in 20 mM cacodylate pH 6.1 and subjected to the PAGE assay. TNM+RA±CYS induce further heparanase activity in U-937 cells, as indicated by a greater decrease in the staining of slower migrating material (upper portion of the gel) in the "TNM+RA 16 hr" and "TNM+CYS+RA 16 hr" lanes compared to the "RA 16 hr" lane.

c. For the ^{35}S-ECM assay, 200 µg of each extract were incubated in duplicate at 37°C for 2 hr on a hydrated ^{35}S-ECM plate in 80 mM cacodylate buffer pH 6.1. Reactions with Hep III (5 mU) in the presence of Hep III buffer (0.25 M sodium acetate pH 8, 2.5 mM $CaCl_2$) were performed in parallel to estimate total counts per minute (cpm) per well. Error bars represent the range of duplicate wells.

Figure 29.

a.
Control 16 hr
Control 0 hr
Control ext
RA 16 hr
RA 0 hr
RA ext
b.
HS
Control 16 hr
Control 0 hr
RA 16 hr
RA 0 hr
GTN 16 hr
GTN 0 hr
GTN+RA 16 hr
GTN+RA 0 hr
HS
TNM+RA 16 hr
TNM+RA 0 hr
TNM+CYS+RA 16 hr
TNM+CYS+RA 0 hr
MOL 16 hr
MOL 0 hr
MOL+RA 16 hr
MOL+RA 0 hr
c.
Counts Released (cpm)
1200
1000
800
600
400
200
Caco Buffer
Hep III Buffer
Control U-937
RA
GTN+RA
MOL+RA
PMNs
Lymphocytes
Hep III (5 mU)

KNRK, leading to variability. This may reflect variations in heparanases between species (i.e., human versus rat).

Degradation of ^{35}S-ECM was also studied as a potential marker for differentiation. Subtle differences observed in the PAGE assay were more apparent using this assay. RA induced in U-937 cells a low level of ^{35}S-ECM-degrading activity in U-937 cells compared to control cells (Figure 29c). GTN and MOL did not further enhance the RA-induced activity. PMNs displayed low activity while lymphocytes were considerably more active in the ^{35}S-ECM assay. These results are consistent with the results of the PAGE assays (Figures 29a, 29b, 17c and 23d). Unfortunately, the TNM+CYS+RA combination of inducers was not tested in the ^{35}S-ECM assay.

U-937 cells and HL-60 cells, human PMNs, macrophage and lymphocytes have previously been shown to possess heparanase activity [94,102,114,116,117,126,127,134]. However, in my studies with the exception of lymphocytes (Figure 17c and 23d), they were relatively inactive compared to KNRK (Figures 17b, 17c, 23b and 23d). Since U-937 cells can be induced to differentiate into monocyte-like cells (Part A), it would have been interesting to see if monocytes possessed heparanase activity.

Neutrophil heparanases have been reported to be localized to specific granules [114]. In the event that heparanase in differentiated U-937 cells was stored in granules, 0.5%(v/v) Triton X-100 was added to the heparanase extraction buffer for PMNs and control or differentiated U-937 cells; however, addition of the detergent did not increase heparanase activity in either cell type (data not shown). It has been postulated that, because heparanase activity in unfractionated neutrophil extract is lower than in specific

granule fractions, heparanase inhibitors may be present in the unfractionated neutrophil extract [114].

TPA (12-*O*-tetradecanoylphorbol-13-acetate) stimulated neutrophils have been shown to exhibit increased heparanase activity relative to unstimulated cells, although neutrophilic heparanase activity is much lower than that of the melanoma heparanase [127]. Stronger activity may have been observed with U-937 cells and PMNs if they were activated in the event that leukocyte heparanase requires stimulus-dependent activation. This possibility was not investigated for U-937, HL-60 cells or PMNs, although it has been reported that U-937 and HL-60 cell lysates exhibited heparanase activity in the absence of TPA stimulation [94,126]. Perhaps, with a more sensitive assay, heparanase activity could have been detected since PMN heparanase activity is relatively low. The possibility that heparanase activity in U-937 cells and PMNs may have a different pH optimum was not investigated.

II.5. *Summary of Section II.3. and II.4.*

KNRK heparanase appears to be less selective in terms of substrate; that is, it is able to digest bovine intestine, kidney and lung HS as well as ^{35}S-ECM. Similarly, B16F10 and lymphocyte heparanases are able to digest bovine kidney and lung HS as well as ^{35}S-ECM. This is unlike the more restrictive human placental α,MM heparanase which is able to digest ^{35}S-ECM well but only weakly digests bovine kidney or lung HS (intestine HS not tested with α,MM). Strongest KNRK heparanase activity is observed with bovine lung HS; thus, it may be more useful as a starting substrate for the proposed fluorescent

assay. Hep III is useful as a positive control for digestibility of both soluble and immobilized HS substrates.

KNRK heparanase appears be most active near pH 6. Calcium ions and reducing agent DTT do not appear to be essential for full activity. KNRK heparanase is inactivated by 10 min boiling, treatment with either 47 mM β-mercaptoethanol, or 0.1% SDS. Bovine lung heparin appears to be a potent inhibitor of KNRK digestion of bovine kidney HS but only a partial inhibitor of bovine lung HS digestion. Fisher heparin is effective as an inhibitor of α,MM heparanase (in the ^{35}S-ECM assay) but not of KNRK heparanase (in either the PAGE or ^{35}S-ECM assay). Thus, KNRK and α,MM heparanase appear to be different in terms of substrate specificity and sensitivity to heparin. Considering its substrate specificity, insensitivity to SAL and sensitivity to bovine lung heparin, its pH optimum, and the relative size of HS fragments produced, KNRK most likely contains an endoglycosidase that is similar to the B16 melanoma heparanases [94,108].

Heparanase activity is only marginally enhanced by RA during U-937 cell differentiation (as seen in the PAGE and ^{35}S-ECM assay). Using bovine lung HS in the PAGE assay, induction of RA-induced heparanase activity is slightly enhanced by TNM±CYS. Due to the relatively low levels of heparanase activity observed in differentiated U-937 cells and/or the possible insufficient sensitivity of the assays used, the use of heparanase activity as another marker of U-937 cell differentiation was not pursued.

CHAPTER III. ATTEMPTS AT DEVELOPING A FLUORESCENCE-BASED HEPARANASE ASSAY

This chapter highlights some of the experiments that were performed in attempts to develop a more sensitive, fluorescence-based heparanase assay (refer to *Introduction* and Figure 13 for the principles of the proposed assay). During its development, the PAGE assay was found to be convenient to monitor intactness and digestibility of the modified HS substrates. It should be noted that HS is not well-defined chemically and this has made the development of the fluorescence-based assay difficult. Although a working assay has not yet been arrived at, progress towards this end are described below. Because of the complexity of the reactions involved, many details have been included that may be potentially useful for future workers.

III.1. *Random-Labelling of Native HS with FITC*

HS randomly labelled with fluorescein isothiocyanate (FITC-HS) was prepared to test and optimize FITC labelling conditions, to assess the digestibility and thus usefulness of a fluorescent substrate, as well as to generate a control substrate for assessment of non-specific binding to various surfaces for later studies.

III.1.1. *N-Desulfation and Conjugation with FITC*

While *O*-sulfate groups are relatively stabile, *N*-sulfate groups are readily removed from *N*-sulfated glucosamine residues under acidic conditions or in the presence of DMSO by a process termed *solvolysis* [135]. After solvolysis, free amino groups remain at sites of *N*-desulfation. Fluorescein can be substituted onto the newly exposed amino groups

using the amine-reactive probe FITC which couples fluorescein to an amine group via an acylation reaction. Since FITC is stable in DMSO, *N*-desulfation and fluorescein labelling can be carried out simultaneously under slightly alkaline conditions. Because previous experiments in our laboratory indicated reduced digestibility of HS with extensive fluorescent probe substitution in the PAGE assay, partial *N*-desulfation was performed under conditions of 50% DMSO (v/v) rather than 95% DMSO (v/v) to achieve limited labelling.

0.5 to 2 mg/mL native bovine kidney HS was reacted with 2.6 mM FITC (freshly prepared as 26 mM in DMSO) in either 0.1 M $NaHCO_3$ pH 8.3 or 0.1 M sodium acetate pH 8 and 50% DMSO (v/v) at RT from 3 hr to overnight in the dark. Control reactions (no HS) were also set up. To convert unreacted FITC into a more soluble form, reaction mixtures were treated with 0.15 M hydroxylamine pH 8 (freshly prepared and pH adjusted using NaOH) for 1 hr at RT. To remove excess probe, the reactions were alcohol precipitated at -20°C overnight with 1/3 volume 1 M to 1/4 volume 4 M sodium acetate pH 8, and 3 to 4 volumes cold 99% ethanol. Following centrifugation at 13,000*g* for 5 min, pellets were washed in cold 99% ethanol, spun again and the washed pellets were resuspended in water, typically at an estimated concentration of 1 µg/µL. To confirm that labelling had occurred, control and HS-containing reactions were spotted on diethylaminoethyl (DEAE)-cellulose TLC strip, chromatographed in 1% acetic acid:75% ethanol. Detection of fluorescein requires pH > 6 since fluorescein exhibits pH-dependent fluorescence. Using a fluorometer (Perkin-Elmer LS-5 Fluorescence Spectrophotometer), the pH for optimal fluorescence of fluorescein-labelled HS was determined to be pH 9.5.

Thus, the TLC strips were sprayed twice with 0.3 M borate pH 9.4 to adjust the pH, and visualized under ultraviolet (UV) light to detect a fluorescent spot at the origin where HS was expected to remain.

Results and Discussion:

Using TLC to monitor the progress of the FITC reaction with HS, a difference from control was observed in about 3 hr as a brighter spot at the origin and 20 hr incubation with FITC resulted in heavier fluorescent probe substitution (see Figure 30c for comparison of relative fluorescence intensities after PAGE separation). Bicarbonate tended to precipitate out slightly during the alcohol precipitation while sodium acetate did not; therefore, sodium acetate was preferred as the reaction buffer. TLC of pellet and supernatant fractions before (Figure 30a) and after alcohol precipitation (Figure 30b) confirmed the effectiveness of the precipitation in removing unconjugated FITC. The above random labelling procedure was also used for biotinylated bovine kidney HS (Section III.3.) to produce FITC-HS-N-XXB.

III.1.2. *Testing for Digestibility of Random Fluorescently-Labelled HS*

The presence of the bulky and hydrophobic fluorescein substitution on HS might affect substrate recognition by heparanase or hinder substrate access to the active site. To test whether heparanase activity was reduced in the presence of the fluorescein substitutions, FITC-HS and FITC-HS-N-XXB (Section III.1.1) were subjected to the PAGE assay as described in Figure 14 (Chapter I).

Results and Discussion:

As shown in Figure 30c, 3 hr and 20 hr labelled FITC-HS were equally digestible

Figure 30. *Thin layer chromatography and PAGE assay of random fluorescein-labelled HS.*

a. Water as a control ("C") or 2 mg/mL unfractionated native bovine kidney HS ("HS") was reacted with 2.6 mM FITC (freshly prepared as 26 mM in DMSO) in 0.1 M $NaHCO_3$ pH 8.3 and 50% DMSO (v/v) at RT for 20 hr in the dark. Reactions were terminated with 0.15 M hydroxylamine pH 8 (freshly prepared and pH adjusted using NaOH) for 1 hr at RT. Reactions were spotted on a DEAE-cellulose TLC strip (CEL 300 DEAE), chromatographed in 1% acetic acid:75% ethanol, sprayed twice with 0.3 M borate pH 9.4, and visualized under UV light. FITC-HS appears as an intense spot at the origin. The higher mobility smear represents the conjugate of FITC with hydroxylamine produced during the termination step.

b. Terminated reactions (from *a.*) were alcohol precipitated at -20°C overnight with 1/3 volume 1 M sodium acetate pH 8, and 3 volumes cold 99% ethanol. The precipitations were microcentrifuged for 5 min, the supernatant recovered, the pellets washed in cold 99% ethanol, spun again and the washed pellet was resuspended in water to a concentration of 1.25 µg/µL. Samples were spotted on a DEAE-cellulose TLC strip, chromatographed in 1% acetic acid: 75% ethanol, sprayed twice with 0.3 M borate pH 9.4, and visualized under UV light. Shown are the pellet ("P") and supernatant ("S") (equivalent amount) fractions for the HS-containing reaction. FITC-HS appears as an intense spot at the origin with the higher mobility FITC-hydroxylamine conjugate removed. (Note: The control pellet lane was empty and the control supernatant lane was identical to the HS reaction supernatant lane (not shown here)).

c. 2.5 µg of fluorescent HS, as the result of a 3 hr ("FITC-HS3") or 20 hr ("FITC-HS20") random labelling with FITC (as in Section III.1.1.), were incubated with either 50 µg KNRK extract in 20 mM cacodylate buffer pH 6.1 or 10 mU Hep III in 0.25 M sodium acetate pH 8, 2.5 mM $CaCl_2$ for 16 hr or 0 hr at 37°C. The reactions were further processed in the PAGE assay (as described in the legend for Figure 14). A methylene blue stained gel (*left panel*) and a UV transilluminated gel (*right panel*) are shown. 3 or 20 hr fluoresceinated HS is digestible by KNRK and Hep III, as indicated by a decrease in the staining of slower migrating material (in the upper portion of the gel) at 16 hr compared to 0 hr or FITC-HS controls.

d. 2 µg HMW#1 bovine kidney HS or bovine kidney FITC-HS-N-XXB were incubated at 37°C for 16 or 0 hr with 60 µg KNRK in 20 mM cacodylate pH 6.1 or 2 mU Hep III in 0.25 M sodium acetate pH 8 and 2.5 mM $CaCl_2$. Reactions were subjected to the PAGE assay as described in Figure 14. A methylene blue stained gel (*left panel*) and a UV transilluminated gel (*right panel*) are shown. Biotinylated and fluoresceinated HS is digestible by KNRK and Hep III, as indicated by a decrease in the staining of slower migrating material (in the upper portion of the gel) at 16 hr compared to 0 hr or FITCHSNXXB controls.

Figure 30.

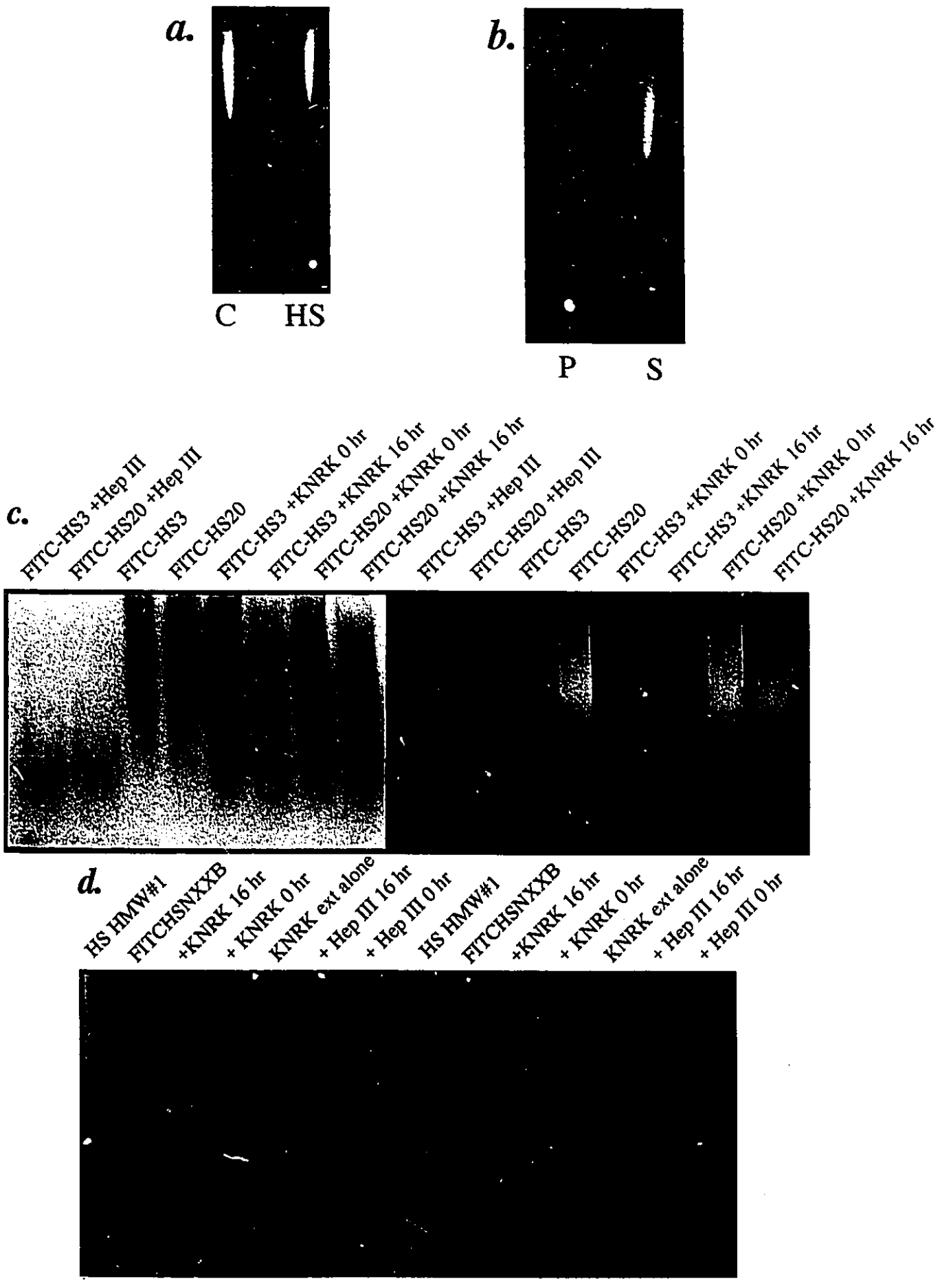
a.
C
HS
b.
P
S
c.
FITC-HS3 +Hep III
FITC-HS20 +Hep III
FITC-HS3
FITC-HS20
FITC-HS3 +KNRK 0 hr
FITC-HS3 +KNRK 16 hr
FITC-HS20 +KNRK 0 hr
FITC-HS20 +KNRK 16 hr
FITC-HS3 +Hep III
FITC-HS20 +Hep III
FITC-HS3
FITC-HS20
FITC-HS3 +KNRK 0 hr
FITC-HS3 +KNRK 16 hr
FITC-HS20 +KNRK 0 hr
FITC-HS20 +KNRK 16 hr
d.
HS HMW#1
FITCHSNXXB
+KNRK 16 hr
+ KNRK 0 hr
KNRK ext alone
+ Hep III 16 hr
+ Hep III 0 hr
HS HMW#1
FITCHSNXXB
+KNRK 16 hr
+ KNRK 0 hr
KNRK ext alone
+ Hep III 16 hr
+ Hep III 0 hr

by Hep III and KNRK in PAGE assay in a manner comparable to unlabelled HS (refer to Figure 17 for example). Biotinylated, fluoresceinated HS (FITC-HS-N-XXB) was similarly digestible by Hep III and KNRK (Figure 30d).

III.1.3. *Assessment of Sensitivity of Detection*

The reductive amination product of HS ($HS\text{-}NH_2$) (Section III.2) was labelled with FITC (as described in Section III.1.1) to determine the lowest amount of the minimally labelled substrate that could be detected using a fluorometer.

Results and Discussion:

Using a Perkin-Elmer LS-5 Fluorescence Spectrophotometer set at excitation wavelength 488 nm, emission wavelength 520 nm and slit widths at 5 and 10 nm respectively, 2 pg of this substrate could be detected in a 25 µL volume in 10 mM borate pH 9.4. This sensitivity of detection was at least 250,000 times greater than that achieved using methylene blue staining in a gel (about 0.5 µg).

III.2. *Reductive Amination of Native HS*

As described in the *Introduction*, one way to introduce a biotin at one end of HS would be to first introduce a terminal primary amine group to which a biotin analogue could later be coupled. Reductive amination of the aldose at the reducing end of HS is theoretically accomplished by incubating HS with ammonia, sodium cyanoborohydride ($NaBH_3CN$), and a polar protic solvent such as methanol (Figure 31a) [136]. This section outlines the various tested and recommended procedures for reductive amination of HS. Reductively aminated HS was designated as "$HS\text{-}NH_2$".

Figure 31. ***Reductive amination: reaction and examples of HS-NH_2 on a TLC strip.***

The reductive amination of an aldose sugar is shown in ***a.*** using glucose as an example. The aldehyde group reacts with ammonia to form an imine (Schiff base). The Schiff base is reduced by the hydride (H^-) donor $NaBH_3CN$ to form a primary amino group. Representative TLC analyses of reductive amination products are shown in ***b.*** and ***c.*** 1 mg/mL bovine kidney HS was incubated at 50°C for 7 days in the presence of 2 M ammonium borate pH 9, 0.4 M $NaBH_3CN$, and 50% methanol. A control reaction with water instead of HS was set up in parallel. The reactions were dialyzed overnight against water in MWCO 12,000-14,000 dialysis tubing and concentrated to 25 µg/µL under vacuum and 50°C heat using a Buchler Vortex-Evaporator. 1 µg of the dialyzed, concentrated control (indicated as "C") and HS-containing (indicated as "HS") reactions were spotted and chromatographed on DEAE-cellulose TLC strips in 0.3 M sodium borate pH 9.4 (shown in ***b.***) or 1% acetic acid:75% ethanol (shown in ***c.***). The TLC strips for the latter were sprayed twice with 0.3 M borate buffer pH 9.4 to adjust the pH. Both strips were then sprayed twice with 15 mg/100 mL fluorescamine in acetone and visualized under UV light. HS-NH_2 stains as a spot at the origin in both solvent systems.

Figure 31.

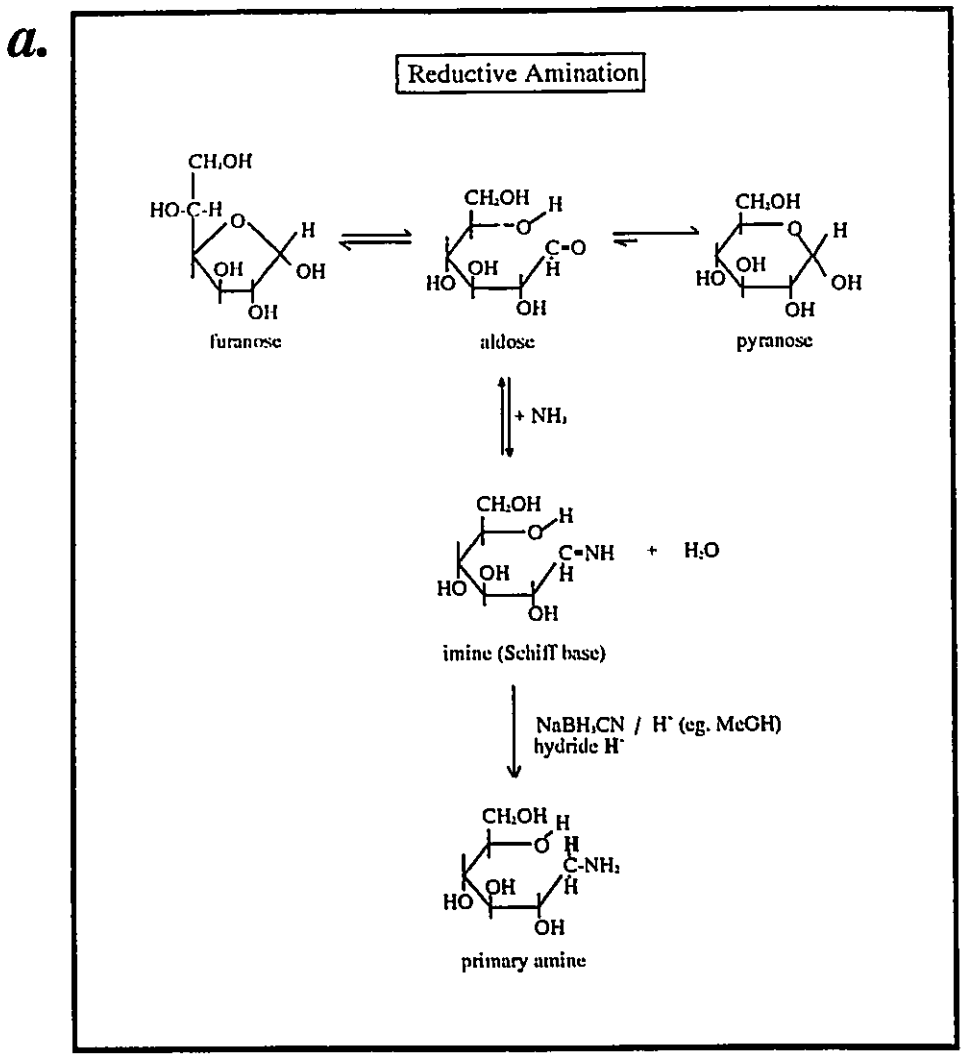
a.
Reductive Amination
furanose
aldose
pyranose
+ NH3
imine (Schiff base)
NaBH3CN / H+ (eg. MeOH)
hydride H-
primary amine

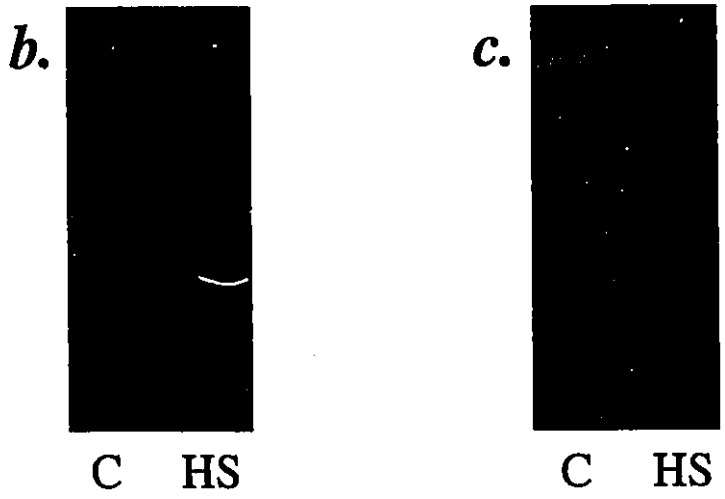
b.
c.
C
HS
C
HS

Of several experimental conditions explored, best results appeared to be obtained using the following procedure. 0.5 to 1 mg/mL HS (or water as a control), 2 M ammonium borate pH 9, and 0.4 M $NaBH_3CN$ (freshly opened or stored under N_2 after opening) in 50% methanol were incubated at 50°C for 6 or 7 days in glass vials with teflon coated caps. Reactions were dialyzed twice against water overnight in dialysis tubing (12,000 to 14,000 molecular weight cutoff (MWCO)) and concentrated to at least 1 mg/mL in a Buchler Vortex-Evaporator under vacuum and 50°C heat. Samples aliquots were analyzed by spotting on DEAE-cellulose TLC strips, chromatographing in 0.3 to 0.4 M borate pH 9.4, and spraying twice with 15 mg/100 mL fluorescamine in acetone to visualize HS-NH_2 as a spot at the origin. Samples were further purified by alcohol precipitation overnight at -20°C with 1/4 volume 4 M sodium acetate pH 8 and 4 volumes cold 99% ethanol, a procedure confirmed to be effective spectrophotometrically by the dimethylmethylene blue (DMMB) precipitation method (described in Appendix II.1.). After microcentrifuging for 5 min, the precipitate was washed in cold 99% ethanol, spun and resuspended in water to 1 to 10 mg/mL. The extent of amine introduction could be improved with a repeated reductive amination.

Results and Discussion:

Using the above procedure, the resulting HS-NH_2 was intact (Figure 32a) and digestible by KNRK as assessed using the PAGE assay (not shown). Samples were chromatographed on DEAE-cellulose TLC in 0.3 M borate pH 9.4 or 1% acetic acid:75% ethanol, sprayed with 0.3 M borate buffer pH 9.4 in the latter case to adjust the pH for subsequent spraying with fluorescamine to detect the presence of primary amines under

UV light [137]. In both running solvents, HS was expected to remain at the origin. The latter solvent was originally used to remove interfering material from the origin when monitoring the progress of the reductive amination reaction (prior to dialysis). This interfering material, either $NaBH_3CN$ itself or a by-product of $NaBH_3CN$ and the reaction buffer, was present in both HS-containing and control reactions and it stained with fluorescamine (and other amine-detecting reagents) thus interfering with TLC analysis. Dialysis against water was effective in removing this interfering material from the sample. After concentrating the samples, fluorescamine-staining material was seen at the origin only for HS-containing samples and not for controls suggesting that reductive amination of HS had occurred (Figure 31b and c). About 0.35 µg of HS-NH_2 could be detected by such TLC analysis.

Several experiments were performed to determine ways to improve the extent of amination. Neither acidification of $NaBH_3CN$ with 1% acetic acid (a process which would destroy borohydride, a contaminant that reduces aldehydes to alcohols rather than amines) or recrystallization (for purification as described in [136]) improved amination. Rather, best results were obtained using fresh $NaBH_3CN$ (not previously exposed to air) stored under N_2. Ammonium borate pH 9 as the reaction buffer seemed preferable to ammonium acetate pH 7; borate ions are reported to facilitate reductive amination [138]. Conversion to the open-ring aldose form of the terminal sugar is the limiting reaction in the overall scheme (Figure 31a). This acyclization is facilitated by increasing the temperature and pH of the reaction and by the addition of borate ions [138], which complexes to vicinyl hydroxyls. Since $NaBH_3CN$ decays upon exposure to aqueous environments, repeated

reductive amination of HS-NH_2 was tested. Re-reductive amination roughly doubled the number of amines using bovine lung HS as a substrate (data not shown).

III.3. *Biotinylation of Reductively Aminated HS with Biotin Succinimidyl Ester*

Biotinylation of the terminal amino group formed from reductive amination can be accomplished using a succinimidyl ester of biotin such as that of 6-((6-((biotinoyl)amino)hexanoyl)amino) hexanoic acid (BXXSE) ("X" denotes a spacer arm unit) (Figure 13 in *Introduction*). Although in theory biotin can be coupled directly to the terminal aldehyde of HS using biotin hydrazide (Figure 13), the extent of biotinylation using this latter method was found to be limited.

III.3.1. *Biotinylation Procedure*

Biotinylation was performed by coupling the amine-reactive BXXSE onto the terminal amino group of HS-NH_2 introduced by reductive amination.

10 mg/mL BXXSE was freshly prepared in dimethyl formamide (DMF). Biotinylation of 1 to 3 µg/µL HS-NH_2 with 1 to 2 mM BXXSE was carried out in 0.1 M sodium acetate pH 8. The reaction was incubated at RT for 2 to 4 days and stopped by incubation with 0.15 M hydroxylamine pH 8 (freshly prepared and pH-adjusted with NaOH) for 1 hr at RT. To remove the biotin-hydroxylamine conjugate, the reaction mixture was alcohol precipitated at -20°C overnight with 1/4 volume 4 M sodium acetate pH 8 and 4 volumes 99% cold ethanol. After microcentrifuging for 5 min, the pellet was washed with cold 99% ethanol, spun again and resuspended in water to 5 to 10 µg/µL. The resulting substrate was designated as "HS-N-XXB".

Results and Discussion:

The extent of biotinylation using the above procedure was determined to be between 25 to 50% as assessed spectrophotometrically by DMMB precipitation (Section III.3.2.) or fluorometrically (Section III.3.3.) after random labelling of HS-N-XXB with FITC using procedures described in Section III.1.1.. It was subsequently found that biotinylation could be improved with repeated additions (twice or three times) of BXXSE during incubation with HS-NH_2 presumably because BXXSE rapidly hydrolyzes in water.

III.3.2. *Spectrophotometric Assessment of Extent of Biotinylation*

To quantify the extent of biotinylation, HS-N-XXB in the presence of 0.5 M ammonium sulfate was introduced to a biotin-capture system, such as streptavidin immobilized to agarose beads (SA-ag), and HS in the total and non-bound fractions was quantified spectrophotometrically by DMMB precipitation (Appendix II.1.).

Results and Discussion:

Unfortunately, both unmodified and modified HS bound non-specifically to SA-ag beads but not to streptavidin-alkaline phosphatase (as assessed by pre-incubation with SA-ag beads or streptavidin-alkaline phosphatase before PAGE separation (not shown)). This would suggest that HS was binding non-specifically to the agarose beads themselves rather than streptavidin. Salts and chaotropic agents (6 and 8 M urea, 2 M perchlorate, 1 M guanidinium thiocyanate, 0.3 M LiCl) were tested to remove HS non-specifically bound to the streptavidin-agarose beads; however, these agents interfered with DMMB precipitation thereby obscuring results. 0.5 M ammonium sulfate during binding and washing seemed to reduce non-specific binding without altering DMMB precipitation. The

estimated % biotinylation of the first HS-N-XXB preparation was about 29%. This technique, however, had a high background and narrow detection range (0.1 to 1 µg HS). The other method (used in remaining studies) to estimate % biotinylation was to measure, by difference, the non-bound fraction after conjugation with fluorescent tag (Section III.3.3.). Using this method, the same preparation was found to be 30 to 33% biotinylated, which was close to that determined by the DMMB method.

III.3.3. *Fluorometric Assessment of the Extent of Biotinylation*

Another method to determine the extent of biotinylation of HS-N-XXB was performed after fluorescent labelling of the substrate (described in Section III.1.1.).

FITC-HS-N-XXB was incubated at 37°C with SA-ag beads and washed with either 1 M-2 M perchlorate in 0.1 M Tris pH 9.5, 4 mM CDTA, or 0.2% SDS in 0.1 M Tris-HCl pH 9.5 to remove non-specifically bound molecules. For quantitative fluorescence measurements, samples were adjusted to pH 9.5 using 0.2 M Tris-HCl pH 9.5 and total fluorescence and that of the washes were read in a Perkin-Elmer Model LS-5 Fluorescence Spectrophotometer at excitation wavelength of 485 nm, emission wavelength of 525 nm with slits set at 5 and 3 nm respectively.

Results and Discussion:

The stability of streptavidin was taken into account in testing wash buffers for complete removal of non-specifically bound randomly labelled fluorescent HS (FITC-HS) (prepared as described in Section III.1.1.). Streptavidin, in addition to having extremely high avidity for biotin, is also extremely stable and actually binds biotin optimally under harsh conditions such as 9 M urea, 1 M NaCl or KCl and 4 M guanidine-HCl [139]. 6 or

8 M urea, 1 or 2 M perchlorate, 1 or 2 M LiCl, NaCl or KCl, 1 M guanidium thiocyanate or guanidine-HCl, 0.5 M ammonium sulfate, 0.5 mg/mL heparin, and 0.2% Triton X-100 were tested as wash buffers. An effective wash buffer for complete removal of non-specifically bound FITC-HS with little quenching of fluorescence was determined to be 1 M or 2 M perchlorate in 0.1 M Tris pH 9.5, 4 mM CDTA. 0.2% SDS in 0.1 M Tris-HCl pH 9.5 as a wash buffer was equally effective, with less fluorescence quenching. Neither perchlorate nor SDS were damaging to HS substrates (Figure 32b). After 1 hr or overnight binding to SA-ag beads and washing with wash buffer, it appeared that biotinylation of HS with BXXSE yielded between 25 to 50% biotinylation on average. This was calculated based on the difference in fluorescence of total and non-bound fractions (i.e. 25-50% of the fluorescence bound to the beads). In contrast, only 8% binding was achieved with the biotin hydrazide reaction product. Thus, BXXSE was the preferred reagent for addition of biotin onto HS.

III.4. *Substrate Purification and Trial Assays*

Because biotinylation of bovine kidney FITC-HS-N-XXB preparations was incomplete (between 25 to 50% due to either incomplete reductive amination and/or biotinylation), in the proposed fluorescent assay this would lead to high background thereby decreasing the sensitivity of the assay. Purification of the substrate further to remove non-biotinylated HS was therefore deemed necessary before use in a soluble assay.

III.4.1. *Substrate Purification on Streptavidin-Agarose Resin*

After binding total substrate to SA-ag beads and washing with wash buffer, various

elution methods to recover the biotinylated fraction were tested. Among these, elution under rather harsh conditions (excess biotin (100 µg/mL), 0.1 M NaOH, 1 mM CDTA, neutralization with 0.1 M acetic acid and buffering with 0.1 M Tris-HCl pH 9.5) initially appeared to be effective (as determined fluorometrically). After concentrating and alcohol precipitating, one such preparation yielded 93% pure substrate that was digested by KNRK and Hep III in both immobilized and soluble digests. Unfortunately, subsequent purifications under similar conditions yielded inconsistent results with only 25 to 50% recovery. After dialysis against water to remove any residual biotin, typically only 40 to 60% of the resulting substrate was able to rebind to SA-ag beads. This would suggest that the substrate was impure (either contaminated with non-biotinylated fluorescent HS or free biotin) or damaged in some way that prevented interaction with SA-ag beads. Damage to the substrate is possible since biotin is unstable at alkaline pH and NaOH may cause "peeling", i.e., sequential cleavage of monosaccharide units from the reducing end of polysaccharides [140]. Treatment with NaOH under the same conditions did not appear to reduce the size of FITC-HS-N-XXB on a PAGE gel (Figure 32a), but this is not a sensitive test for the loss of a few residues at one end which would release the attached biotin. Longer incubation with NaOH did change the mobility of native HS and FITC-HS-N-XXB size, as seen on a PAGE gel (Figure 32b(i) and (ii)). These factors might explain why full rebinding was not achieved.

Biotinylated cytochrome c was prepared as a positive control for the biotinylation reaction by BXXSE and to test gentler elution methods for substrate purification (Appendix II.2.). Excess biotin ± DMF was not able to elute biotinylated cytochrome c from SA-ag

Figure 32. ***PAGE separation of native and modified HS substrates after treatment with alkali ± biotin and other substances.***

a. 2 µg HS-NH_2 or HS-N-XXB (2 preparations labelled as "HSNXXB1" and "HSNXXB2") and 1 µg FITC-HS-N-XXB (2 preparations labelled as "FITCHSNXXB1" and "FITCHSNXXB2") with or without treatment with 0.1 N NaOH ("NaOH") or elution buffer ("EB" = 0.1 N NaOH, 0.1 µg/µL biotin) at 37°C for 1 hr were loaded onto a 7.5% PAGE gel, electrophoresed and stained as described in Section I.1. Reductively aminated, biotinylated, and fluoresceinated substrates appear to be intact since they produce the characteristic smear in the gel (although their relative amounts or ability to be stained have decreased). Treatment with NaOH or elution buffer do not further alter mobility.

b. Samples of 1.3 µg native HS or FITC-HS-N-XXB were incubated overnight at 37°C in the presence or absence of 0.1 N HCl, 0.1 N NaOH, 1 M perchlorate (containing 8 mM Tris-HCl pH 8, 4 mM CDTA), 5 µg proteinase K, or 0.2% SDS. After incubation, the HCl and NaOH treated samples were neutralized with NaOH and HCl respectively. All samples were loaded onto a 7.5% PAGE gel, electrophoresed and stained as described in Section I.1. Panel *(i)* shows the methylene blue stained gels and panel *(ii)* shows the gel containing fluorescent HS under UV light. Methylene blue staining and fluorescence visualization are decreased by the various treatments. HCl and NaOH treatments appear to produce faster migrating material compared to the FITC-HS-N-XXB control.

Figure 32.

a.
HS-NH2
HSNXXB1
HSNXXB2
FITCHSNXXB1
FITCHSNXXB2
FITCHSNXXB2+NaOH
FITCHSNXXB2+EB
b.
(i)
FITCHSNXXB
+ 0.1 N HCl
+ 0.1 N NaOH
+ 1 M perchlorate
+ proteinase K
+ 0.2% SDS
native HS
+ 0.1 N HCl
+ 0.1 N NaOH
+ 1 M perchlorate
+ proteinase K
+ 0.2% SDS
(ii)
+ 0.2% SDS
+ proteinase K
+ 1 M perchlorate
+ 0.1 N NaOH
+ 0.1 N HCl
FITCHSNXXB

beads. Since separation of biotin from SA or avidin is essentially irreversible (Ka ~ 10^{15} M^{-1}) [139] and SA was found to be extremely resistant to the harshest denaturation conditions, alternative means of biotin capture were investigated.

III.4.2. *Substrate Purification on Moromeric Streptavidin Resin*

Monomeric avidin has been reported to have reduced affinity for biotin [141]. Non-reversible biotin-binding (high affinity) sites are blocked by biotin. Reversible biotin-binding sites are revealed by stripping with a low pH glycine buffer. Biotinylated substrates introduced to monomeric avidin can then be eluted with excess biotin.

Attempts to prepare a monomeric SA equivalent were made using SA-ag beads on the premise that elution from monomeric streptavidin, assuming it behaves like monomeric avidin, should occur with excess biotin. SA-ag beads were incubated in the presence of excess biotin to block high affinity sites. Biotin was stripped from lower affinity sites with 0.1 M glycine pH 3 and the resin was washed with 0.1 M Tris pH 7.5. Biotinylated substrates were bound, washed with 0.1 M Tris pH 7.1 and eluted with excess biotin.

Results and Discussion:

It was found that indeed biotinylated cytochrome c was released with 100% efficiency (as determined spectrophotometrically). In a small scale purification, 48% biotinylated FITC-HS-N-XXB substrate was released with 93% efficiency (as determined fluorometrically). However, after extensive dialysis against water to remove excess biotin, only 63% bound to SA-ag beads. When the same was applied to larger scale purifications, yields were low (20%) and only 56-70% was able to rebind back to SA-ag beads. The background, although slightly improved, was still unsuitable for a sensitive soluble assay.

III.4.3. *Substrate Purification by Immobilized Monoclonal Antibodies to Biotin*

Biotinylated molecules can also be purified by immunoaffinity chromatography using commercially available monoclonal antibodies to biotin that are immobilized onto agarose beads. Binding of biotinylated molecules occurs with an affinity of a typical antigen-antibody interaction; therefore, elution from the resin should be easier.

Commercial resin bearing immobilized monoclonal antibodies to biotin was blocked with 10 mg/mL bovine serum albumin fraction V in 10 mM phosphate pH 7.2, 0.5 M NaCl. After washing, biotinylated substrate was applied to the column. Elution was performed with 0.1 M glycine pH 2.4, 0.15 M NaCl, 0.2 mg/mL biotin and fractions were neutralized with 50 mM phosphate pH 8.

Results and Discussion:

Using biotinylated cytochrome c to test elution conditions, the above procedure resulted in 100% recovery (as determined spectrophotometrically). With FITC-HS-N-XX-B, only 45-50% recovery of that which did bind (<10%) was achieved (i.e. <5% recovery) (as determined fluorometrically). Blocking with 1 mg/mL native HS to reduce non-specific binding to the resin did not improve recovery. After the purified substrate was dialyzed and concentrated, it demonstrated 57-74% rebinding. Although promising, digestion by KNRK extract in the soluble phase appeared to be limited since incubated digests applied to SA-ag beads did not result in significant increases in the non-bound fluorescence. Furthermore, column capacity was low leading to low yields, and column reusability was poor. Purification in bulk to generate usable quantities of substrate would thus require multiple rounds of purification.

III.4.4. *Treatment of Soluble Digests With Proteinase K Prior to Binding*

Soluble digests did not fully bind to various biotin-capture systems suggesting that binding of substrate was reduced in the presence of extract. Treatment of digests with proteinase K prior to binding was performed in an attempt to improve binding.

Results and Discussion:

Treatment of Hep III and KNRK digests with proteinase K ± SDS prior to binding *increased* rather than decreased the non-bound fraction on several occasions. To test the possibility that proteinase K was digesting the amide bonds of the spacer arm "XX" of BXXSE conjugates, the newly acquired fluorescein-X-biotin, which contained a similar spacer arm, was tested for susceptibility to proteinase K digestion. After 48 hr incubation of 25 nmol of fluorescein-X-biotin at 37°C with 0, 0.5 or 1 mg/mL proteinase K, in 0.1 M Tris pH 9.5 ± 0.1 %SDS, aliquots of digests were incubated with SA-ag beads for 1 hr and the fluorescence of the non-bound fractions were read. With proteinase K ± SDS, the % bound did not change (98 versus 97%). Therefore, there seems to be negligible digestion of the spacer arm (or inhibition of binding to SA-ag) by proteinase K. It is possible that endogenous biotin or other interfering substances in extracts might have been released upon proteinase K digestion which resulted in inhibition of substrate binding to SA-ag.

III.5. *Digestion of Immobilized Substrate As An Alternative to Purification*

Due to the great difficulties encountered in purifying FITC-HS-N-XXB for use in a soluble assay, experiments were performed to test the utility of the substrate in an immobilized assay. Upon immobilizing the biotinylated fluorescent substrate,

non-biotinylated fluorescent molecules could be washed away to lower the background. The fluorescence of HS fragments liberated upon endoglycosidic cleavage would be quantified in a fluorometer as a measure of heparanase activity.

Digestion was more apparent with SA-ag immobilized substrate than soluble substrate due to the lower background with immobilized substrate after washing. Although there was some dose-dependence with Hep III or KNRK, digestion was limited (less than 10-50% off). Because SA-ag beads might sterically hinder enzyme access to the immobilized substrate, alternative methods of immobilization were tested.

III.5.1. *NeutrAvidin-Immobilized Substrate*

Because KNRK and Hep III were active in the ^{35}S-ECM assay (Figure 28), a similar configuration was adopted to immobilize fluorescent biotinylated substrate. 96-well polystyrene plates coated with NeutrAvidin (NA) were prepared for such use. NA is a commercially available deglycosylated form of avidin that exhibits reduced non-specific binding. The procedures for preparation of the NA-coated plates and immobilization of FITC-HS-N-XXB onto such plates are detailed in Appendix II.3.

Results and Discussion:

Using a NA-coated 96-well plate, immobilized FITC-HS-N-XXB was digested by 5 mU Hep III but minimally by KNRK (Figure 33a). When soluble digests were performed with the same substrate (which was 48% biotinylated) and subsequently bound to NA-coated wells, Hep III was quite active while KNRK was relatively inactive (Figure 33b). The background was quite high using the soluble substrate. Boiling of KNRK extract typically resulted in a slight increase in fluorescence of the unbound fraction rather

Figure 33. ***Digestion of immobilized and soluble bovine kidney FITC-HS-N-XXB using a NeutrAvidin coated 96-well polystyrene plate as a biotin capture system.***

NeutrAvidin coated 96-well polystyrene plates were prepared and coated with bovine kidney FITC-HS-N-XXB as described in Appendix II.3.

a. Immobilized digest. 50 µL of Hep III buffer (0.25 M sodium acetate pH 8, 2.5 mM $CaCl_2$) ± 5 mU Hep III or 20 mM cacodylate buffer pH 6.1 ± 50 µg KNRK extract ± boiling for 10 min or 5 µg proteinase K was added to FITC-HS-N-XXB coated wells and incubated at 37°C in a humidified chamber overnight. Digests were removed from the wells. Wells were washed with 50 µL 0.2 M Tris-HCl pH 9.5 and washes were pooled with the digest. Fluorescence of the digests was read in a Perkin-Elmer LS-5 Fluorescence Spectrophotometer at excitation and emission wavelengths of 485 and 525 nm respectively and slit widths set at 5 and 3 nm respectively. Shown in *a.* are mean ± SEM of triplicate determinations.

b. Soluble digest. 0.6 ng/µL FITC-HS-N-XXB was incubated at 37°C overnight with Hep III buffer ± 5 mU Hep III or 20 mM cacodylate buffer pH 6.1 ± KNRK extract (9.3 to 93 µg) that had or had not been boiled for 10 min. 50 µL of the digests were introduced to wells of a NA-coated plate and incubated at RT for 1 hr. The well contents were removed, the wells were washed with 0.2 M Tris pH 9.5 and washes were pooled with the digests. For a measure of total fluorescence units introduced to each well, 50 µL of original digest was mixed with 50 µL 0.2 M Tris pH 9.5. The fluorescence of total and unbound fractions were read in a Perkin-Elmer LS-5 Fluorescence Spectrophotometer at excitation and emission wavelengths of 485 and 525 nm respectively and slit widths set at 5 and 3 nm respectively. The % of the fluorescence units unbound was calculated. Shown in *b.* are the mean ± SEM of triplicate determinations.

Figure 33.

a.

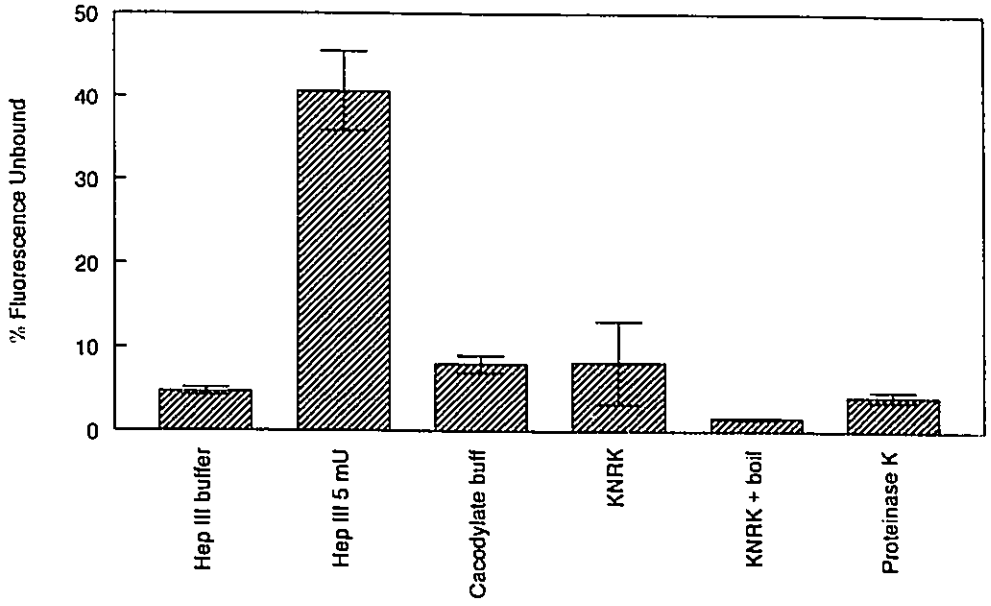
% Fluorescence Unbound
50
40
30
20
10
0
Hep III buffer
Hep III 5 mU
Cacodylate buff
KNRK
KNRK + boil
Proteinase K

b.

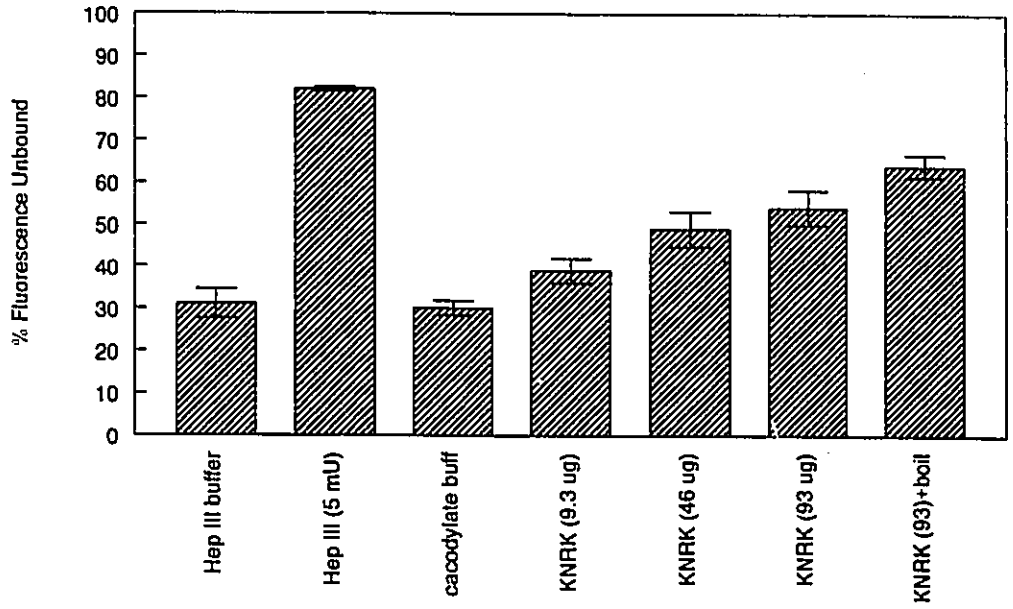
% Fluorescence Unbound
100
90
80
70
60
50
40
30
20
10
0
Hep III buffer
Hep III (5 mU)
cacodylate buff
KNRK (9.3 ug)
KNRK (46 ug)
KNRK (93 ug)
KNRK (93)+boil

than a decrease. The increase in unbound fluorescence with increasing amounts of extract was perhaps due to intrinsic fluorescence of the extract itself or release of endogenous biotin in the extracts. The fact that Hep III and KNRK were very active in the PAGE assay on the same substrate as well as in the ^{35}S-ECM immobilized assay but less than 40% release resulted with NA-immobilized digests suggested that multiple biotinylation of the substrate might have occurred instead of the desired one biotin per molecule.

III.6. *Amine Analyses of Bovine Kidney and Bovine Lung HS*

The presence of amines in the native HS substrate could lead to subsequent multiple biotinylation. Not only would purification become more difficult, but the presence of more than one biotin per molecule would substantially reduce the sensitivity of the proposed assay, since more extensive digestion would have to occur to detect a signal (seen earlier with Hep III versus KNRK digestion of substrate). Several experiments were performed to determine whether native bovine kidney HS actually contained free amines, and if so, where they were located.

Results and Discussion

By reacting HS with fluorescamine in solution and comparison of its fluorescence with a glucosamine standard (as described in Appendix II.4.), native bovine kidney HS was found to contain amines. The number of amines per HS was on average 1.1 which rose to 1.6 amines per molecular after reductive amination (HS-NH_2) (assuming M_r of 15,000).

In an attempt to determine if amines were present on bovine kidney HS itself rather than in a contaminant, the HS stock solution was microcentrifuged to remove possible

insoluble material and scanned in the spectrophotometer. The absence of nucleic acid (A_{260}) was confirmed. If basic proteins had co-purified with the acidic HS, they would have migrated away from the origin when separated on DEAE-cellulose TLC and thus stained with fluorescamine above the origin. To test this, HS from centrifuged stock was alcohol precipitated and run on a DEAE-cellulose TLC strip in 0.5 M NaCl, 0.4 M borate pH 9.4, conditions that should allow proteins to migrate. When stained with fluorescamine, there was only one spot that, upon subsequent methylene blue staining, was found to co-migrate with HS. (Another co-migrating, precipitable, anionic species is also possible but unlikely.) To confirm the absence of contaminating acidic protein, HS stock samples with or without proteinase K treatment (0.25 µg per µg HS at 37°C overnight) were alcohol precipitated and run on DEAE-cellulose TLC in 0.4 M borate pH 9.4. Staining with fluorescamine did not reveal any reduction in the fluorescence of the spot at the origin. Also, running native HS on PAGE ± proteinase K treatment did not alter mobility in the gel or reduce staining by methylene blue (Figure 32b(i)). Thus, it appeared that the free amine-containing material was probably not protein but was likely on the HS molecule itself.

Free amines could be present on *N*-desulfated glucosamine residues as a result of the HS isolation procedure or they could be due to amino acids remaining after incomplete removal of the protein components from the initial proteoglycan. In the case of HSPG, serine, the terminal amino acid to which HS is linked, is often difficult to remove [98]. Reaction with dansyl chloride (an amine-reactive probe [142]), hydrolysis to monosaccharides by boiling in 1 N HCl (a condition that would normally hydrolyze

polysaccharides, although not confirmed for HS in a PAGE analysis), separation of monomers on polyamide TLC sheets, and comparison to dansylated amino acid and glucosamine standards was performed (Figure 34). Although a longer run combined with two-dimensional chromatography and more standards would have provided greater separation and certainty of identification, in this system, it appeared that most of the amine-reactive material in HS was glucosamine that was still present after reductive amination but in much smaller amounts (not visible in the photograph in Figure 34). A faint spot corresponding to serine in HS but not in HS-NH_2 suggested that serine might have been present in the native material but had been removed during reductive amination. Therefore, *N*-desulfation of glucosamine residues might have occurred during initial purification of HS if it were exposed to acidic conditions or DMSO. Also, *N*-deacetylated glucosamine residues may exist as intermediate biosynthetic products but the proportion would be small since *N*-deacetylated residues are converted simultaneously to *N*-sulfated residues during biosynthesis of HS [97,98].

To determine the location of free amines and quantify their relative proportions, native bovine kidney was reacted with FITC in 50% DMSO and the resulting FITC-HS substrate was treated with 0.1 N NaOH at 37°C overnight to remove associated amino acids by alkali β-elimination [140]. After neutralization and precipitation to remove smaller residues, it appeared that NaOH released 35% of the fluorescence suggesting the presence of terminal amino acids in the original substrate. The other 65% of the fluorescence, stable to alkali treatment, could represent internal glucosamine residues that were *N*-desulfated in DMSO. Similar results were found for bovine lung HS except the

Figure 34. ***TLC of hydrolyzed dansylated derivatives of bovine kidney HS.***

Dansyl chloride (5-dimethylaminonapthalene-1-sulfonyl chloride) was prepared fresh as a 25 mg/mL stock in DMF. 5 mg/mL bovine kidney HS and HS-NH_2 and 2.5 mg/mL glucosamine were prepared in 0.1 M $NaHCO_3$. The pH was checked with pH paper (8.5 to 9). An equal volume of 25 mg/mL dansyl chloride was added and the mixture was incubated overnight at RT in the dark. A control (no HS or glucosamine) was set up in parallel. To hydrolyze HS conjugates into monomers, HS-containing reactions were dried down in a Speedvac Concentrator (Savant) and were treated with 1 N HCl with boiling for 1 hr. After neutralization with NaOH, 2 volumes of 10% formic acid (v/v) were added. The glucosamine reaction was diluted with 0.5 volume 10% formic acid. Dansylated serine was prepared freshly as a 0.6 mg/mL stock in 10% formic acid (v/v). Equimolar amounts of dansylated HS ("HS"), glucosamine ("Glc-NH_2 (1x)") and serine ("SER") derivatives or concentrated dansyl-glucosamine ("Glc-NH_2 (50x)") were spotted on a polyamide TLC sheet. The sheet was chromatographed in (200:3) (v/v) H_2O:90% formic acid and visualized under UV light (image shown in ***a.***). A more detailed diagram is shown in ***b.*** depicting the observed colours of spots and fainter bands that did not show up in *a.*

Figure 34.

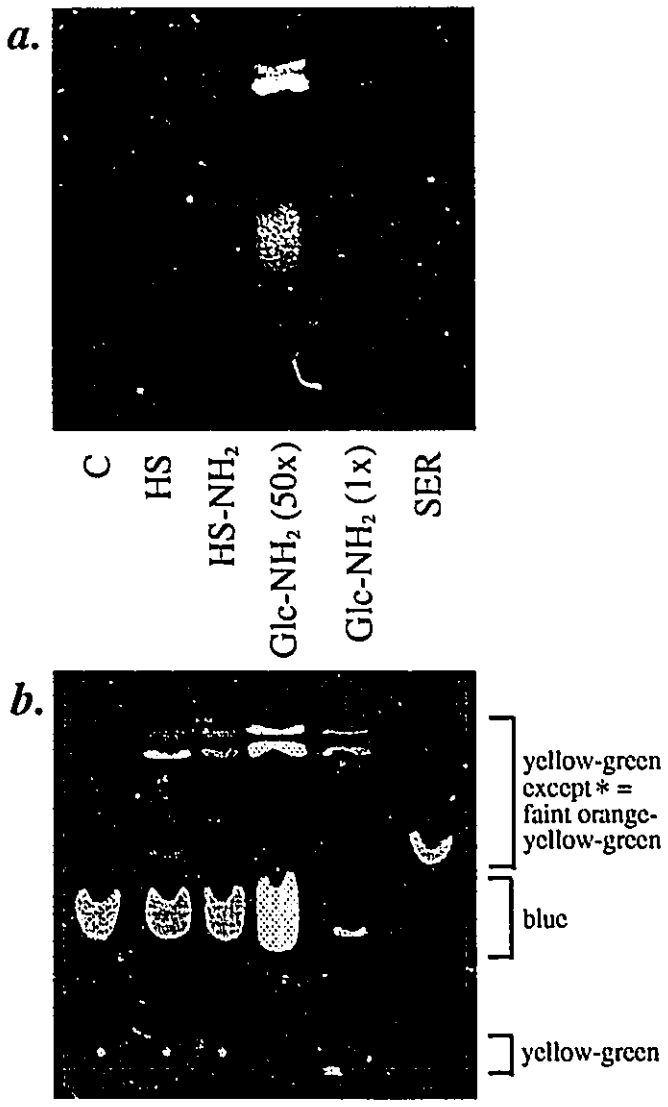
a.
C
HS
HS-NH2
Glc-NH2 (50x)
Glc-NH2 (1x)
SER
b.
yellow-green
except * =
faint orange-
yellow-green
blue
yellow-green

fluorescence intensity was 1/20th to 1/25th of that for bovine kidney HS.

Native bovine kidney HS appeared to contain internal amines which was unsatisfactory for our purposes. By contrast, using the procedures outlined in Appendix II.4., native bovine lung HS was found to contain fewer amines (0.07 per molecule on average) of which the number increased with reductive amination (0.3 per molecule), decreased with biotinylation (0 per molecule), and increased with a modified *N*-desulfation procedure described in the next section (23 to 37 amines per molecule). Thus, bovine lung HS was the more promising starting material.

III.7. *Preparation of Bovine Lung Biotinylated Fluorescent HS Using Modified N-Desulfation Procedure*

Since native bovine lung HS was found to contain fewer amines and was more digestible than bovine kidney HS in the PAGE assay, attempts were made to similarly label bovine lung HS with biotin and fluorescein. When the *N*-desulfation/FITC-labelling procedure described earlier (Section III.1) was applied to bovine lung HS, bovine lung HS, although as digestible by KNRK as the unlabelled substrate (such as in Figure 23c), was found to have low incorporation of fluorescein compared to labelled bovine kidney HS (about 1/20 to 1/25th of bovine kidney HS as assessed using a fluorometer and qualitatively seen in Figure 35. This substrate was somehow resistant to *N*-desulfation in 50% DMSO. Alternative means of *N*-desulfation were employed.

Using a more conventional *N*-desulfation procedure for partial *N*-desulfation, bovine lung HS substrates were first converted to their pyridinium salts by ion exchange chromatography [135]. An 0.8 x 0.6 cm column of Amberlite IR120 cation exchanger

Figure 35. ***PAGE assays comparing digestibility and fluorescence intensities of random FITC-labelled bovine kidney and lung substrates.***

2 µg unfractionated bovine kidney ("bk") or lung ("bl") FITC-HS (i.e., randomly labelled with fluorescein) were incubated for 16 or 0 hr at 37°C with 60 µg KNRK extract in 20 mM cacodylate pH 6.1 or 3 mU Hep III in 0.25 sodium acetate pH 8, 2.5 mM $CaCl_2$. Reactions were subjected to the PAGE assay as described in Figure 14. A methylene blue stained gel is shown in panel ***a*** while the UV transilluminated gel is shown in ***b***. As with unlabelled substrate (such as in Figure 23), bovine lung FITC-HS is digested more strongly by KNRK than bovine kidney FITC-HS, as indicated by a greater decrease in the staining of slower migrating material (in the upper portion of the gel) in "bl+KNRK 16 hr" compared to "bk+KNRK 16 hr". The fluorescence intensity of the lung substrate is much less than the kidney substrate as seen in ***b***.

Figure 35.

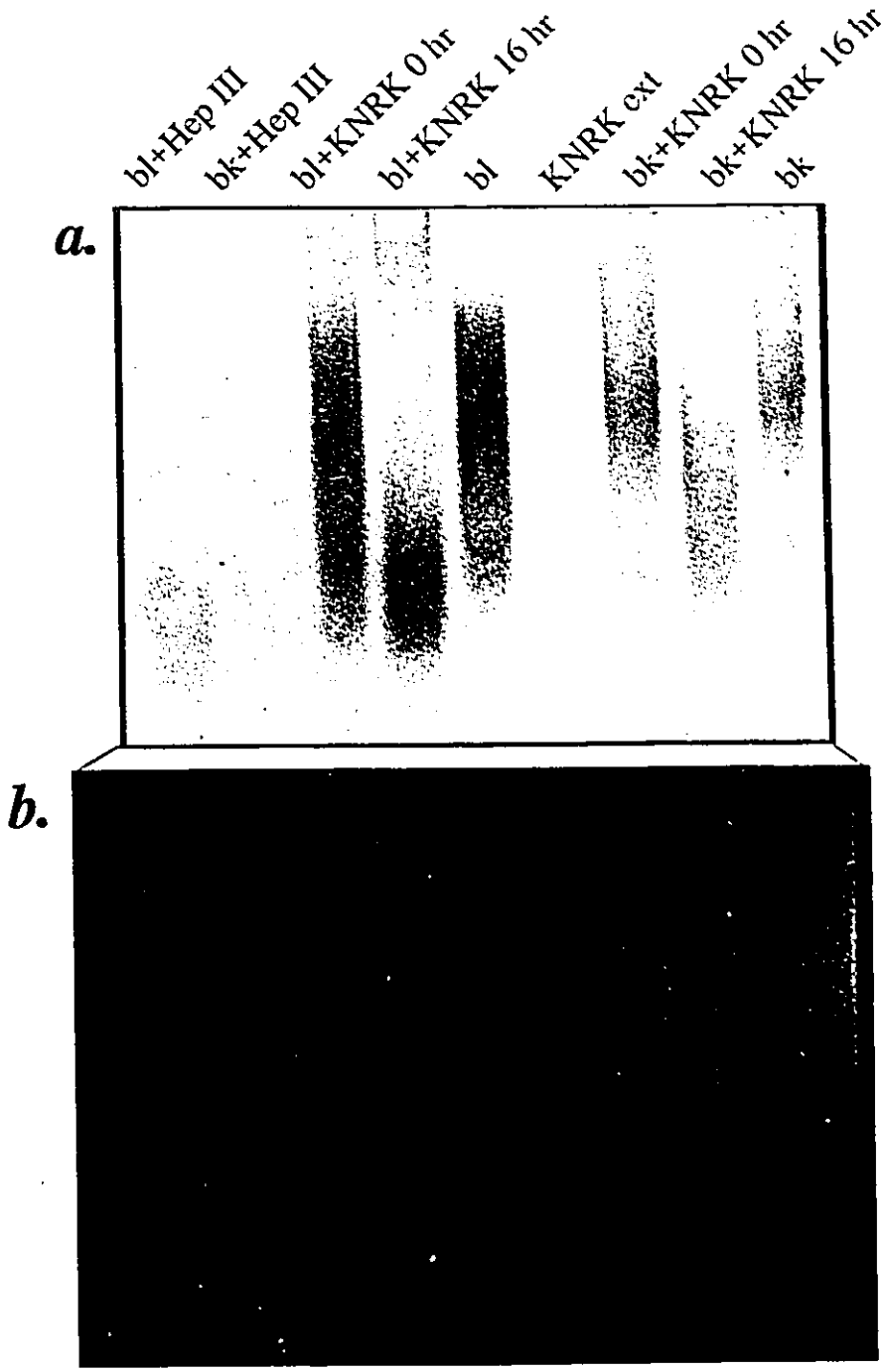
bl+Hep III
bk+Hep III
bl+KNRK 0 hr
bl+KNRK 16 hr
bl
KNRK ext
bk+KNRK 0 hr
bk+KNRK 16 hr
bk
a.
b.

resin in acid (H^+) form was prepared in a Millipore Ultrafree-MC Durapore 0.22 µm filter unit contained inside a 1.5 mL Eppendorf tube with the lid removed. After washing (by centrifugation) with water several times until the pH of the washes reached pH 6, 100 µg HS (Na^+ salt) was applied to the column and incubated 15 min at RT to convert it to acid form. The flow-through fraction was collected by centrifugation and was neutralized with 1 µL pyridine. Being volatile, excess pyridine was removed under vacuum using a Speedvac Concentrator (Savant) with heat for 5 min. Most of the HS eluted in the first flow-through fraction as determined by spotting on Hybond-N membrane and staining with methylene blue. *N*-desulfation of the pyridinium salt of HS was carried out in 95% (v/v) DMSO in water for 1 hr at RT. After diluting 1:2 with water and adjusting the pH to 9.5 with NaOH, the reactions were dialyzed against running water overnight in 12,000-14,000 MWCO dialysis tubing to remove DMSO. Using a Speedvac with heating, the dialysates were concentrated to about 0.5 µg/µL.

Results and Discussion:

As a negative control for the above procedure, DMF was used in place of DMSO. Surprisingly, both DMF and DMSO appeared to be equally effective in introducing free amines as assessed by TLC/fluorescamine (Figure 36a) and quantitative fluorescamine assay for amines (from 0.5 amines per molecule to 23 or 37 amines per molecule for DMF and DMSO respectively). The extent of amine introduction was now greatly improved and was comparable to native bovine kidney HS while acid treatment of native bovine lung HS using HCl was not as effective (note: treatment with 0.1 N HCl did not appear to hydrolyze HS (Figure 32b)).

Figure 36. ***Fluorescamine-stained TLC of acid, DMF or DMSO solvolyzed bovine lung HS and PAGE assay of fluorescein conjugates.***

a. Bovine lung HS was converted to a pyridinium salt, *N*-desulfated in DMF (shown as "HS/pyr-DMF") or DMSO (shown as "HS/pyr-DMSO") as described in Section III.7. For comparison of DMF or DMSO solvolysis to acid solvolysis, bovine lung HS was treated with 0.1 N HCl at 37°C overnight and then neutralized with 0.1 N NaOH (shown as "HS/HCl"). As a control, bovine lung HS was incubated in water at 37°C overnight and then treated with 0.1 N HCl and 0.1 N NaOH simultaneously (shown as "HS-C for HCl"). 0.5 µg of each was spotted on a DEAE-cellulose strip along with native lung HS ("bl HS") and native bovine kidney HS ("bk HS"), chromatographed in 0.4 M borate pH 9.4, sprayed twice with 15 mg/100 mL fluorescamine in acetone and visualized under UV light.

b. Water ("C") or 50 µg/mL DMSO ("DMSO-FITC") or DMF ("DMF/FITC") solvolyzed pyridinium salts of HS were reacted at RT overnight with 2.6 mM FITC in 0.1 M sodium acetate pH 8 and 50% DMF. The reactions were stopped with 0.15 M hydroxylamine pH 8.5 for 1 hr at RT. The reactions were alcohol precipitated at -20°C with 1/4th volume 4 M sodium acetate pH 8 and 4 volumes cold ethanol overnight. After microcentrifugation, washing twice with cold ethanol and resuspending the pellets in water, 0.1 µg of each was spotted on a DEAE-cellulose TLC strip, chromatographed in 0.4 M borate pH 9.45 and visualized under UV light. Similar results were obtained when *N*-desulfated HS was labelled with FITC in 50% DMSO.

c. 0.5 µg of unmodified HS, and fluoresceinated DMF-solvolyzed (shown as "FITC-HS (DMF)") or DMSO-solvolyzed (shown as "FITC-HS (DMSO)") bovine lung HS was incubated for 16 or 0 hr at 37°C with 60 µg KNRK extract in 20 mM cacodylate pH 6.1 and subjected to the PAGE assay as described in Figure 14. Fluoresceinated DMF- and DMSO-solvolyzed substrates are digestible by KNRK at 16 hr, as indicated by a decrease in the staining of slower migrating material (in the upper portion of the gel) compared to FITC-HS controls. In the methylene blue stained gel shown, there is some interfering high molecular weight material due to the KNRK extract. (Note: A lesser amount of HS than usual was used in the PAGE assay due to limited quantities of the substrates; such small amounts in the gel were not easily photographed when UV transilluminated).

Figure 36.

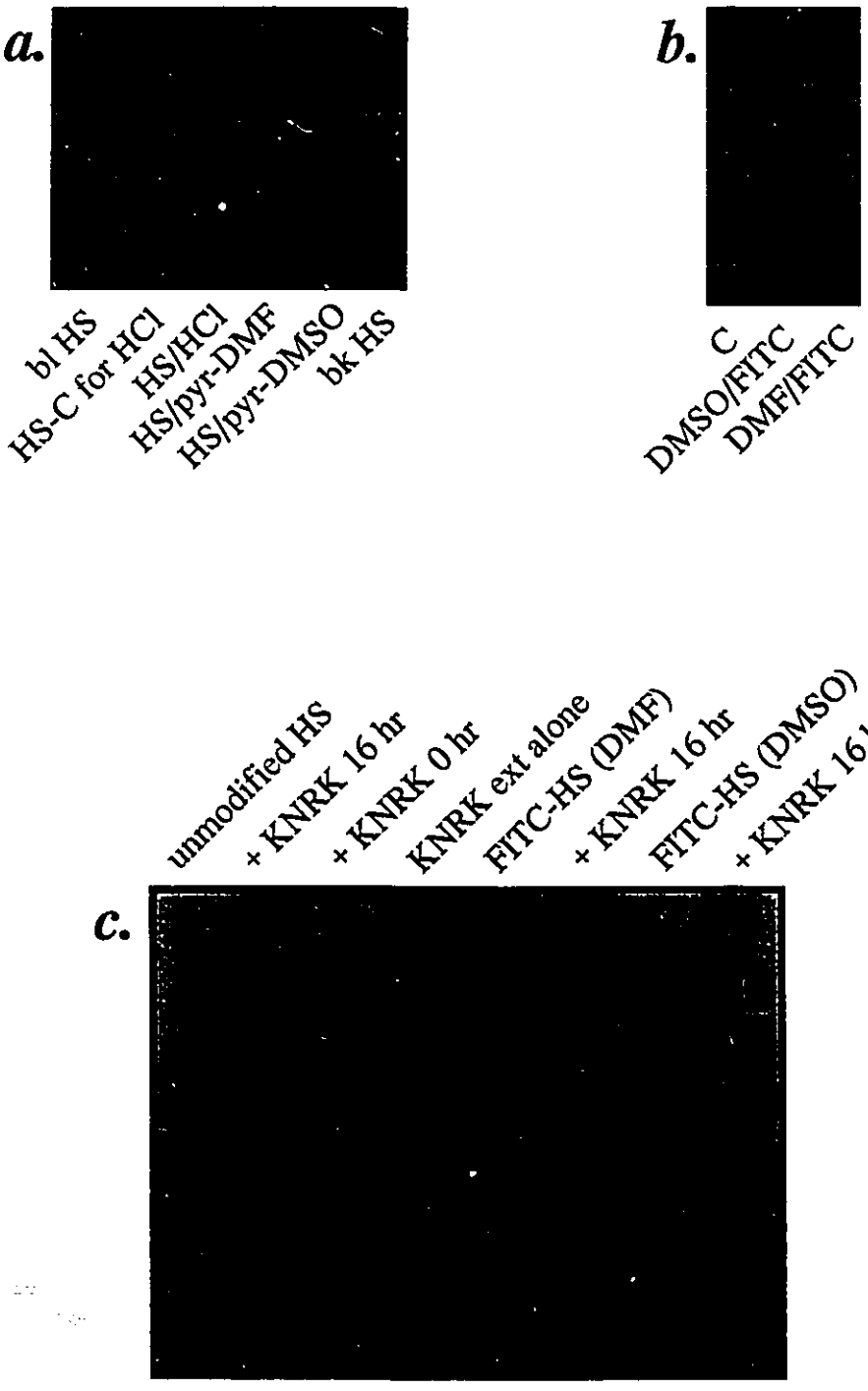
a.
bl HS
HS-C for HCl
HS/HCl
HS/pyr-DMF
HS/pyr-DMSO
bk HS
b.
C
DMSO/FITC
DMF/FITC
c.
unmodified HS
+ KNRK 16 hr
+ KNRK 0 hr
KNRK ext alone
FITC-HS (DMF)
+ KNRK 16 hr
FITC-HS (DMSO)
+ KNRK 16 hr

The substrate was subsequently labelled with FITC as described in Section III.1. Again, DMF and DMSO *N*-desulfated HS were similarly labelled with fluorescein (Figure 36b). Furthermore, both substrates were intact and digestible by KNRK as shown in the PAGE assay (Figure 36c).

III.8. *Purification of Bovine Lung FITC-HS-N-XX-B on Soft-Link Soft-Release Resin and Trial Heparanase Assays*

Because only about 13% of the molecules were biotinylated (even with repeated biotinylation which slightly improved % biotinylation to 21%), purification of the substrate (bovine lung FITC-HS-N-XXB) was still necessary.

The commercially available Soft-link Soft-Release (SLSR) resin, which is essentially monomeric avidin (refer to Section III.4.2.) immobilized to more stable and rigid methacrylate beads, was chosen for this purpose. Using bovine kidney FITC-HS, appropriate wash buffer (to remove non-specific binding) was determined to be 0.05 M Tris pH 8, 0.1% Triton X-100 and 0.15 M NaCl. Fluorescein-X-biotin was used to test purification procedures. The SLSR resin was rinsed with 0.1 M sodium phosphate pH 7 and blocked with 3 volumes of 5 mM biotin in 0.1 M phosphate pH 7 for 30 min at RT. After microcentrifuging 10 seconds, the supernatant was removed. The blocking step was repeated. The resin bed was stripped of biotin twice by incubation with 20 volumes of 10% acetic acid for 10 min RT with microcentrifuging and removal of supernatant in between. After washing twice with 20 volumes of 0.1 M phosphate pH 7 and twice with 20 volumes of SLSR equilibration buffer (50 mM Tris pH 8, 150 mM NaCl, 0.1% Triton X-100), fluorescein-X-biotin diluted in SLSR equilibration buffer was incubated with the

resin at RT for 2 hr. Washes with SLSR equilibration buffer (with 10 min RT incubation between washes) were saved for reading. Elutions with 5 mM biotin in SLSR equilibration buffer were collected and saved for reading after incubation at RT for 10 min.

Results and Discussion:

Using the above procedure, fluorescein-X-biotin was found to be 94% biotinylated and was recovered with 97% efficiency from the SLSR resin. When the procedure was applied to the purification of bovine lung FITC-HS-N-XXB followed by extensive dialysis against water and concentration in a Speedvac, the % biotinylated substrate was improved from 16-21% biotinylated to 51-54% using SA-ag beads and 80-88% using SLSR resin as a biotin capture system. (Greater % biotinylation seen with SLSR resin may be due to greater biotin-binding capacity or better access to the substrate since the exclusion limit is smaller.)

Digestion of the purified FITC-HS-N-XXB in soluble phase by 20 mU Hep III and binding to SLSR beads resulted in a decrease in % bound fluorescence from 80 to 34%. Digestion with 77 µg KNRK resulted in a decrease from 88 to 58% bound. With 0.5 µg KNRK, % bound dropped from 70 to 35; unexpectedly, with increasing amounts of extract (5 to 50 µg protein), % bound began to increase (58-62%). After boiling 50 µg KNRK for 10 min prior to digestion (a procedure which should inhibit KNRK activity as in the PAGE assay (Figure 25)), the % bound remained the same. This may have been due to intrinsic fluorescence of the extract or scattering of light due to fine precipitates in the extract. Because of this, soluble digests using lower amounts of KNRK (0.005 to 0.5 µg protein) were performed and bound to SLSR resin. From Figure 37, heparanase activity

Figure 37. ***Soluble digest of purified bovine lung FITC-HS-N-XXB by KNRK followed by binding to SLSR resin.***

0, 0.005, 0.05, or 0.5 µg KNRK extract ± boiling for 10 min was incubated with about 2 ng purified bovine lung FITC-HS-XXB in 20 mM cacodylate pH 6.1 at 37°C overnight in a 10 µL volume. After the incubation, 10 µL of equilibration buffer (50 mM Tris-HCl pH 8, 150 mM NaCl, 0.1% Triton X-100) was added to each reaction. 7.5 µL of each mixture was incubated at 37°C for 1 hr with 5 µL SLSR resin washed in equilibration buffer or 5 µL equilibration buffer alone. 37.5 µL equilibration buffer was added, mixed and the resin was pelleted by brief microcentrifugation for 10 sec. The fluorescence of the supernatant was read in a Perkin-Elmer LS-5 Fluorescence Spectrophotometer at excitation and emission wavelengths set at 485 and 525 nm respectively and slit widths set at 5 and 10 nm respectively, zeroing on equilibration buffer. The percentage fluorescence that did not bind to the resin was calculated and is shown as % fluorescence unbound. The results shown represent the mean ± range of duplicates.

Figure 38. ***Digestion of NA-immobilized bovine kidney FITC-HS-N-XXB by Hep III.***

About 7 ng of unpurified 48% biotinylated bovine kidney FITC-HS-N-XXB substrate in 25 µL PBST (10 mM potassium phosphate pH 7.4, 150 mM NaCl, 0.1% (v/v) Tween 20, 0.02% (w/v) NaN_3) were incubated in NA-coated wells of a 96-well plate. On average, 25% of the substrate bound to the wells. The wells were washed with 25 µL PBST. Varying amounts of Hep III (0 to 5 mU) in 10 µL of 1x Hep III buffer (0.25 M sodium acetate pH 8, 2.5 mM $CaCl_2$) were introduced to the wells and incubated for 10 min at RT. At the end of the incubation, 40 µL PBST was added to each well, the contents were removed and the fluorescence of each supernatant was measured in a Perkin-Elmer LS-5 Fluorescence Spectrophotometer at excitation and emission wavelengths of 485 and 525 nm respectively and slit widths set at 5 and 10 nm respectively. The instrument was zeroed on PBST. Points from 0.01 to 0.5 mU represent the mean ± range of two determinations. The other points represent the mean ± SEM of four to six determinations. Similar results were obtained using bovine lung substrate.

Figure 37.

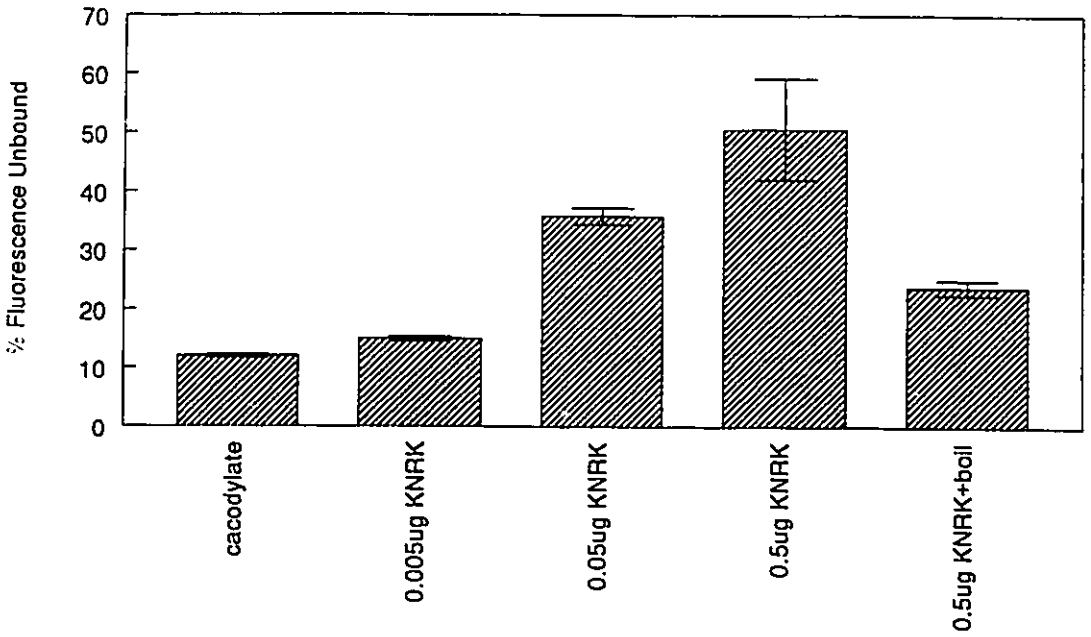

Figure 38.

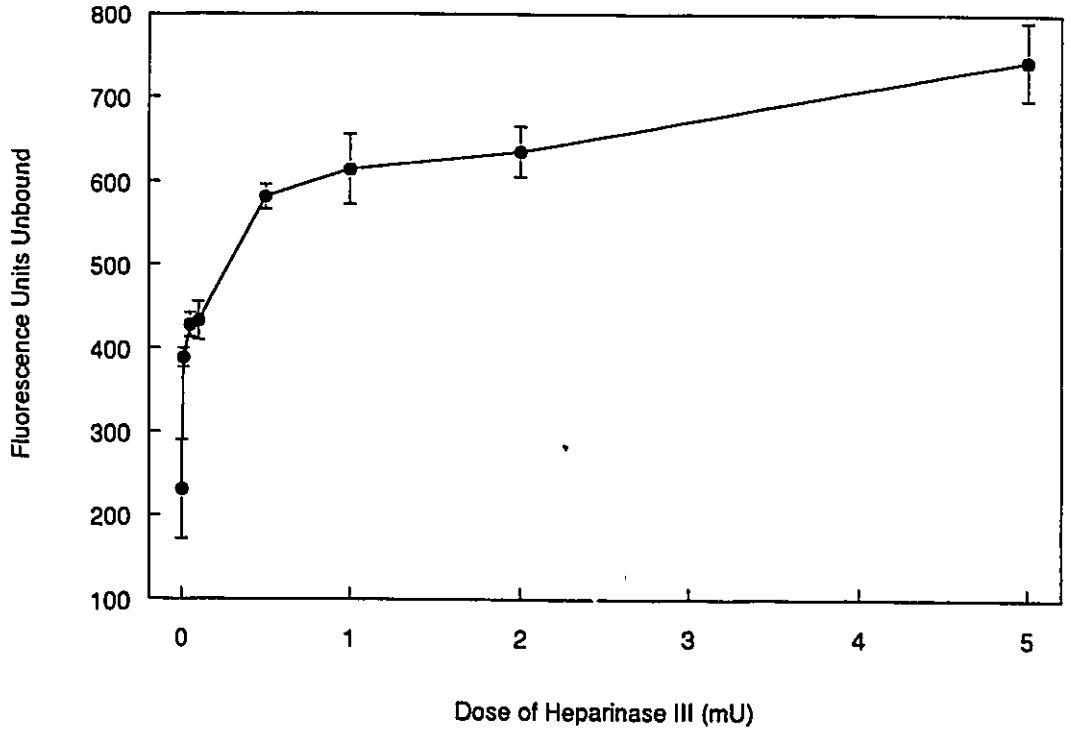

was even detected at 0.05 µg KNRK protein. Boiling 0.5 µg KNRK protein largely destroys heparanase activity. This promising assay, utilizing 2 ng of substrate which was 1/1000th of that required in the PAGE assay, could detect 100 times less KNRK heparanase (50 ng versus 5 µg protein).

For yet to be explained reasons, when other substrates were prepared in the same manner, the above results could not be reproduced. The substrates seemed to be unstable as the % biotinylation appeared to decrease with time leading to high background in soluble assays. Digestion by KNRK extract of immobilized substrate continued to be limited with interference from the extract. Nevertheless, the NA-coated plate configuration was still useful for immobilization and digestion of FITC-HS-N-XXB kidney or lung substrates by Hep III (Figure 38).

III.9. *Summary for Chapter III*

HS has been successfully reductively aminated, biotinylated and fluorescently labelled, although the exact locations of these modifications are unclear since the monosaccharide composition and primary sequence of our HS substrates are unknown. The completion of a working heparanase assay using modified HS substrates has been very difficult and, even after consulting with others in the field, the problem at hand remains complex and unresolved. It is clear that substrates from different sources vary not only in their digestibility but also in their quality and chemical properties. Perhaps using a better characterized substrate could a functional assay have resulted. Since HS, which is so heterogeneous in composition, is one of the most complex of all mammalian carbohydrates

[97,98], it may be difficult to apply standard techniques in carbohydrate chemistry to characterize HS. Fortunately, the field of GAG research is expanding as more techniques are becoming available. Although further investigation into this problem is necessary, our approach has been promising.

Having successfully fluorescently labelled HS, however, there are still some possibilities for sensitive, quantitative heparanase assays that could be developed using fluorescent HS without further modifications. For instance, an assay based on a selective precipitation or selective ion exchange of high molecular weight HS from lower molecular weight digestion products could be employed. The fluorescence of the soluble fragments could be detected with high sensitivity and could be quantified with relative ease. To further improve the sensitivity, the fluorescein labels could be replaced with a chemiluminescent label such as isoluminol, a smaller, less bulky and less hydrophobic label. This may render the substrate more digestible and its detection may be less subject to interference by intrinsic fluorescence of the extract.

OVERALL CONCLUSION OF THESIS

In Part A of this thesis, I have described conditions that induce a very high level of differentiation of U-937 cells with respect to their ability to produce $O_2^{\cdot-}$. RA was found to be a potent inducer of U-937 differentiation. The effects of RA were potentiated by known NO· donors (GTN, MOL, CAS 936) and TNM (a potential NO· or other reactive nitrogen intermediate donor). While RA is a known inducer of U-937 differentiation, reported here is the first evidence that NO· or other reactive nitrogen intermediates may also enhance RA-induced differentiation of these cells. RA-induced differentiation is also accompanied by a slight increase in heparanase activity, an effect enhanced when combined with TNM (Part B). This suggests that RA and reactive nitrogen intermediates might also be involved in the induction of heparanase.

The PAGE-based heparanase assay, the preferred assay at this point, has proven to be useful and reliable in terms of detecting heparanase activity in a variety of cell types and using a variety of HS substrates. It is clear that different heparanases digest different HS substrates and differ in sensitivity to inhibition by heparin. From the PAGE studies, KNRK cells have been shown to possess an active heparanase which may be similar to the metastatic melanoma enzyme. The PAGE assay, although semi-quantitative and time-consuming, could still be used for screening purposes since it is moderately sensitive. The PAGE and fluorescence studies have considerably increased our understanding of the nature of heparanases and HS substrates, although much remains to be learned.

REFERENCES

1. Bimboim, H. C. & Jevcak, J. J. (1981) Fluorometric method for rapid detection of DNA strand breaks in human white blood cells produced by low doses of radiation. *Cancer Res.* 41: 1889-1892.

2. Bimboim, H. C. (1982) DNA strand breakage in human leukocytes exposed to a tumor promoter, phorbol myristate acetate. *Science* 215: 1247-1249.

3. Bimboim, H. C. (1982) Factors which affect DNA strand breakage in human leukocytes exposed to a tumor promoter, phorbol myristate acetate. *Can.J.Physio.Pharmacol.* 60: 1359-1366.

4. Bimboim, H. C. & Kanabus-Kaminska, M. (1985) The production of DNA strand breaks in human leukocytes by superoxide anion may involve a metabolic process. *Proc.Natl.Acad.Sci.USA* 82: 6830-6824.

5. Bimboim, H. C. (1988) Superoxide anion may trigger DNA strand breaks in human granulocytes by acting at a membrane target. In: Annals of the New York Academy of Sciences. Vol. 551. Membrane in Cancer Cells (Galeotti, T., Cittadini, A., Neri, G. & Scarpa, A. eds.), pp. 83-94. The New York Academy of Sciences, New York.

6. Bimboim, H. C. (1990) Fluorometric analysis of DNA unwinding to study strand breaks and repair in mammalian cells. *Methods Enzymol.* 186: 550-555.

7. Cross, A. R. & Jones, O. T. G. (1991) Enzymic mechanisms of superoxide production. *Biochim.Biophys.Acta* 1057: 281-298.

8. Baggiolini, M. & Wymann, M. P. (1990) Turning on the respiratory burst. *Trends Biochem.Sci.* 15: 69-72.

9. Dinauer, M. C. (1993) The respiratory burst oxidase and the molecular genetics of chronic granulomatous disease. *Crit.Rev.Clin.Lab.Sci.* 30: 329-369.

10. Segal, A. W. & Abo, A. (1993) The biochemical basis of the NADPH oxidase of phagocytes. *Trends Biochem.Sci.* 18: 43-47.

11. Bokoch, G. M. (1994) Regulation of the human neutrophil NADPH oxidase by the Rac GTP-binding proteins. *Curr.Opin.Cell Biol.* 6: 212-218.

12. Jones, O. T. G., Jones, S. A., Hancock, J. T. & Topley, N. (1993) Composition and organization of the NADPH oxidase of phagocytes and other cells. *Biochem.Soc.Trans.* 21: 343-346.

13. Rotrosen, D., Yeung, C. L., Leto, T. L., Malech, H. L. & Kwong, C. H. (1992)

Cytochrom b558: the flavin-binding component of the phagocyte NADPH oxidase. *Science* 256: 1459-1462.

14. Royer-Pokora, B., Kunkel, L. M., Monaco, A. P., Goff, S. C., Newburger, P. E., Baehner, R. L., Cole, F. S., Curnutte, J. T. & Orkin, S. H. (1986) Cloning the gene for an inherited human disorder-chronic granulomatous disease-on the basis of its chromosomal location *Nature* 322: 32-38.

15. Volpp, B. D., Nauseef, W. M. & Clark, R. A. (1988) Two cytosolic neutrophil oxidase components absent in autosomal chronic granulomatous disease. *Science* 242: 1295-1297.

16. Baggiolini, M., Boulay, F., Badwey, J. A. & Curnutte, J. T. (1993) Activation of neutrophil leukocytes: chemoattractant receptors and respiratory burst. *FASEB J.* 7: 1004-1010.

17. Wientjes, F. B., Hsuan, J. J., Totty, N. F. & Segal, A. W. (1993) $p40^{phox}$, a third cytosolic component of the activation complex of the NADPH oxidase to contain *src* homology 3 domains. *BiochemJ.* 296: 557-561.

18. Sadler, K. L. & Badwey, J. A. (1988) Second messengers involved in superoxide production by neutrophils. Function and metabolism. *Hematol.Oncol.Clin.North.Am.* 2: 185-200.

19. Lemarchand, P., Vaglio, M., Mauel, J. & Marker, M. (1992) Translocation of a small cytosolic calcium-binding protein (MRP-8) to plasma membrane correlates with human neutrophil activation. *J.Biol.Chem.* 267: 19379-19382.

20. Francis, J. W., Balazovich, K. J., Smolen, J. E., Margolis, D. I. & Boxer, L. A. (1992) Human neutrophil annexin I promotes granule aggregation and modulates Ca^{2+}-dependent membrane fusion. *J.Clin.Invest.* 90: 537-544.

21. Nishizuka, Y. (1992) Intracellular signalling by hydrolysis of phospholipids and activation of protein kinase C. *Science* 258: 607-613.

22. Zimmer, H.-G. (1992) The oxidative pentose phosphate pathway in the heart: regulation, physiological significance, and clinical implications. *Basic Res Cardiol* 87: 303-316.

23. Schreck, R. & Baeuerle, P. A. (1991) A role for oxygen radicals as second messengers. *Trends Cell Biol.* 1: 39-42.

24. Fialkow, L., Chan, C. K., Grinstein, S. & Downey, G. P. (1993) Regualtion of tyrosine phosphorylation in neutrophils by the NADPH oxidase. *J.Biol.Chem.* 268: 17131-17137.

25. Trudel, S., Paquet, M. R. & Grinstein, S. (1991) Mechanism of vanadate-induced

activation of tyrosine phosphorylation and of the respiratory burst in HL-60 cells. *Biochem.J.* 276: 611-619.

26. Menon, S. D., Qin, S., Graeme, R. G. & Tan, Y. H. (1993) Differential induction of nuclear NF-kappaB by protein phosphatase inhibitors in primary and transformed human cells. *J.Biol.Chem.* 268: 26805-26812.

27. Schieven, G. L., Kirihara, J. M., Myers, D. E., Ledbetter, J. A. & Uckun, F. M. (1993) Reactive oxygen intermediates activate NF-kappaB in a tyrosine-kinase dependent mechanism and in combination with vanadate activate the $p56^{lck}$ and $p59^{fyn}$ tyrosine kinases in human lymphocytes. *Blood* 82: 1212-1220.

28. Schreck, R., Rieber, P. & Baeuerle, P. A. (1991) Reactive oxygen intermediates as apparently widely used messengers in the activation of the NF-kappaB transcription factor and HIV-1. *EMBO J.* 10: 2247-2258.

29. Schulze-Osthoff, K., Beyaert, R., Vandevoorde, V., Haegeman, G. & Fiers, W. (1993) Depletion of the mitochondrial electron transport abrogates the cytotoxic and gene-inductive effects of TNF. *EMBO J.* 12: 3095-3104.

30. Stevenson, M. A., Pollock, S. S., Coleman, C. N. & Calderwood, S. K. (1994) X-irradiation, phorbol esters, and H_2O_2 stimulate mitogen-activated protein kinase activity in NIH 3T3 cells through the formation of reactive oxygen intermediates. *Cancer Res.* 54: 12-15.

31. Pelech, S. L. & Sanghera, J. S. (1992) MAP kinases: charting the regulatory pathways. *Science* 257: 1355-1356.

32. Li, S. & Sedivy, J. M. (1993) Raf-1 protein kinase activates the NF-kappaB transcription factor by dissociating the cytoplasmic NF-kappaB-I-kappaB complex. *Proc.Natl.Acad.Sci.USA* 90: 9247-9251.

33. Park, J.-H. & Levitt, L. (1993) Overexpression of mitogen-activated protein kinase (ERK 1) enhances T-cell cytokine gene expression: role of AP1, NF-AT, and NF-kappaB. *Blood* 82: 2470-2477.

34. Eggleston, L. V. & Krebs, H. A. (1974) Regulation of the pentose phosphate cycle. *Biochem.J.* 138: 425

35. DeChatelet, L. R. & Parce, J. W. (1981) Hexose monophosphate shunt activity and oxygen uptake. In: Methods for Studying Mononuclear Phagocytes (Adams, D. O., Edelson, P. J. & Koren, H. eds.), pp. 477-488. New York, Academic Press, Inc.

36. Kletzien, R. F., Harris, P. K. W. & Foellmi, L. A. (1994) Glucose-6-phosphate dehydrogenase: a "housekeeping" enzyme subject to tissue-specific regulation by hormones,

nutrients, and oxidant stress. *FASEB J.* 8: 174-181.

37. Harris, P. & Ralph, P. (1985) Human leukemic models of myelomonocytic development: a review of the HL-60 and U937 cell lines. *J.Leukoc.Biol.* 37: 407-422.

38. Zhang, L., Nakaya, K., Yoshida, T. & Kuroiwa, Y. (1992) Induction by bufalin of differentiation of human leukemia cells HL-60, U-937, and ML1 toward macrophage/monocyte-like cells and its potent synergistic effect on the differentiation of human leukemia cells in combination with other inducers. *Cancer Res.* 52: 4634-4641.

39. Olsson, I. L., Breitman, T. R. & Gallo, R. C. (1982) Priming of human myeloid leukemic cell lines HL-60 and U-937 with retinoic acid for differentiation effects of cyclic adenosine 3':5'-monophosphate-inducing agents and a t-lymphocyte-derived differentiation factor. *Cancer Res.* 42: 3928-3933.

40. Olsson, I. L., Breitman, T. R. & Gallo, R. C. (1982) Induction of differentiation of the human histiocytic lymphoma cell line U-937 by retinoic acid and cyclic adenosine 3':5'-monophosphate-inducing agents. *Cancer Res.* 42: 3924-3927.

41. Taimi, M., Chateau, M.-T., Cabane, S. & Marti, J. (1991) Synergistic effect of retinoic acid and 1,25-dihydroxyvitamin D_3 on the differentiation of the human monocytic cell line U937. *Leuk.Res.* 15: 1145-1152.

42. Petkovich, M., Brand, N. J., Krust, A. & Chambon, P. (1987) A human retinoic acid receptor which belongs to the family of nuclear receptors. *Nature* 330: 444-450.

43. Mangelsdorf, D. J., Ong, E. S., Dyck, J. A. & Evans, R. M. (1990) Nuclear receptor that identifies a novel retinoic acid response pathway. *Nature* 345: 224-229.

44. Yu, V. C., Delsert, C., Andersen, B., Holloway, J. M., Devary, O. V., Naar, A. M., Kim, S. Y., Boutin, R.-M., Glass, C. K. & Rosenfeld, M. G. (1991) RXRβ: a coregulator that enhances binding of retinoic acid, thyroid hormone, and vitamin D receptors to their cognate response elements. *Cell* 67: 1251-1266.

45. Tsai, S. & Collins, S. J. (1993) A dominant negative retinoic acid receptor blocks neutrophil differentiation at the promyelocyte stage. *Proc.Natl.Acad.Sci.U.S.A.* 90: 7153-7157.

46. McBurney, M. W., Costa, S. & Pratt, M. A. C. (1993) Retinoids and cancer: a basis for differentiation therapy. *Cancer Invest.* 11: 590-598.

47. Lubbert, M., Herrmann, F. & Koeffler, H. P. (1991) Expression and regulation of myeloid-specific genes in normal and leukemic myeloid cells. *Blood* 77: 909-924.

48. Gullberg, U., Nilsson, E., Einhorn, S. & Olsson, I. (1985) Combinations of

interferon-gamma and retinoic acid or 1α,25-dihydroxycholecalciferol induce differentiation of the human monoblast leukemia cell line U-937. *Exp.Hematol.* 13: 675-679.

49. Peck, R. & Bollag, W. (1991) Potentiation of retinoid-induced differentiation of HL-60 and U937 cell lines by cytokines. *Eur.J.Cancer* 27: 53-57.

50. Olsson, I., Gullberg, U., Ivhed, I. & Nilsson, K. (1983) Induction of differentiation of the human histiocytic lymphoma cell line U-937 by 1alpha.25-dihydroxycholecalciferol. *Cancer Res.* 43: 5862-5867.

51. Laskin, D. L., Beavis, A. J., Sirak, A. A., O'Connell, S. M. & Laskin, J. D. (1990) Differentiation of U-937 histiocytic lymphoma cells towards mature neutrophilic granulocytes by dibutyryl cyclic adenosine-3',5'-monophosphate. *Cancer Res.* 50: 20-25.

52. Kamijo, R., Takeda, K., Nagumo, M. & Konno, K. (1990) Effects of combinations of transforming growth factor-β_1 and tumor necrosis factor on induction of differentiation of human myelogenous leukemic cell lines. *J.Immunol.* 144: 1311-1316.

53. Boss, G. R. (1989) cGMP-induced differentiation of the promyelocytic cell line HL-60. *Proc.Natl.Acad.Sci.U.S.A.* 86: 7174-7178.

54. Ignarro, L. J. (1991) Signal transduction mechanisms involving nitric oxide. *Biochem.Pharmacol.* 41: 485-490.

55. Schmidt, H. H. H. W., Lohmann, S. M. & Walter, U. (1993) The nitric oxide and cGMP signal transduction system: regulation and mechanism of action. *Biochim.Biophys.Acta Mol.Cell Res.* 1178: 153-175.

56. Nathan, C. (1992) Nitric oxide as a secretory product of mammalian cells. *FASEB J.* 6: 3051-3064.

57. Noack, E. & Feelisch, M. (1991) Molecular mechanisms of nitrovasodilator bioactivation. *Basic Res Cardiol* 86: 37-50.

58. Ignarro, L. J., Lippton, H., Edwards, J. C., Baricos, W. H., Hyman, A. L., Kadowitz, P. J. & Gruetter, C. A. (1981) Mechanisms of vascular smooth muscle relaxation by organic nitrates, nitrites, nitroprusside and nitric oxide: evidence for the involvement of S-nitrosothiols as active intermediates. *J.Pharmacol.Exp.Ther.* 218: 739-749.

59. Magrinat, G., Mason, S. N., Shami, P. J. & Weinberg, J. B. (1992) Nitric oxide modulation of human leukemia cell differentiation and gene expression. *Blood* 80: 1880-1884.

60. Kurz, M. A., Boyer, T. D., Whalen, R., Peterson, T. E. & Harrison, D. G. (1993) Nitroglycerin metabolism in vascular tissue: role of glutathione S-transferases and

relationship between NO· and NO_2- formation. *Biochem J.* 292: 545-550.

61. Kuhn, M., Otten, A., Frolich, J. C. & Forstermann, U. (1991) Glyceryl trinitrate increases platelet cyclic GMP after metabolism in fibroblasts. *Eur.J.Pharmacol.* 200: 175-178.

62. Kowaluk, E. A. & Fung, H.-L. (1991) Vascular nitric oxide-generating activities for organic nitrites and organic nitrates are distinct. *J.Pharmacol.Exp.Ther.* 259: 519-525.

63. Feelisch, M. (1991) The biochemical pathways of nitric oxide formation from nitrovasodilators: appropriate choice of exogenous NO donors and aspects of preparation and handling of aqueous NO solutions. *J.Cardiovasc.Pharmacol.* 17(Suppl.3): S25-S33.

64. Bimboim, H. C. (1983) A rapid alkaline extraction method for the isolation of plasmid DNA. *Methods Enzymol.* 100: 243-256.

65. Piechaczyk, M., Blanchard, J. M., Marty, L., Dani, C., Panabieres, F., Sabouty, S. E., Fort, P. & Jeanteur, P. (1984) Post-transcriptional regulation of glyceraldehyde-3-phosphate dehydrogenase gene expression in rat tissues. *Nucleic Acids Res.* 12: 6951-6963.

66. Bimboim, H. C. (1993) Extraction of high molecular weight RNA and DNA from cultured mammalian cells. *Methods Enzymol.* 216: 154-160.

67. Kikuchi, K., Nagano, T., Hayakawa, H., Hirata, Y. & Hirobe, M. (1993) Detection of nitric oxide production from a perfused organ by a luminol-H_2O_2 system. *Anal.Chem.* 65: 1794-1799.

68. DeVouge, M. W., Yamazaki, A., Bennett, S. A. L., Chen, J.-H., Shwed, P. S., Couture, C. & Bimboim, H. C. (1994) Immunoselection of GRP94/endoplasmin from a KNRK cell-specific lambda-gt11 library using antibodies directed against a putative heparanase amino-terminal peptide. *Int.J.Cancer* 56: 286-294.

69. Elferink, J. G. R. (1984) Measurement of the metabolic burst in human neutrophils: a comparison between cytochrome c and NBT reduction. *Res.Commun.Chem.Path.Pharm.* 43: 339-342.

70. Stamler, J. S., Singel, D. J. & Loscalzo, J. (1992) Biochemistry of nitric oxide and its redox-activated forms. *Science* 258: 1898-1902.

71. Stamler, J. S., Simon, D. I., Osborne, J. A., Mullins, M. E., Jaraki, O., Michel, T., Singel, D. J. & Loscalzo, J. (1992) S-nitrosylation of proteins with nitric oxide: synthesis and characterization of biologically active compounds. *Proc.Natl.Acad.Sci.U.S.A.* 89: 444-448.

72. Myers, P. R., Minor, R. L.,Jr., Guerra, R. ,Jr., Bates, J. N. & Harrison, D. G. (1990)

Vasorelaxant properties of the endothelium-derived relaxing factor more closely resemble S-nitrosocysteine than nitric oxide. *Nature* 345: 161-163.

73. Chong, S. & Fung, H.-L. (1991) Biochemical and pharmacological interactions between nitroglycerin and thiols. Effects of thiol structure on nitric oxide generation and tolerance reversal. *Biochem.Pharmacol.* 42: 1433-1439.

74. Stamler, J. S., Jaraki, O., Osborne, J., Simon, D. I., Keaney, J., Vita, J., Singel, D., Valeri, C. R. & Loscalzo, J. (1992) Nitric oxide circulates in mammalian plasma primarily as an *S*-nitroso adduct of serum albumin. *Proc.Natl.Acad.Sci.U.S.A.* 89: 7674-7677.

75. Clancy, R. M. & Abramson, S. B. (1992) Novel synthesis of S-nitrosoglutathione and degradation by human neutrophils. *Anal.Biochem.* 201: 365-371.

76. Yamazaki, A. & Bimboim, H. C. (1995) Potentiation of retinoic acid-induced U-937 differentiation into respiratory burst-competent cells by nitric oxide donors. *Leuk.Res.* 19: 325-335.

77. Kikuchi, K., Nagano, T., Hayakawa, H., Hirata, Y. & Hirobe, M. (1993) Real time measurement of nitric oxide produced *ex vivo* by luminol-H_2O_2 chemiluminescence method. *J.Biol.Chem.* 268: 23106-23110.

78. Radi, R., Cosgrove, T. P., Beckman, J. S. & Freeman, B. A. (1993) Peroxynitrite-induced luminol chemiluminescence. *Biochem.J.* 290: 51-57.

79. Rodaway, A. R. F., Teahan, C. G., Casimir, C. M., Segal, A. W. & Bentley, D. L. (1990) Characterization of the 47-kilodalton autosomal chronic granulomatous disease protein: tissue-specific expression and transcriptional control by retinoic acid. *Mol.Cell.Biol.* 10: 5388-5396.

80. Barker, K. A., Orkin, S. H. & Newburger, P. E. (1988) Expression of the X-CGD gene during induced differentiation of myeloid leukemia cell line HL-60. *Mol.Cell.Biol.* 8: 2804-2810.

81. Levy, R., Rotrosen, D., Nagauker, O., Leto, T. L. & Malech, H. L. (1990) Induction of the respiratory burst in HL-60 cells: correlation of function and protein expression. *J.Immunol.* 145: 2595-2601.

82. Cassatella, M. A., Hartman, L., Perussia, B. & Trinchieri, G. (1989) Tumor necrosis factor and immune interferon synergistically induce cytochrome b-245 heavy-chain gene expression and nicotinamide-adenine dinucleotide phosphate hydrogenase oxidase in human leukemic myeloid cells. *J.Clin.Invest.* 83: 1570-1579.

83. Saito, H., Kuroki, T. & Nose, K. (1989) Decrease in CuZn-superoxide dismutase mRNA level during differentiation of human monocytic and promyelotic leukemia cells.

FEBS Lett. 249: 253-256.

84. Auwerx, J. H., Chait, A., Wolfbauer, G. & Deeb, S. S. (1989) Loss of copper-zinc superoxide dismutase gene expression in differentiated cells of myelo-monocytic origin. *Blood* 74: 1807-1810.

85. Diggs, L. W., Sturm, D. & Bell, A. (1985) The morphology of human blood cells. Ed.5th, pp. 1-92. Abbott Laboratories, Abbott Park, IL.

86. Lowenstein, C. J. & Snyder, S. H. (1992) Nitric oxide, a novel biologic messenger. *Cell* 70: 705-707.

87. Henry, Y., Lepoivre, M., Drapier, J.-C., Ducrocq, C., Boucher, J.-L. & Guissani, A. (1993) EPR characterization of molecular targets for NO in mammalian cells and organelles. *FASEB J.* 7: 1124-1134.

88. Rabini, J., Mulac, W. A. & Matheson, M. S. (1965) The pulse radiolysis of aqueous tetranitromethane. I. Rate constants and the extinction coefficient of e^-_{aq}. II. Oxygenated solutions. *J.Phys.Chem.* 69: 53-70.

89. Ischiropoulos, H., Zhu, L., Chen, J., Tsai, M., Martin, J. C., Smith, C. D. & Beckman, J. S. (1992) Peroxynitrite-mediated tyrosine nitration catalyzed by superoxide dismutase. *Arch.Biochem.Biophys.* 298: 431-437.

90. Beckman, J. S., Ischiropoulos, H., Zhu, L., van der Woerd, M., Smith, C., Chen, J., Harrison, J., Martin, J. C. & Tsai, M. (1992) Kinetics of superoxide dismutase- and iron-catalyzed nitration of phenolics by peroxynitrite. *Arch.Biochem.Biophys.* 298: 438-445.

91. Makishima, M., Honma, Y., Hozumi, M., Sampi, K., Hattori, M., Umezawa, K. & Motoyoshi, K. (1991) Effects of inhibitors of protein tyrosine kinase activity and/or phosphatidylinositol turnover on differentiation of some human myelomonocytic leukemia cells. *Leuk.Res.* 15: 701-708.

92. Katagiri, K., Katagiri, T., Kajiyama, K., Uehara, Y., Yamamoto, T. & Yoshida, T. (1992) Modulation of monocytic differentiation of HL-60 cells by inhibitors of protein tyrosine kinases. *Cell.Immunol.* 140: 282-294.

93. Constantinous, A., Kiguchi, K. & Huberman, E. (1990) Induction of differentiation and DNA strand breakage in human HL-60 and K-562 leukemia cells by genistein. *Cancer Res.* 50: 2618-2624.

94. Nakajima, M., Irimura, T., Di Ferrante, D., Di Ferrante, N. & Nicolson, G. L. (1983) Heparan sulfate degradation: relation to tumor invasive and metastatic properties of mouse B16 melanoma sublines. *Science* 220: 611-613.

95. Darnell, J., Lodish, H. & Baltimore, D. (1990) Molecular cell biology, Ed.2nd, pp. 1-1105. Scientific American Books, Inc. New York.

96. Nakajima, M., Irimura, T. & Nicolson, G. L. (1988) Heparanases and tumor metastasis. *J.Cell.Biochem.* 36: 157-167.

97. Gallagher, J. T., Lyon, M. & Steward, W. P. (1986) Structure and function of heparan sulphate proteoglycans. *Biochem.J.* 236: 313-325.

98. Fransson, L.-A. (1985) Mammalian glycosaminoglycans. In: The polysaccharides, Vol. III (Aspinall, G. D. ed.), pp. 337-415. Academic Press, Inc. New York.

99. Gallagher, J. T. (1989) The extended family of proteoglycans: social residents of the pericellular zone. *Curr.Opin.Cell Biol.* 1: 1201-1218.

100. David, G. (1993) Structural and functional diversity of the heparan sulfate proteoglycans. *Adv.Exp.Med.Biol.* 313: 69-78.

101. Kjellen, L. & Lindahl, U. (1991) Proteoglycans: structures and interactions. *Annu.Rev.Biochem.* 60: 443-475.

102. Vlodavsky, I., Bar-Shavit, R., Ishai-Michaeli, R., Bashkin, P. & Fuks, Z. (1991) Extracellular sequestration and release of fibroblast growth factor: a regulatory mechanism? *Trends Biochem.Sci.* 16: 268-271.

103. Iozzo, R. V., Cohen, I. R., Grassel, S. & Murdoch, A. D. (1994) The biology of perlecan: the multifaceted heparan sulphate proteoglycan of basement membranes and pericellular matrices. *Biochem.J.* 302: 625-639.

104. Freeman, C. & Hopwood, J. (1992) Lysosomal degradation of heparin and heparan sulfate. *Adv.Exp.Med.Biol.* 313: 121-134.

105. Alexander, C. M. & Werb, Z. (1989) Proteinases and extracellular matrix remodelling. *Curr.Opin.Cell Biol.* 1: 974-982.

106. Nicolson, G. L. (1989) Metastatic tumor cell interactions with endothelium, basement membrane and tissue. *Curr.Opin.Cell Biol.* 1: 1009-1019.

107. Yahalom, J., Eldor, A., Fuks, Z. & Vlodavsky, I. (1984) Degradation of sulfated proteoglycans in the subendothelial extracellular matrix by human platelet heparitinase. *J.Clin.Invest.* 74: 1842-1849.

108. Nakajima, M., Irimura, T., Di Ferrante, N. & Nicolson, G. L. (1984) Metastatic melanoma cell heparanase: characterization of heparan sulfate degradation fragments produced by B16 melanoma endoglucuronidase. *J.Biol.Chem.* 259: 2283-2290.

109. Ricoveri, W. & Cappelletti, R. (1986) Heparan sulfate endoglycosidase and metastatic potential in murine fibrosarcoma and melanoma. *Cancer Res.* 46: 3855-3861.

110. Hoogewerf, A. J., Leone, J. W., Reardon, I. M., Howe, W. J., Asa, D., Heinrikson, R. L. & Ledbetter, S. R. (1995) CXC chemokines connective tissue activating peptide-III and neutrophil activiting peptide-2 are heparin/heparan sulfate-degrading enzymes. *J.Biol.Chem.* 270: 3268-3277.

111. Bar-Ner, M., Kramer, M. D., Schirrmacher, V., Ismai-Michaeli, R., Fuks, Z. & Vlodavsky, I. (1985) Sequential degradation of heparan sulphate in the subendothelial extracellular matrix by highly metastatic lymphoma cells. *Int.J.Canccr* 35: 483-491.

112. Oosta, G. M., Favreau, L. V., Beeler, D. L. & Rosenberg, R. D. (1982) Purification and properties of human platelet heparitinase. *J.Biol.Chem.* 257: 11249-11255.

113. Gallagher, J. T., Walker, A., Lyon, M. & Evans, W. H. (1988) Heparan sulphate-degrading endoglycosidase in liver plasma membranes. *BiochemJ.* 250: 719-726.

114. Matzner, Y., Vlodavsky, I., Bar-Ner, M., Ishai-Michaeli, R. & Tauber, A. I. (1992) Subcellular localization of heparanase in human neutrophils. *J.Leukoc.Biol.* 51: 519-524.

115. Matzner, Y., Bar-Ner, M., Yahalom, J., Ishai-Michaeli, R., Fuks, Z. & Vlodavsky, I. (1985) Degradation of heparan sulfate in the subendothelial extracellular matrix by a readily released heparanase from human neutrophils. *J.Clin.Invest.* 76: 1306-1313.

116. Savion, N., Disatnik, M.-H. & Nevo, Z. (1987) Murine macrophage heparanase: inhibition and comparison with metastatic tumor cells. *J.Cell.Physiol.* 130: 77-84.

117. Naparstek, Y., Cohen, I. R., Fuks, Z. & Vlodavsky, I. (1984) Activated T lymphocytes produce a matrix-degrading heparan sulphate endoglycosidase. *Nature* 310: 241-244.

118. Tekotte, H., Engel, M., Margolis, R. U. & Margolis, R. K. (1994) Disaccharide composition of heparan sulfates: brain, nervous tissue storage organelles, kidney and lung. *J.Neurochem.* 62: 1126-1130.

119. Jin, L., Nakajima, M. & Nicolson, G. L. (1990) Immunochemical localization of heparanase in mouse and human melanomas. *Int.J.Cancer* 45: 1088-1095.

120. Jin, L., Nakajima, M. & Nicolson, G. L. (1992) Molecular cloning and expression of human heparanase cDNA. *Proc.Am.Assoc.Cancer Res.* 33: 57(abs)

121. Bashkin, P., Razin, E., Eldor, A. & Vlodavsky, I. (1990) Degranulating mast cells secrete an endoglycosidase that degrades heparan sulfate in subendothelial extracellular matrix. *Blood* 75: 2204-2212.

122. Moller, H. J., Heinegard, D. & Poulsen, J. H. (1993) Combined alcian blue and silver staining of subnanogram quantities of proteoglycans and glycosaminoglycans in sodium dodecyl sulfate-polyacrylamide gels. *Anal.Biochem.* 209: 169-175.

123. Nakajima, M., Irimura, T. & Nicolson, G. L. (1986) A solid-phase substrate of heparanase: its application to assay of human melanoma for heparan sulfate degradative activity. *Anal.Biochem.* 157: 162-171.

124. Irimura, T., Nakajima, M. & Nicolson, G. L. (1986) Chemically modified heparins as inhibitors of heparan sulfate specific endo-beta-glucuronidase (heparanase) of metastatic melanoma cells. *Biochemistry* 25: 5322-5328.

125. Vlodavsky, I., Fuks, Z., Bar-Ner, M., Ariav, Y. & Schirrmacher, V. (1983) Lymphoma cell mediated degradation of sulfated proteoglycans in subendothelial extracellular matrix: relation to tumor cell metastasis. *Cancer Res.* 43: 2704-2711.

126. Yahalom, J., Fibach, E., Bar-Tana, R., Fuks, Z. & Vlodavsky, I. (1988) Differentiating human leukemia cells express heparanase that degrades heparan sulfate in subendothelial extracellular matrix. *Leuk.Res.* 12: 711-717.

127. Aeed, P. A., Nakajima, M. & Welch, D. R. (1988) The role of polymorphonuclear leukocytes (PMN) on the growth and metastatic potential of 13762NF mammary adenocarcinoma cells. *Int.J.Cancer* 42: 748-759.

128. Graham, L. D. (1994) Tumour rejection antigens of the hsp90 family (gp96) closely resemble tumour-associated heparanase enzymes. *Biochem.J.* 301: 917-918.

129. Nicolson, G. L. & Nakajima, M. (1994) Tumour rejection antigens of the hsp90 family (gp96) closely resemble tumour-associated heparanase enzymes: reply. *Biochem.J.* 301: 918

130. Srivastava, P. K. (1994) Endo-beta-D-glucuronidase (heparanase) activity of heat-shock protein/tumour rejection antigen gp96. *Biochem.J.* 301: 919

131. Nakanishi, H., Oguri, K., Yoshida, K., Itano, N., Takenaga, K., Kazama, T., Yoshida, A. & Okayama, M. (1992) Structural differences between heparan sulphates of proteoglycan involved in the formation of basement membranes *in vivo* by Lewis-lung-carcinoma-derived cloned cells with different metastatic potentials. *Biochem.J.* 288: 215-224.

132. Godder, K., Vlodavsky, I., Eldor, A., Weksler, B. B., Haimovitz-Freidman, A. & Fuks, Z. (1991) Heparanase activity in cultured endothelial cells. *J.Cell.Physiol.* 148: 274-280.

133. Bame, K. J. (1993) Release of heparan sulfate glycosaminoglycans from

proteoglycans in chinese hamster ovary cells does not require proteolysis of the core protein. *J.Biol.Chem.* 268: 19956-19964.

134. Sewell, R. F., Brenchley, P. E. C. & Mallick, N. P. (1989) Human mononuclear cells contain an endoglycosidase specific for heparan sulphate glycosaminoglycan demonstrable with the use of a specific solid-phase metabolically radiolabelled substrate. *Biochem J.* 264: 777-783.

135. Nagasawa, K. & Inoue, Y. (1980) De-N-sulfation. *Methods Carbohydr.Chem.* 8: 291-294.

136. Lane, C. F. (1975) Sodium cyanoborohydride - a highly selective reducing agent for organic functional groups. *Synthesis* March: 135-146.

137. Udenfriend, S., Stein, S., Bohlen, P., Dairman, W., Leimbruber, W. & Weigele, M. (1972) Fluorescamine: a reagent for assay of amino acids, peptides, proteins, and primary amines in the picomole range. *Science* 178: 871-872.

138. Roy, R., Katzenellenbogen, E. & Jennings, H. J. (1984) Improved procedures for the conjugation of oligosaccharides to protein by reductive amination. *Can.J.Biochem.Cell Biol.* 62: 270-275.

139. Updyke, T. V. & Nicolson, G. L. (1986) Immunoaffinity isolation of membrane antigens with biotinylated monoclonal antibodies and streptavidin-agarose. *Methods Enzymol.* 121: 717-725.

140. Beeley, J. G. (1985) Laboratory technigues in biochemistry and molecular biology, volume 16: glycoprotein and proteoglycan techniques, pp. 1-462. Elsevier Science Publishers B.V. (Biomedical Division), Amsterdam.

141. Kohanski, R. A. & Lane, M. D. (1990) Monovalent avidin affinity columns. *Methods Enzymol.* 184: 194-200.

142. Gray, W. R. (1972) End-group analysis using dansyl chloride. *Methods Enzymol.* 25: 121-139.

APPENDIX I: LIST OF MATERIALS, SUPPLIERS AND SOLUTION COMPOSITIONS

α.MM	Dr. I. Vlodavsky; 80 µg/µL in 10 mM phosphate citrate pH 6.1, 1 mM NaCl, 0.25 M α.methyl mannoside; stored at -20°C
acrylamide/bisacrylamide mix	BDH; Electran Acrylogel 5 mix
Amberlite IR120 H^+ form	BDH
ammonium persulfate	Bio-Rad
aprotinin	Sigma; 2 mg/mL stock in water, stored at -20°C
Aquasol 2 scintillation fluid	Dupont-NEN Research Products
azide, sodium	Fisher
B16F10	Dr. R. Liteplo
bacterial clone for pGAPDH	Dr. R. Hawley
bacterial clones for $p47^{phox}$, $gp91^{phox}$ G6PD, SOD	American Type Culture Collection (ATCC)
BioGel Wrap	BioDesign, Inc.
biotin	Sigma; stock prepared as 0.5 to 1 mg/mL in water with heating at 50 to 60°C to facilitate dissolving, stored at 4°C
biotin hydrazide	Sigma; 4 mM stock in 90% DMF:10% H_2O; used with 2 mg/mL HS at 0.4 mM in 0.2 M $NaHCO_3$ pH 8.3 RT; reactions terminated with 50 mM glucose
β-mercaptoethanol	BDH
bovine intestine HS (Na^+ salt)	Sigma; 10 mg/mL stock in water, stored at -20°C
bovine kidney HS (Na^+ salt)	Sigma (pbs or pfs); 10 mg/mL stock in water, stored at -20°C
bovine lung heparin	Dr. I. Vlodavksy (from Kabi-Pharmacia); stock 1 mg/mL in water, stored at -20°C
bovine lung HS	Dr. I. Vlodavsky (from Dr. C.-M. Svahn of Kabi Pharmacia); ~ 30 mg/mL in water, stored at -20°C
BSS	137 mM NaCl, 5 mM KCl, 0.8 mM $MgSO_4$, 10 mM HEPES, pH 7.4; stored at 4°C
BXXSE	Molecular Probes; freshly prepared as 18 mM stock in DMF
cacodylate, sodium	BDH; 10x buffer = 0.2 M pH 6.1, stored at -20°C
CAS	Hoechst-Roussel Canada Inc. (Dr. B. Carter); 30 µM in RPMI 1640 + 10% fetal calf serum prepared fresh in subdued light, filtered through 0.2 µm filter and used immediately
catalase (EC 1.11.1.6)	Sigma; ~ 135,000 U/mL stock in H_2O, stored at 4°C
CDTA	Sigma
CEL 300 DEAE TLC sheets	Whatman
CHAPS	Sigma

chymostatin	Sigma; 10 mM in DMSO, stored at -20°C
CT	10 mM Tris-HCl, pH 7.5, 1 mM CDTA
Cu,Zn-SOD	Diagnostic Data Inc.; 2.5 mg/mL stock in BSS
cytochrome c	ICN; 1.6 mM in water and stored at 4°C
CYS	BDH Inc.; freshly prepared as a 30 mM solution in 10 mM HCl and filtered through a 0.2 µm filter
dansyl chloride	Dr. Anderson and Sigma
dansylated serine	Dr. Anderson and Sigma
[^{32}P]dCTP	Amersham; 3000 Ci/mmol stock stored at -20°C
desferal (desferrioxamine mesylate)	CIBA; 15 mM stock in water, stored at 4°C
100x Denhardt's solution	2% (w/v) Ficoll (400,000 mw), 2% (w/v) polyvinylpyrrolidone (40,000 mw), 2% (w/v) bovine serum albumin fraction V, 1 mM CDTA
dialysis tubing	Spectrum Medical Industries, Inc.; Spectra/Por Molecular Porous Membrane Tubing, diameter 15.9 mm, MWCO 12,000 to 14,000
DMEM	GIBCO BRL
DMMB	Aldrich Chemical Co.; see Appendix II.1. for preparation procedure
DMSO	J.T. Baker or Fisher
DMF	BDH
DTT	Sigma
ethidium bromide	Sigma; stock 1 mg/mL in H_2O, stored at 4°C in dark
fetal calf serum	Flow Laboratories, Inc.
FITC (isomer I)	Sigma; freshly prepared as 26 mM in DMSO
fluorescamine	Sigma; 15 mg/100 mL in acetone, stored at RT shielded from the light
fluorescein-X-biotin	Molecular Probes (Dr. J. Stahl); 5 mM stock in DMF, stored at -20°C
formaldehyde	Fisher
GF/A glass fibre filter (2.5 cm dia.)	Whatman
glass powder suspensions	plasmid purification systems developed in our lab
glass scintillation vials	Kimble
glycerol	BRL
glucosamine	BDH; 5 mg/mL stock in water, stored at -20°C
D-glucose	BDH; 1 M stock in water, stored at 4°C
D-[1-^{14}C]glucose	Amersham Canada Ltd.; supplied as a 200 µCi/mL (54 µCi/µmol) stock, stored at -20°C
GTN	Dupont Canada Inc.; supplied as a sterile 22 mM solution in 30% ethanol and 30% propylene glycol; stored at 4°C
Hep III (EC 4.2.2.7)	IBEX Technologies; 10 mU/µL in 20 mM Tris pH 7.5, stored at -20°C
2x Hep III reaction buffer	0.5 M Na acetate pH 8, 5 mM $CaCl_2$, stored at -20°C
heparanase extraction buffer	50 mM MOPS pH 7.5, 5 mM NEM, 0.05% (w/v)

(stock)	sodium azide, 0.1 mM CDTA; stored at -20°C
heparanase extraction buffer (working)	stock heparanase extraction buffer + freshly added 1 mM PMSF, 50 µM chymostatin, 2 µg/mL aprotinin
heparin (Na^+ salt), laboratory grade	Fisher; stock 1 mg/mL in water, stored at -20°C
HL-60	ATCC
HSC 93	Dr. M. Buchwald, Hospital for Sick Children
Hybond-N nylon membrane	Amersham
hydrogen peroxide (30% v/v)	Fisher or BDH
hydroxylamine hydrochloride	Canlab; freshly prepared as 1.5 M stock and pH adjusted to pH 8 with 10 N NaOH
KNRK	ATCC
luminol (5-amino-2,3-dihydro -1,4-phthalazinedione)	Sigma; 0.5 mM stock in DMSO, stored at -20°C.
lysozyme	BMC
β-mercaptoethanol	BDH
methylene blue	Allied Chemical Corp.; 0.1% (w/v) in 50% ethanol/water (v/v)
MNase	Sigma; 200 U/mL in 5x MNase buffer + 30% (v/v) glycerol, stored at -20°C
5x MNase buffer	5 mM $CaCl_2$, 50 mM Tris-HCl pH 9.5, stored at -20°C
MOL	Hoechst-Roussel Canada Inc. (Dr. B. Carter); 0.05 M stock in H_2O prepared fresh in subdued light, filtered through 0.2 µm filter and used immediately
monoclonal antibodies to biotin immobilized on agarose beads	Sigma; stored at 4°C and washed prior to use
MOPS	Sigma
$NaBH_3CN$	Aldrich; stored under N_2 at RT; prepared fresh as a 0.8 M stock in methanol immediately before use
NBT	Sigma; 12.2 mM stock in H_2O, stored at 4°C
NEM	Sigma
NeutrAvidin	Pierce
NIH 3T3	ATCC
NRK	ATCC
oligolabelling kit	Pharmacia LKB Biotechnology
PAGE gels	7.5% in 1x TAC (prepared from 30% acrylamide-bisacrylamide (19:1) mix) containing 0.025% (w/v) ammonium persulfate and 0.1% (v/v) TEMED
PBS	2.7 mM KCl, 1.5 mM KH_2PO_4, 137 mM NaCl, 4.3 mM Na_2HPO_4
PBS + trypsin	PBS containing 1x trypsin (see below)
PBST	10 mM potassium phosphate pH 7.4, 150 mM NaCl, 0.1% (v/v) Tween 20, 0.02% (w/v) NaN_3
PMSF	Sigma; 20 mM in methanol, stored at -20°C

polyamide TLC sheets	Dr. Peter Anderson
polystyrene tissue culture plates	Falcon or Corning (10 or 15 cm; 12 or 96 well)
proteinase K	BDH; 5 or 10 mg/mL in water; stored at -20°C
proteinase K/urea (lyophilized)	5 µg proteinase K, 5.8 µL 10 M urea, lyophilized
pyridine	BDH
RA	Sigma; 10 mM stock in ethanol; stored at -20°C
Rec	Rat embryo cells prepared by Steffany Bennett
RecRas	*ras*-transformed Rec cells prepared by S. Bennett
restriction enzymes (EcoRI, Bgl II, Hind III, Pst I)	Pharmacia; stored at -20°C as glycerol stocks
RPMI 1640	GIBCO BRL
SA-ag	Sigma; resin stored at 4°C, washed prior to use
SAL	Sigma; 0.2 M stock in water adjusted to pH 6.1 with NaOH
^{35}S-ECM plate	Dr. I. Vlodavsky; stored sealed at 4°C
Sephadex G-75 resin	Pharmacia; hydrated in and equilibrated with CT
SLSR resin	Promega
SLSR resin equilibration buffer	50 mM Tris-HCl pH 8, 150 mM NaCl, 0.1% Triton X-100
10x SSC	1.5 M NaCl, 0.15 M sodium citrate pH 6.1
1x TAC	40 mM Tris/20 mM sodium acetate, pH 7.8, 1 mM CDTA
TEMED	Bio-Rad
TK6	ATCC
Teflon-coated silicone septum	Pierce Chemical Co.
TNM	Aldrich Chemical Co., Inc.; freshly prepared in subdued light as a 50 mM solution in 99% ethanol
TPA	LC Services Corp.; stored at -20°C as a 1×10^{-4} M stock in DMSO
Triton X-100	BDH
trypan blue stain	mix 4 parts 0.2% trypan blue with 1 part 4.25% NaCl prior to use; mix with cells in a 1:1 (v/v) ratio
10x trypsin-EDTA	Gibco; 0.5% trypsin, 5.3 mM EDTA·4Na
U-937 cells	ATCC
Ultrafree-MC Durapore 0.22 µm filter unit	Millipore
xanthine	Sigma; freshly prepared as 10 mM in 75 mM NaOH
xanthine oxidase (EC 1.1.3.22)	Sigma, Grade 1; freshly diluted from a 19 U/mL stock to 50 mU/mL stock in BSS

APPENDIX II: MISCELLANEOUS PROCEDURES FOR PART B

Appendix II.1. *Dimethylmethylene Blue (DMMB) Assay for HS*

Dimethylmethylene blue (DMMB) is a cationic dye that binds negatively charged molecules (such as HS, nucleic acids, acidic proteins, etc.). When binding to polyanions, the intercalating dye molecules stack due to hydrophobic interactions causing a precipitate to form. The precipitate is insoluble in aqueous solutions; however, it can be solubilized in ethanol/SDS and quantified spectrophotometrically. The formation of the precipitate is accelerated by elevated temperature and vigorous mixing. This assay is subject to interference by salts and chaotropes. The following procedure was used to determine HS concentrations using DMMB.

0.006% (w/v) DMMB in 0.2 N sodium acetate pH 5 was prepared from a 1 mg/mL stock solution in 99% ethanol, filtered through a 0.45 µm filter, and could be stored at 22-25°C in an air-tight glass bottle for several months. 0.1 to 1.0 µg HS standards and unknowns were diluted into 200 µL water and 200 µL of 0.006% (w/v) DMMB was added to each. After vortexing vigorously for a few seconds, the mixtures were incubated at 37°C for 1 hr and microfuged for 5 min. The pellets were washed with 0.5 mL water, spun again and resuspended in 250 µL 0.5% SDS/95% ethanol with vortexing. The samples were read in a Perkin-Elmer Lambda 5 Spectrophotometer in a 200 µL microcuvette at 652 nm.

Using this protocol, DMMB detection was linear to 1 µg HS. DMMB precipitation tended to occur in the presence of salts (such as NaCl, LiCl) and was inhibited by the presence of SDS, Triton X-100, sarkosyl, and chaotropic agents such as urea, perchlorate, guanidinium thiocyanate. The lowest background and most reliable results were obtained using water as the diluent.

Appendix II.2. *Biotinylation of Cytochrome C With Biotin Succinimidyl Ester*

0.8 mM cytochrome c (freshly prepared in water as 1.6 mM) was incubated with 2 mM BXXSE (freshly prepared as 100 mM in DMF) in 0.2 M sodium borate pH 9.4 for 2 hr at RT then overnight at 4°C. A control reaction (no BXXSE) was also set up in parallel. The reactions were stopped by incubation with 10 mM glycine at RT for 1.5 hr and dialyzed overnight against water at 4°C to remove excess biotin-glycine conjugates. After binding to SA-ag beads, % biotinylation was determined spectrophotometrically (ε_m(oxidized cytochrome c)=8,900; ε_m(dithionite-reduced cytochrome c)=29,000) to be ~ 55-65%.

Appendix II.3. *Preparation of Immobilized FITC-HS-N-XXB Using NA Plates*

a) Preparation of the NeutrAvidin (NA) Coated 96-Well Polystrene Plates

50 µL of 0.1 mg/mL or 1 mg/mL NA in 50 mM $NaHCO_3$ pH 9.6 was added to each well. After overnight incubation at 4°C, NA was removed and wells were washed several times with PBST (10 mM phosphate pH 7.4, 150 mM NaCl, 0.1% Tween 20, 0.02% NaN_3). To prevent drying of wells or evaporation and thus concentration of samples, lids of the 96 well plates were lined with Whatman No. 1 paper moistened with water. Plates were stored at 4°C sealed with parafilm until use.

b) Immobilization of FITC-HS-N-XXB Onto NA-Coated 96-Well Polystyrene Plates

50 µL substrate diluted in PBST at less than 1 µg/mL was bound to the wells for 1 to 2 hr at RT with gentle shaking. Unbound substrate was removed, wells were washed with an equal volume of PBST or 0.2 M Tris pH 9.5 and pooled with the first fraction. Substrate that had not been introduced to the plate was similarly diluted to allow for determination of the amount of fluorescence bound to each well. Coating with a higher concentration of NA increased substrate binding capacity of the well (at least 0.05 µg versus 0.01 to 0.02 µg HS). To conserve NA, 0.1 mg/mL NA was routinely used thereafter to coat wells. Pre-washing of wells distilled water prior to coating with NA was found to improve reproducibility of substrate binding. Freshly prepared plates were able to bind more substrate.

Appendix II.4. *Quantitative Amine Analysis Using Fluorescamine*

The molar ratios of amines to molecules was determined using fluorescamine as an amine reactive probe. Fluorescamine reacts with primary amines [137]. While fluorescamine is rapidly degraded in water thus abolishing its fluorescence, the fluorescamine-amine conjugate is stable. Quantification of amines in HS substrates is accomplished by comparison of the fluorescence of fluorescamine-HS conjugates of known molar amount to that of a standard of known amine content per mole. The standard used in the assay described below was glucosamine which has one amine per molecule.

Samples to be analyzed for amine content were first standardized for their concentrations using the DMMB assay (above) with bovine kidney HS as a standard.

Glucosamine was prepared as a 5 mg/mL stock (= 23 mM) in water. For amine analysis, glucosamine was diluted 1:100 in water. HS samples to be analyzed were diluted with water in the range of 1 to 5 mg/mL. In separate 0.5 mL microcentrifuge tubes, 2.5, 5 and 10 µL aliquots of standard or samples were made up to a total volume of 10 µL using water. To each tube was added 10 uL of a solution of 0.3 M sodium borate pH 9.4, 0.15% SDS, 5 mM CDTA. After vortexing, 40 µL of 15 mg/100 mL fluorescamine in acetone were added to each tube. The tubes were vortexed and incubated at RT in the dark for 10 min to allow conjugation of fluorescamine with amines to occur. The reaction was stopped and unreacted fluorescamine destroyed upon addition of 20 µL water. After vortexing, the fluorescence of the standards and samples were read in a microcuvette using a Perkin-Elmer LS-5 Fluorescence Spectrophotometer at excitation and emission wavelengths set at 390 and 475 nm respectively and slits set at 5 and 10 nm respectively. The instrument was zeroed on water. Controls (i.e. without HS) were also subject to the assay to determine the background. Using linear regression analysis of the standards, the number of amines per molecule of HS was determined (average molar mass of 15,000 was used to convert mass of HS to moles).

CURRICULUM VITAE

Personal Data:

Name:	Amy Yamazaki
Present Address:	22 Alderbrook Drive Nepean, ON K2H 5W5
Telephone No.:	(613) 828-9937
Date of Birth:	August 21, 1968
Place of Birth:	Ottawa, ON

Education:

1994 to 1995	University of Ottawa *B. Education* (Int/Senior Divisions, Full-Time Field-Based Program) (degree and OTC conferred June 1995, Summa Cum Laude)
1992 to 1995	University of Ottawa *M. Science in Biochemistry* (Full and Part-Time) (qualifications to be completed in Winter 1996)
1988 to 1992	University of Ottawa *B. Science Honours in Biochemistry* (Full-Time) (degree conferred in Spring 1992, Summa Cum Laude)
1987 to 1988	Carleton University *First Year of B. Industrial Design* (Full-Time)

Research and Teaching Experience:

June 1995 to present	Adult High School, Ottawa, ON *Night School Teacher for OAC Biology*
July to Aug. 1995	St. Pius X High School, Nepean, ON *Summer Day School Teacher for 11A Chemistry*
May 1995 to present	Ottawa Board of Education *Supply Teacher*
Jan. to Apr., Sept. 1993	University of Ottawa, Department of Biochemistry *Demonstrator for Undergraduate Labs (BCH 2936, 3046)*

Sept. 1991 to present	Dr. H. C. Bimboim, University of Ottawa, Department of Biochemistry, Ottawa Regional Cancer Centre *Summer, Fourth Year Honours, and Graduate Student*
May to Sept. 1991	Dr. I. Altosaar, University of Ottawa, Faculty of Science *NSERC Summer Research Student*

Scholarships and Academic Awards:

University of Ottawa Silver Medal (Faculty of Education) (1995)
Professional Training Scholarship (Faculty of Education and the University of Ottawa Scholarship Committee) (1994 to 1995)
MRC Studentship (tenured at University of Ottawa, 1992 to 1994)
NSERC and OGS Studentships (awarded 1992; declined)
University of Ottawa Supplementary Research Scholarship (1992 to 1994)
A+ Excellence Award (University of Ottawa) (1992)
The Plaque of the Department of Biochemistry (University of Ottawa) (1992)
The Society of Chemical Industry Plaque (University of Ottawa, 1992)
NSERC Summer Undergraduate Research Scholarship (tenured at U. of Ottawa, 1991)
Dean's Honour List (University of Ottawa) (1989, 1991, 1992)
President's Scholarship (Carleton University) (1987 to 1988)
Ontario Scholar (Sir Robert Borden H.S.) (1987)
Bells Corners Arts League Award (Sir Robert Borden H.S.) (1987)

Publications and Abstracts:

Full Papers:

1) Yamazaki, A. and Bimboim, H. C. (1995) Potentiation of retinoic acid-induced U-937 differentiation into respiratory burst competent cells by nitric oxide donors. *Leuk. Res.* **19**, 325-335.

2) DeVouge, M. D., Yamazaki, A., Bennett, S. A. L., Chen, J.-H., Shwed, P. S., Couture, C., and Bimboim, H. C. (1994) Immunoselection of GRP94/endoplasmin from a KNRK cell-specific λgt11 library using antibodies directed against a putative heparanase amino-terminal peptide. *Int. J. Cancer*, **56**, 286-294.

Abstracts:

1) Yamazaki, A. and Bimboim, H. C. (1993) Combinations of nitric oxide-generating agents and retinoic acid induce capacity for respiratory burst and alkaline phosphatase activity in U-937 cells. *FASEB J.*, 7, A1098.